
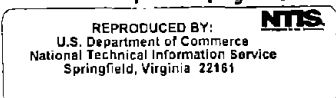


1. Report No. FHWA-RD-76-102		2. Government Accession No. PB268701 	
4. Title and Subtitle Simple Procedure for Fatigue Characterization of Bituminous Concrete		5. Report Date June 1976	
		6. Performing Organization Code	
7. Author(s) G. W. Maupin, Jr. and J. R. Freeman, Jr.		8. Performing Organization Report No. FHWA-RD-76-102	
9. Performing Organization Name and Address Virginia Highway and Transportation Research Council P. O. Box 3817, University Station Charlottesville, Virginia 22903		10. Work Unit No. (TRAIS) FCP-34A2-194	
		11. Contract or Grant No. DOT-FH-11-8324	
12. Sponsoring Agency Name and Address Offices of Research and Development Federal Highway Administration U. S. Department of Transportation Washington, D. C. 20590		13. Type of Report and Period Covered Final	
		14. Sponsoring Agency Code M-0325	
15. Supplementary Notes FHWA Contract Manager: Stewart R. Spelman			
16. Abstract The objective of this project was to develop a simple test to design bituminous concrete mixtures for fatigue resistance. Included are two literature reviews: (1) current fatigue testing procedures, and (2) simple test methods that offer possibilities for fatigue prediction. Seven bituminous concretes representing five areas of the United States were tested by a beam fatigue apparatus and several selected simple test methods. Correlations were performed between fatigue results and simple test results, and the best correlations were obtained with the indirect tensile test. Indirect tensile test results correlate with the stress-fatigue life curve under the constant stress fatigue test mode and the strain-fatigue life curve under the constant strain fatigue test mode. The main conclusion is that the indirect tensile test can be used to predict the fatigue characteristics of bituminous concretes and a simple test method is recommended. ✕			
17. Key Words simple test, fatigue correlations, constant stress fatigue test, constant strain fatigue test, indirect tensile test, predict fatigue life.		18. Distribution Statement No restrictions. This document is available to the public through the National Technical Information Service, Springfield, Virginia 22151.	
19. Security Classif. (of this report) Unclassified	20. Security Classif. (of this page) Unclassified	22. Price PCA07 MFA01	



ACKNOWLEDGEMENTS

The research reported here was administered under the Federal Coordinated Program of Research and Development in Highway Transportation (FCP), Project 4A — Minimize Early Deterioration of Bituminous Concrete. The funding was provided by the U. S. Department of Transportation under contract No. DOT-FH-11-8324.

Appreciation is expressed to the following persons for providing aggregates and asphalt cements used in the laboratory mixes: E. S. Lindow, Pennsylvania Transportation Institute; Dale E. Peterson and Joseph C. McBride, Utah State Department of Highways; F. M. Williams and R. A. Luce, Ohio Department of Transportation; and Professor Carl L. Monismith, University of California.

Appreciation is expressed to J. H. Dillard for encouragement in the project, and to C. S. Hughes III for general guidance and advice on the statistical analysis.

L. E. Wood, Jr., laboratory supervisor, is acknowledged for the scheduling and performance of the many laboratory tests; and thanks go to S. A. Kelley, computer programmer, for running the computer analysis program.

GENERAL DISCLAIMER

This document may be affected by one or more of the following statements

- **This document has been reproduced from the best copy furnished by the sponsoring agency. It is being released in the interest of making available as much information as possible.**
- **This document may contain data which exceeds the sheet parameters. It was furnished in this condition by the sponsoring agency and is the best copy available.**
- **This document may contain tone-on-tone or color graphs, charts and/or pictures which have been reproduced in black and white.**
- **This document is paginated as submitted by the original source.**
- **Portions of this document are not fully legible due to the historical nature of some of the material. However, it is the best reproduction available from the original submission.**

TABLE OF CONTENTS

	<u>Page</u>
ACKNOWLEDGEMENTS	ii
LIST OF FIGURES	v
LIST OF TABLES	viii
CHAPTER I. INTRODUCTION	1
CHAPTER II. LITERATURE REVIEW OF LABORATORY FATIGUE TESTS	2
Methods of Testing	3
Testing Modes	3
Load Variables	5
Definition of Failure	7
Fatigue Tests	8
Beam Specimen	8
Plate Specimen	20
Cylindrical Specimen	22
Trapezoidal Specimen	22
Pell Specimen	25
Evaluation of Test Methods	27
Beam Specimen	27
Plate Specimen	27
Cylindrical Specimen	28
Trapezoidal Specimen	28
Pell Specimen	28
Summary	28
CHAPTER III. LITERATURE REVIEW OF SIMPLE TEST METHODS	29
Purpose and Scope	29
Methods of Testing	29
Indirect Tensile Test	29
Resilient Modulus Indirect Tensile Test	42
Double Punch Test	43
Cohesimeter Test	45
Direct Tension	49
Flexural Beam Test	51
Sonic Test	55
Summary and Evaluation of Test Methods	55
CHAPTER IV. LABORATORY INVESTIGATION OF SIMPLE TEST METHODS	60
Objective and Scope	60

TABLE OF CONTENTS (Cont.)

	<u>Page</u>
General Approach	60
Materials	60
Testing Scheme	64
Testing Methods	64
Fatigue Tests	64
Indirect Tensile Test	68
Punch Test	69
Resilient Modulus	69
Flexure Test	71
Resonant Frequency Tests	74
Pulse Velocity Tests	74
Results	77
Fatigue Tests	77
Simple Tests	82
Indirect Tensile Test	82
Punch Test	85
Resilient Modulus	85
Flexure Test	87
Resonant Frequency and Pulse Velocity Tests	88
Correlation of Simple Test and Fatigue Test Results	89
Constant Stress Fatigue Tests	89
Constant Strain Fatigue Tests	91
CONCLUSIONS	99
RECOMMENDATIONS	100
REFERENCES	109
APPENDIX A FINGERPRINTING DATA ON ORIGINAL ASPHALT CEMENTS	114
APPENDIX B ASPHALT CEMENT SLIDING PLATE VISCOSITIES	115
APPENDIX C PREDICTION OF FATIGUE LIFE RELATIONS BY INDIRECT TENSILE TEST	116

LIST OF FIGURES

	<u>Page</u>
Figure 1. Controlled Stress Fatigue Test	4
Figure 2. Controlled Strain Fatigue Test	4
Figure 3. Block Pattern for Simple Loading	6
Figure 4. Block Pattern for Compound Loading	6
Figure 5. Repeated Flexure Apparatus	9
Figure 6. Details of Components of Repeated Flexure Apparatus	10
Figure 7. Load and Deflection vs. Time	12
Figure 8. Basic Loop of Electrohydraulic Testing System	14
Figure 9. Comparison of Rates of Crack Propagation	19
Figure 10. Deflectometer Flexure Fatigue Tester	21
Figure 11. Loading Head with Rigid Parallel Patens	23
Figure 12. Trapezoidal Specimen	24
Figure 13. Trapezoidal Specimen Loading Apparatus	24
Figure 14. Pell Testing Apparatus	26
Figure 15. Stresses in a Circular Disk	30
Figure 16. Notation for Rectangular Stress Components	32
Figure 17. Stress Distributions on x-Axis	33
Figure 18. Stress Distributions on y-Axis	34
Figure 19. Stiffness Modulus for Asphalt as Function of Loading Time	35
Figure 20. Stress Components in Specimen Using Loading Strips	36
Figure 21. Stress Distributions Along Principal Axes with 0.4 in. (10.2 mm) Wide Loading Strips	37

	<u>Page</u>
Figure 22. Generalized Characterization of Load- Horizontal Deformation Data	41
Figure 23. Failure Mechanism of Double Punch Test	44
Figure 24. Hveem Cohesimeter	47
Figure 25. Experimental Approach to Correlation Analysis	48
Figure 26. Diametrical Direct Tension Test	52
Figure 27. Direct Tension Testing Apparatus	53
Figure 28. Variation of log K with Bulk Modulus	56
Figure 29. Fatigue Test	67
Figure 30. Indirect Tensile Test	68
Figure 31. Typical Indirect Tensile Test Recording	70
Figure 32. Punch Test	71
Figure 33. Typical Punch Test Recording	72
Figure 34. Resilient Modulus Test	73
Figure 35. Flexure Test	73
Figure 36. Typical Flexure Test Recording	75
Figure 37. Resonant Frequency Test	76
Figure 38. Pulse Velocity Test	77
Figure 39. Constant Stress Tests — Fatigue Life vs. Maximum Bending Stress	78
Figure 40. Constant Stress Tests — Fatigue Life vs. Initial Maximum Bending Strain	80
Figure 41. Constant Strain Tests — Fatigue Life vs. Maximum Bending Strain	81
Figure 42. Constant Strain Tests — Fatigue Life vs. Initial Maximum Bending Stress	83
Figure 43. Constant Stress Fatigue Curves (Virginia AC-20 mix)	92

	<u>Page</u>
Figure 44. Constant Stress Fatigue Curves (Virginia 50-60 pen. mix)	93
Figure 45. Constant Stress Fatigue Curves (Virginia 120-150 pen. mix)	94
Figure 46. Constant Stress Fatigue Curves (Pennsylvania mix)	95
Figure 47. Constant Stress Fatigue Curves (Ohio mix)	96
Figure 48. Constant Stress Fatigue Curves (Utah mix)	97
Figure 49. Constant Stress Fatigue Curves (California mix)	98
Figure 50. Constant Strain Fatigue Curves (Virginia AC-20 mix)	103
Figure 51. Constant Strain Fatigue Curves (Pennsylvania mix)	104
Figure 52. Constant Strain Fatigue Curves (Ohio mix)	105
Figure 53. Constant Strain Fatigue Curves (Utah mix)	106
Figure 54. Constant Strain Fatigue Curves (California mix)	107
Figure 55. Fatigue Design of Bituminous Concrete, Constant Stress Failure Mode	108

LIST OF TABLES

	<u>Page</u>
Table 1. Coefficients for Modulus of Elasticity by Double Punch Test	46
Table 2. Parameters Used in Correlation Analysis	50
Table 3. Rating Simple Test Methods	57
Table 4. Asphaltic Concrete Mixtures	61
Table 5. Mix Designs	62
Table 6. Asphalt Cement Properties	63
Table 7. Number of Required Tests	65
Table 8. Average Mixture Properties	66
Table 9. Constant Stress Fatigue Relationships	79
Table 10. Constant Strain Fatigue Relationships	82
Table 11. Indirect Tensile Test Results	84
Table 12. Punch Test Results	86
Table 13. Resilient Modulus Results	87
Table 14. Flexure Test Results	88
Table 15. Resonant Frequency and Wave Velocity Test Results	89
Table 16. Correlation Between Constant Stress Fatigue and Simple Tests	90
Table 17. Correlation Between Constant Strain Fatigue and Simple Tests	102

CHAPTER I. INTRODUCTION

Pavements must be designed for the repeated loadings caused by traffic if they are to give satisfactory service over a reasonable period of time. Although several authors — including F. J. Grumm⁽¹⁾ and O. J. Porter⁽²⁾ — have reported on this subject, F. N. Hveem⁽³⁾ was one of the first to investigate the effects of repeated loadings.

Hveem established three major factors related to the failure of bituminous pavements: (1) flexural strength, (2) the weight of the mix on the subgrade, and (3) the flexibility to withstand repeated bending. Experience and empirical design procedures such as those developed by Marshall and Hveem have enabled engineers to design mixtures against the most common premature failure mechanisms such as rutting and bleeding, but, because of its complex nature, fatigue failure is difficult to analyze and to design against.

When investigating pavement flexibility, Hveem developed a fatigue testing device capable of testing small beams cut from asphaltic pavements. Other tests were developed in the early stages of fatigue testing by Hennes and Chen,⁽⁴⁾ Nijboer,⁽⁵⁾ Van der Poel,⁽⁶⁾ and Monismith⁽⁷⁾. Hennes and Chen tested beam specimens in flexure with a device in which the specimens were supported on a steel leaf spring. Nijboer and Van der Poel developed a repeated loading device that tested cylindrical bars of asphaltic concrete in a rotational cantilever mode. This test method was further developed by Pell⁽⁸⁾ and is discussed in detail in Chapter II. Monismith developed a repeated flexure testing apparatus with a spring base intended to simulate the base-subgrade combination in the pavement structure.

As fatigue testing has progressed, engineers have become more aware of the complexities entailed and many approaches for analyzing the fatigue life of pavements have been adopted. Monismith and others^(9,10,11,12,13) have developed and refined test methods using beam specimens. Jimenez has studied the effects of flexure loadings on circular plate specimens.⁽¹⁴⁾ Several tests have been performed using various odd shaped specimens such as trapezoidal ones.^(15,16) Methods of analysis have advanced, with Majidzadeh et al. having introduced analysis by fracture mechanics.⁽¹⁷⁾

Fatigue behavior can be quantitatively defined for a particular mix by performing a series of cyclic fatigue tests utilizing the variety of specimens and testing devices mentioned previously. The required equipment is usually quite expensive and the time required to obtain fatigue data

for a particular mix is about 2 to 3 weeks; therefore, this test method is not practical in routine design laboratories. A simple test method capable of determining fatigue behavior of asphaltic concrete mixtures is needed if fatigue design can be considered in design laboratories.

Monismith and his co-workers recognized the need for a simple test method.(18) Work is in progress at Georgia Tech Research Institute by Dr. Richard Barksdale to develop equipment for evaluating the fatigue characteristics of asphaltic concrete. Also Dr. Kamran Majidzadeh is conducting research at Ohio State University on the development of a simple fatigue design procedure. Thus the recent emphasis on the development of a simple test method is evident. The Virginia Highway and Transportation Research Council contracted with the Federal Highway Administration to develop a simple test method.

The three main objectives of the contract were to conduct -

1. a literature review of existing fatigue testing equipment, the data acquired, and analytical methods used;
2. a literature review of possible simple test methods that might be used to delineate the fatigue properties of bituminous mixtures; and
3. a laboratory investigation which would hopefully result in the development of a simple test method for predicting the fatigue behavior of asphaltic concrete mixes.

The results of the efforts toward these three objectives are given in the following three chapters of this report.

CHAPTER II. LITERATURE REVIEW OF LABORATORY FATIGUE TESTS

This literature review focused on fatigue test methods and equipment, the data acquired in these tests, and the analytical methods used to evaluate the test results. The discussion presented is directed primarily toward experimental laboratory fatigue testing; however, in some instances it includes the use of the test results in pavement design.

Methods of Testing

Prior to the discussion of the various types of fatigue tests and equipment used, a general discussion of the testing modes used, the load variables, and definitions of the types of failure found in fatigue testing is presented.

Testing Modes

Laboratory fatigue testing methods predominately have used two modes of loading for bituminous specimens.⁽¹⁰⁾ These modes, controlled stress and controlled strain, are designed to hold either the stress or strain at a desired value while an unconstrained variable is monitored.

Controlled Stress

The controlled stress mode of testing requires that a load of constant value be applied to the specimen throughout the testing process as illustrated in Figure 1. When this testing mode is used, the deflection of the specimen is monitored to determine the strain corresponding to the applied load. The controlled stress test mode is used to test the bituminous materials which provide the primary structural support of the roadway, i.e., materials placed in thicknesses greater than 4 in. (10.2 cm).

Controlled Strain

The controlled strain mode of testing is performed by maintaining the strain at a desired level and monitoring the corresponding stress. In this mode, a predetermined value of deflection, or strain, is placed on the specimen, and the load required to produce this deflection is recorded throughout the test. Graphic illustrations of strain vs. cycles to failure and stress vs. cycles to failure are given in Figure 2.

The controlled strain test is used to test bituminous materials used as thin surface layers, the reason being that the surface layer of a bituminous roadway gives little if any structural support and deflects an amount controlled by the subgrade, base material, and bituminous base.

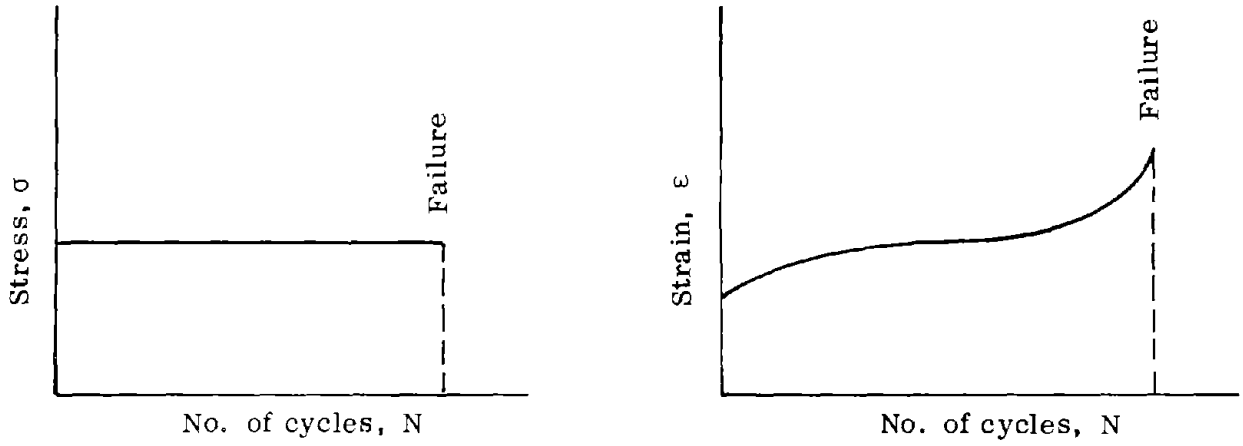


Figure 1. Controlled stress fatigue test. ⁽¹⁰⁾

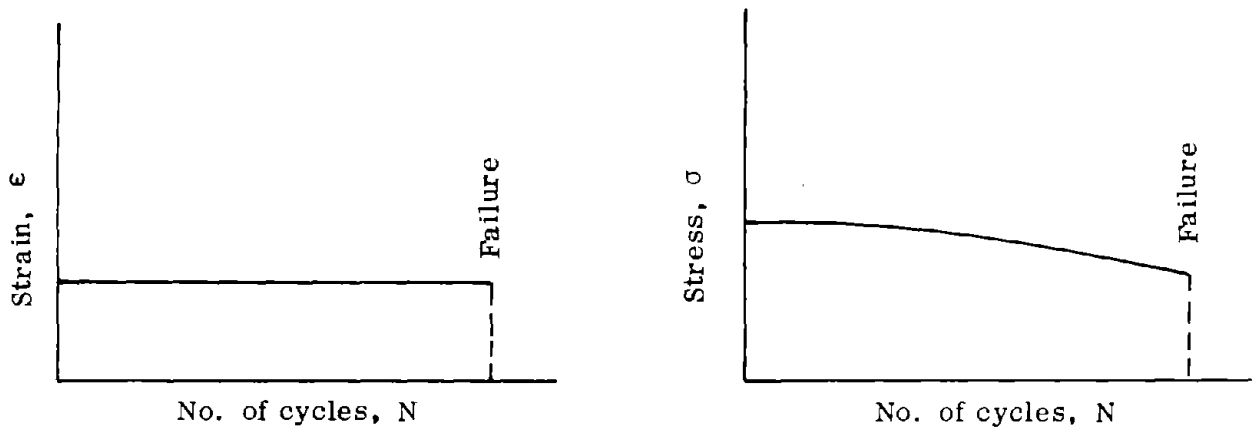


Figure 2. Controlled strain fatigue test. ⁽¹⁰⁾

Load Variables

Many types of loadings can be used in a laboratory fatigue test. The primary variables are the load history, the rate of load application, and the pattern of applying the load.

Load History

A specimen may be subjected to two types of load history — simple and compound.⁽⁹⁾ In simple loading, whether controlled stress or controlled strain, the load condition remains unchanged throughout the fatigue test. In compound loading there are changes in the load condition during the test, with a change being defined as a change in the amount of stress or strain applied to the specimen or a change in the environment, such as an increase or decrease in temperature.

Compound loadings can be preprogrammed to simulate the loadings a pavement receives from traffic; however, the process is quite involved, so simple loadings are more widely used.

Load Rate

The rate of loading is the number of load applications made over a specified period of time. It has been proven that the fatigue life varies with the rate of loading. Tests by Monismith and Deacon indicated that over loading rates ranging from 30 to 100 repetitions per minute, there was a significant decrease in fatigue life as the loading rate increased.⁽⁹⁾ In tests performed by Taylor, it was found that loading rates of less than 200 repetitions per minute caused a greater variation in specimen service life than did higher loading rates.⁽¹⁹⁾

Patterns of Applying Loads

The load patterns commonly used are block, sinusoidal, and haversine.^(9,18) The block pattern for a simple loading is shown in Figure 3. As was previously discussed, for a simple load rate the level of stress or strain is kept constant throughout the test. When applying a compound loading, as shown in Figure 4, the levels of stress or strain are varied. Compound loading tests are done predominately with the block pattern; however, haversine and sinusoidal patterns may also be used.

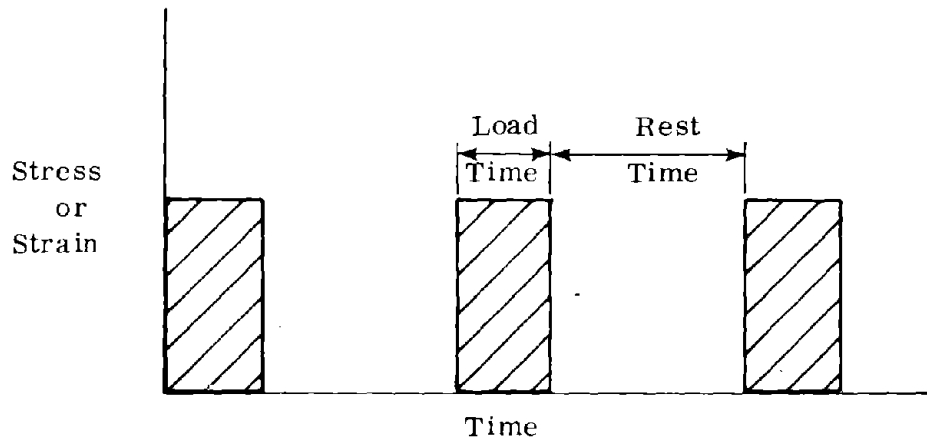


Figure 3. Block pattern for simple loading. ⁽⁹⁾

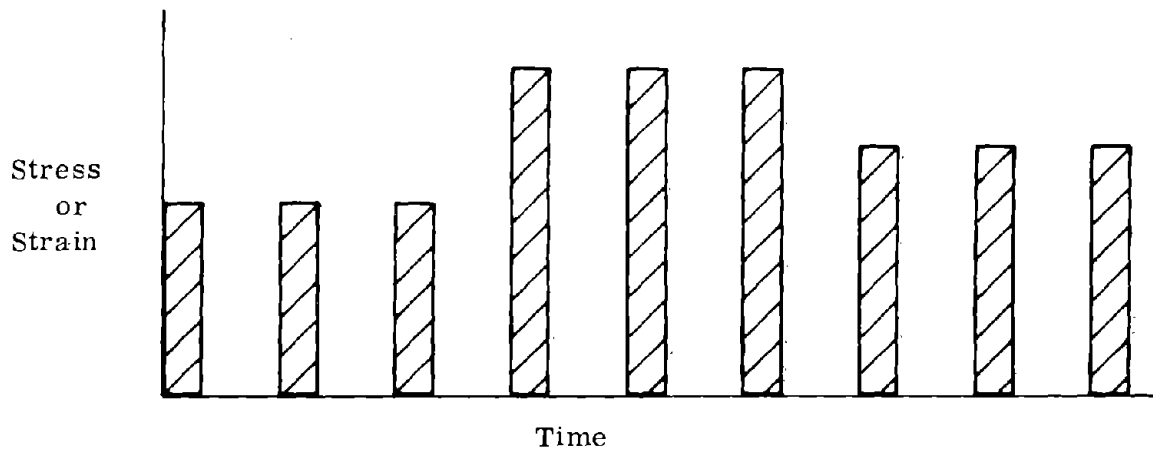


Figure 4. Block pattern for compound loading. ⁽⁹⁾

There are two ways in which a compound loading can be applied — sequentially or randomly. Sequential loading is performed by applying a fixed number of loadings under one load condition, then another fixed number under a different condition. This pattern, which is illustrated in Figure 4, is continued until the specimen fails. In random loading each load applied is selected randomly so that the probability of any load being selected is equal to that of any other load, regardless of the preceding order of applied load conditions.

The haversine pattern is used mostly for simple loading rather than compound loading. It constitutes the compressive half of the sine curve, in which the simply supported beam is loaded and then enough tension is applied to force it back to the neutral axis. This pattern is preferred over the sinusoidal pattern because it more closely resembles the loadings of roadway pavements. The surface layer of a roadway undergoes both tensile and compressive forces during a wheel loading; however, the compressive forces far outweigh the tensile forces.

Definition of Failure

Failure of a specimen is generally defined as the point at which it no longer has the ability to satisfactorily withstand a desired load.⁽⁹⁾ For fatigue tests, the failure condition varies depending on the mode of testing used.

In the controlled stress mode of testing, fatigue life is defined as the number of loadings required for the specimen to completely fracture. In the controlled strain mode of testing the dynamic load applied to the specimen is recorded after the first 200 to 300 load applications, and the fatigue life is reached when the dynamic load reduces to a predetermined percentage of the initial dynamic load. This percentage usually varies between 50% and 75%. It has been reported by Epps and Monismith that 25% and 50% reductions in stiffness correspond to small and extensive crack propagations, respectively.⁽¹⁸⁾

Another method used to determine failure involves gluing foil strips to the tensile sides of the specimen, 1/2 in. (1.27 cm) from each bottom edge.⁽²⁰⁾ The strips are wired in parallel so that both must be broken for failure to be reached. This method of determining failure is used primarily in constant stress testing.

Fatigue Tests

The following discussion focuses on the various types of fatigue tests. The test methods are grouped by the type of specimen (beam, plate, Marshall, etc.) used, and the discussion under each type of specimen covers (1) the type of fatigue testing equipment needed and the capabilities of this equipment, (2) the data acquired from the test, and (3) the analytical methods used in evaluating the data.

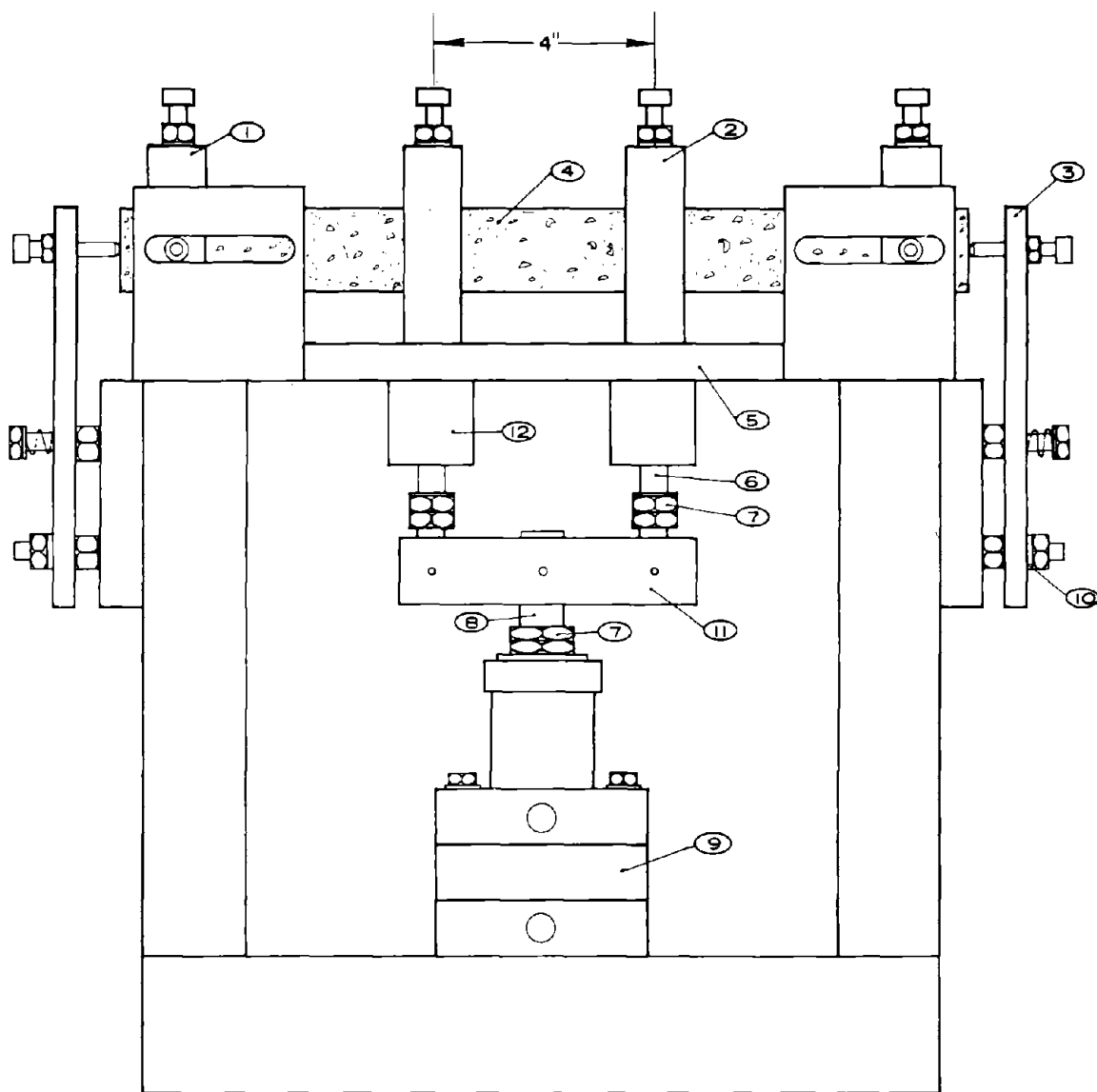
Beam Specimen

Equipment

The fatigue testing equipment that has been developed for beam specimens has two major components — the repeated-flexure apparatus and the control and loading systems. The repeated-flexure apparatus^(9,12) is basically the same for any control and loading system used.^(9,10,11,12,13) The only variations in the apparatus would be changes made to accommodate various sizes of specimens. The control and loading systems are of two types — air or pneumatic pressure systems and electrohydraulic systems.

Repeated-Flexure Apparatus. The repeated-flexure apparatus,⁽⁹⁾ often termed the testing frame, is used to hold the specimen so that the loadings can be applied. This apparatus, shown in Figure 5, is designed so that a symmetrical, two-point load is applied to a simply supported beam and results in unidirectional bending stresses.

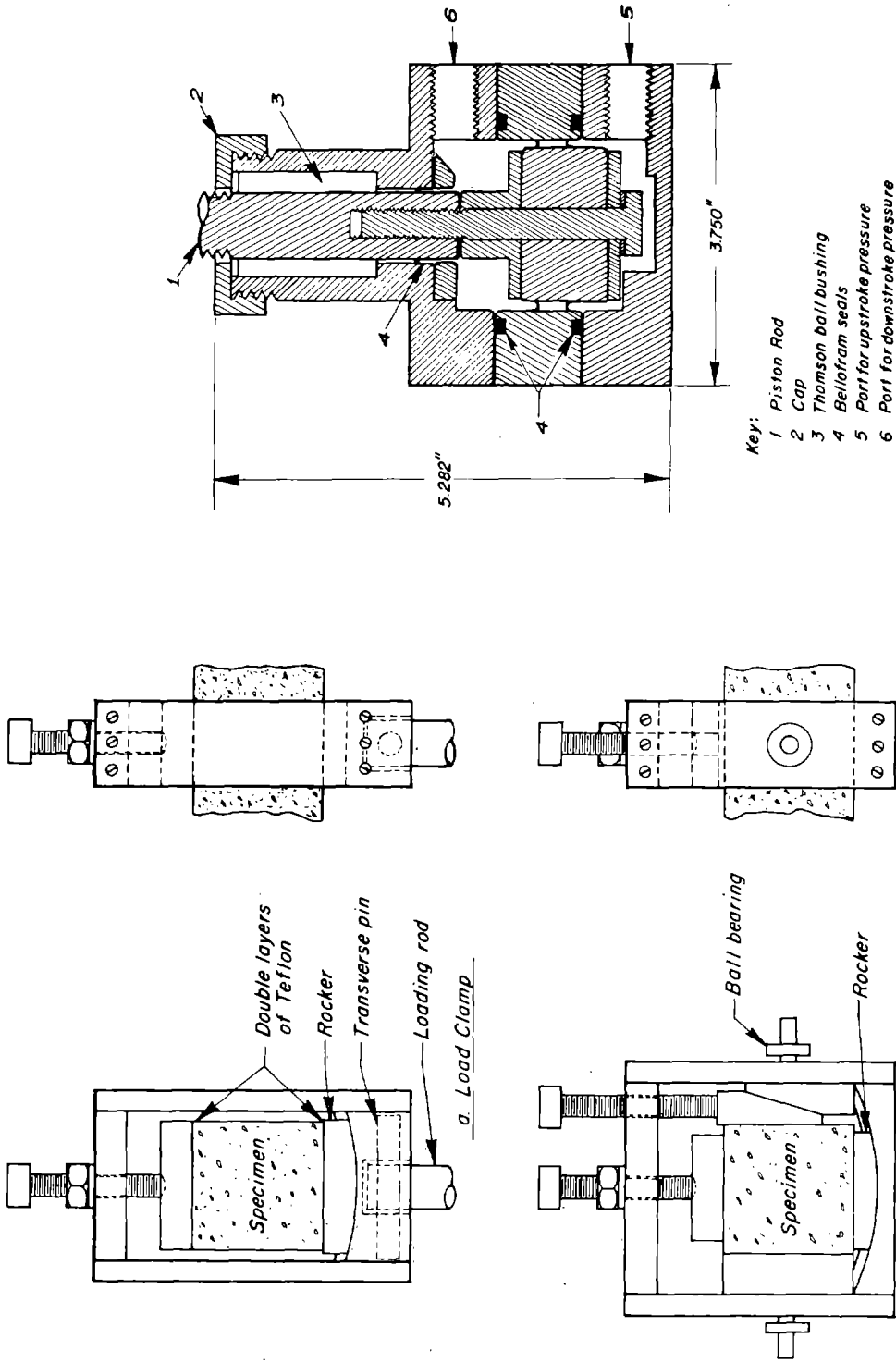
The specimen is held in position by four clamps, two of which apply the load (load clamps) while the other two (reaction clamps) support the specimen. These clamps, as shown in detail in Figure 6, have lubricated rockers that eliminate torsional stresses resulting from the specimen.



Key:

- | | | |
|-------------------|----------------|--------------------------------------|
| 1. Reaction clamp | 5. Base plate | 9. Double-acting, Bellofram cylinder |
| 2. Load clamp | 6. Loading rod | 10. Rubber washer |
| 3. Restrainer | 7. Stop nut | 11. Load bar |
| 4. Specimen | 8. Piston rod | 12. Thomson ball bushing |

Figure 5. Repeated flexure apparatus.⁽⁹⁾



c. Double-acting, Bellofram Load Cylinder

b. Reaction Clamp

Figure 6. Details of components of repeated flexure apparatus. (9)
(1 in. = 2.54 cm.)

not being perfectly square. The reaction clamps are designed so that there is no relative movement between the clamps and the specimen. These clamps are also equipped with ball bearings that allow longitudinal movement and rotation under load. The load clamps have a transverse pin that allows rotation during loading and thus eliminates any bending movement which may be introduced. To allow longitudinal movement of the specimen, a lubricant must be used to minimize friction between the specimen and the load clamp. Teflon tape and Molykote powder can be used for this purpose.

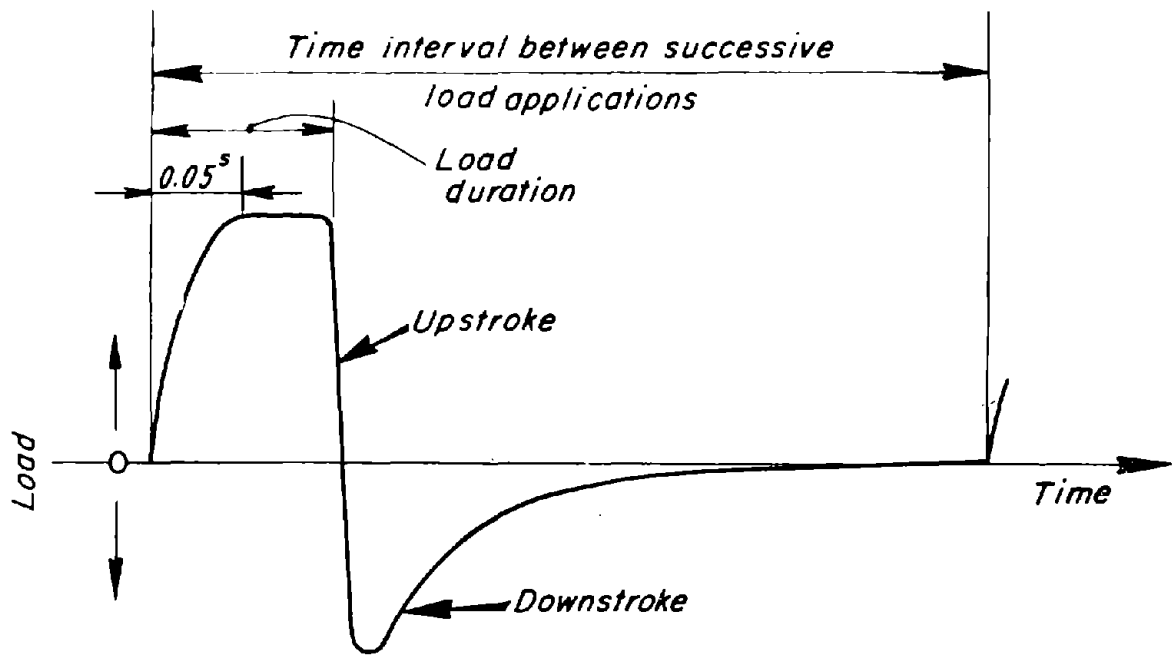
The apparatus is designed to fit one specific size beam. Square beam sizes used have varied from a vertical cross section of 1.5 in. x 1.5 in. (3.8 cm x 3.8 cm)^(9,11) to 3.0 in. x 3.0 in. (7.6 cm x 7.6 cm).^(10,12) Beams not having a square cross section have been tested by Kirk,⁽¹³⁾ who used a beam having cross sectional dimensions of 2 in. x 2 3/4 in. (5 cm x 7 cm). The beams are usually 15 in. (38.1 cm) in length; however, Kirk varied this dimension also and used a beam 13 3/4 in. (35 cm) in length.

Control and Loading Systems. As stated earlier, two systems are used to generate and control the applied load. These systems, the air or pneumatic pressure^(9,11) and the electrohydraulic,^(12,13) are discussed in detail below.

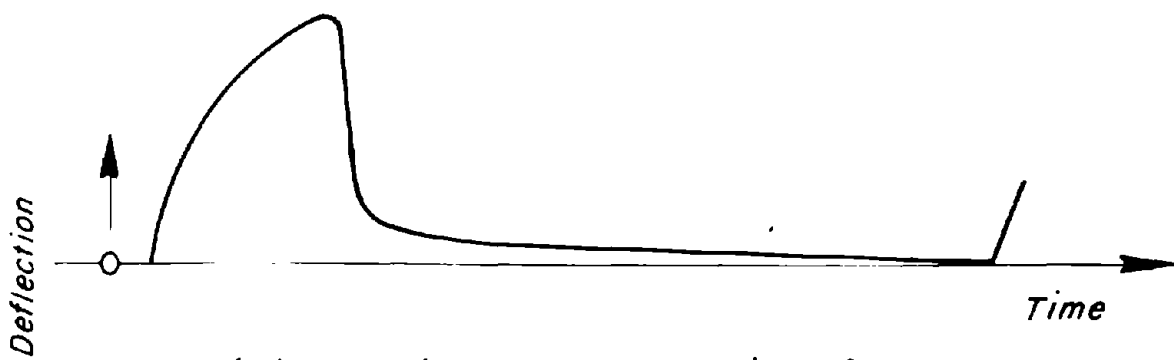
Air or Pneumatic System. The air or pneumatic pressure system developed by Deacon⁽⁹⁾ supplies a controlled pneumatic pressure to a double-acting Bellofram cylinder. The Bellofram cylinder, shown in Figure 5 and in more detail in Figure 6, applies the load to the specimen. The pneumatic pressure is controlled by mechanical air control (MAC) valves regulating the air pressure between the air tanks and the Bellofram cylinder. These valves are three-way, solenoid-operated pressure valves activated by the control system. The MAC valve is designed to allow air to enter either the upstroke chamber or the downstroke chamber, or to completely block off the flow of air into the Bellofram cylinder.

The frequency of loading is regulated through the central system by a mechanically powered cam and microswitch arrangement. The frequency of loading is approximately 120 applications per minute, with the duration of the load increasing from a minimum of 0.05 second. An illustration of the load vs. time and deflection vs. time is shown in Figure 7.

The magnitude of the load is controlled by the pneumatic pressure system through a pressure cylinder under an



(a) Idealized Load-time Curve.



(b) Idealized Deflection-time Curve.

Figure 7. Load vs. time and deflection vs. time relationships for constant stress test equipment.⁽⁹⁾

air pressure regulated to provide the desired loading. A compound block load can be applied by use of a series of pressure cylinders with MAC valves connected to the Bellofram cylinder. By programming the control system to switch the various MAC valves on and off, changes of load magnitudes can be accomplished. The design of this system allows the block loading pattern to be used with either simple or compound loading and either the controlled stress or controlled strain testing mode.

The air or pneumatic pressure system is used predominantly for tests in the controlled stress mode, because of the difficulty in varying the load to maintain a constant strain in the controlled strain test. To perform a controlled strain test with this equipment, the test must be constantly monitored so that the adjustments in the load necessary to maintain a constant strain level can be made manually.

Electrohydraulic System. The electrohydraulic system^(12,13) is very different from the air pressure system, both in the control mechanism and in the generation of the load. This system uses a totally electronic control subsystem to activate the hydraulic subsystem that generates the load.

The testing system operates in a closed loop,⁽²¹⁾ as shown in Figure 8, initiated by an electrical signal (load, deflection or strain) from the manual command control in the input module (performed by operator). This input is applied to the specimen, and the system then compares the polarity and the magnitude of the command signal to those given by the feedback transducer. If the difference between the command signal and that of the feedback transducer is not zero, the controller makes the necessary adjustment by signaling the loading system.

The hydraulic supply is the link between the control system and the loading system. The control system, through a servo valve, regulates the flow of hydraulic fluid moving the piston. The movement of the piston provides the loading that the repeated-flexure apparatus applies to the specimen.

This type of equipment can perform in both the controlled stress and controlled strain modes. The tests are generally performed with a simple haversine load pattern, but other patterns may be used.

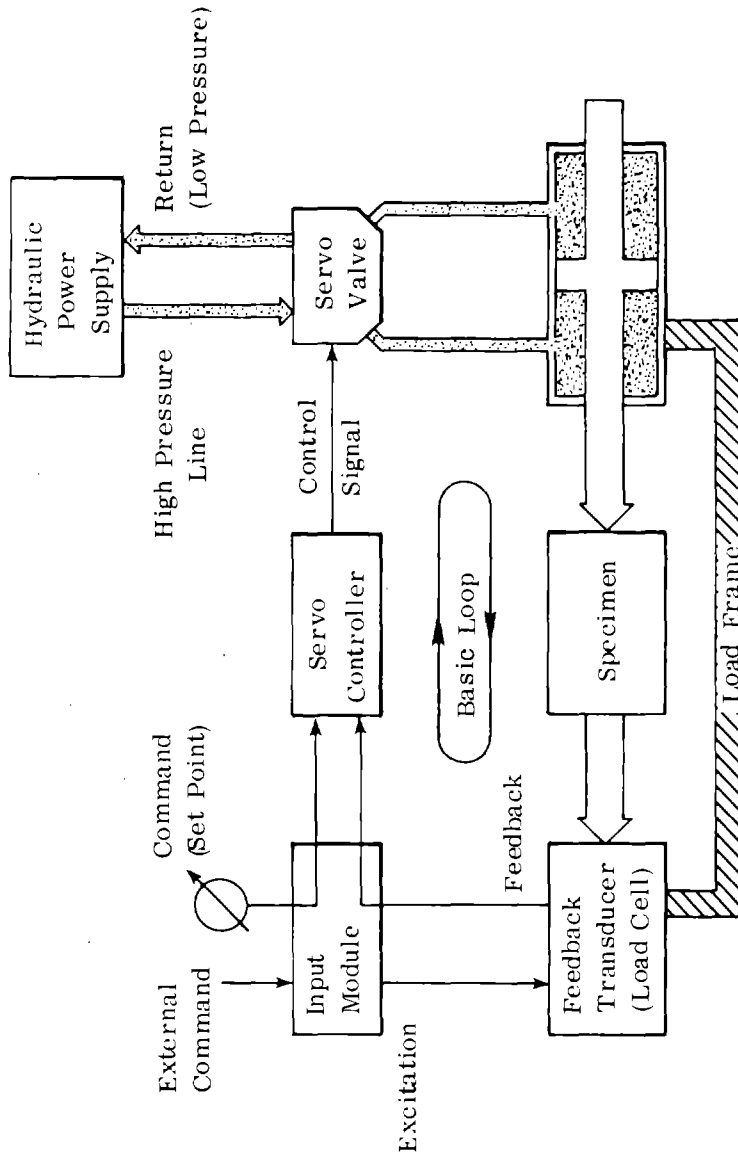


Figure 8. The basic loop of the electrohydraulic testing system. (21)

Data Collection

Because of the general acceptance of the repeated-flexure apparatus for loading the specimen, the data collection methods and equipment are generally the same regardless of the control and loading system used. The only major differences are in the methods in which the load is applied to the specimen and the deflections are recorded. The electrohydraulic system has a load cell in the repeated-flexure apparatus which determines the load applied to the specimen.⁽¹²⁾ The air pressure system can measure the load directly from the pressure maintained in the air pressure tank, provided it has been calibrated with a load cell.⁽⁹⁾

The centerline beam deflection is measured by a linear, variable, differential transformer (LVDT). The value measured by the LVDT is recorded on a strip chart recorder.

Analytical Methods

Linear Fatigue Life Relationships. The methods used to analyze the data are the same regardless of the size of the specimen used. The basic equations for extreme fiber stress, stiffness modulus, and extreme fiber strain are listed below.⁽¹²⁾ The equations apply to a beam of uniform cross section which is simply supported at the ends and loaded by two symmetrical, concentrated loads applied near the center.

$$\sigma = \frac{3aP}{bt^2} \quad (1)$$

$$E_s = \frac{Pa(3l^2 - 4a^2)}{48Id} \quad (2)$$

$$\epsilon = \frac{12td}{(3l^2 - 4a^2)} \quad (3)$$

where

σ = extreme fiber stress, psi (1 psi = 6890 Pa)

a = 1/2 (reaction span length - distance between load clamps), in. (1 in. = .0254 m)

P = dynamic load applied to deflect beam, lb.
(1 lb. = 4.45 N)

- b = specimen width, in. (1 in. = .0254 m)
- t = specimen depth, in. (1 in. = .0254 m)
- E_s = flexural stiffness modulus based on deflection, psi (1 psi = 6890 Pa)
- ℓ = reaction span length in. (1 in. = .0254 m)
- I = specimen moment of inertia, in.⁴ (1 in.⁴ = 41.6 cm⁴)
- d = dynamic deflection of beam center, in. (1 in. = .0254 m)
- ϵ = extreme fiber strain of mix in region of equal moment calculated from deflection of beam center, in./in. (mm/mm)

The stress, σ , and fatigue life, N_f , can be correlated using a least squares regression analysis that results in a linear log-log plot of σ versus N_f .⁽¹²⁾ This relationship is shown in the form:

$$N_f = K_1 (1/\sigma)^{n_1} \quad (4)$$

where

N_f = number of load applications to failure

K_1 = constant depending on the mix

σ = extreme fiber bending stress, psi
(1 psi = 6890 Pa)

n_1 = constant (slope of regression line)

With the above equation, the fatigue life for a given bending stress can be estimated.

A similar relationship can be established for strain, ϵ , versus fatigue life, N_f . This relationship is also obtained from a least squares regression analysis,⁽¹²⁾ and is shown as

$$N_f = K_2 (1/\epsilon)^{n_2} \quad (5)$$

where

- N_f = number of load applications to failure
- K_2 = constant depending on the mix
- ϵ = initial bending strain based on center point deflection of specimen
- n_2 = constant (slope of regression line)

Fracture Mechanics. The fatigue behavior of bituminous pavements has been analyzed from the fracture mechanics viewpoint by Majidzadeh et al.⁽¹⁷⁾ This analysis has been developed using beam specimens tested in a controlled stress mode with loading of 0.1 sec. duration and a 1.0 sec. rest period. During loading it is necessary to measure the crack length or determine it by indirect methods. The direct methods are X-ray, ink-staining, and visual observation. The indirect method uses the inverse slope of the load/deflection diagram for each loading cycle to represent the compliance of the beam, with an increase in compliance being directly related to an increase in crack depth. The fracture mechanics analysis uses the equation

$$N_f = \int_{C_o}^{C_f} \frac{1}{AK^n} dc \quad (6)$$

where

- N_f = number of cycles of load to failure
- A = crack growth parameter relative to materials
- K^n = the stress intensity factor with n being a material constant
- dc = the rate of crack propagation
- C_f = the critical crack depth
- C_o = the original crack depth
- n = crack growth parameter relative to foundation stiffness

The stress intensity factor, K^n , can be determined by using the equation

$$K^n = P \sqrt{\frac{E}{2(1-\nu^2)} \frac{\partial L}{\partial C}} \quad (7)$$

where

- L = compliance, which is the inverse slope of the load/deflection diagram under each loading cycle
- C = crack depth, in. (1 in. = .0254 m)
- P = load, lb. (1 lb. = 4.45 N)
- E = Young's modulus, psi (1 psi = 690 Pa)
- ν = Poisson's ratio

The values of parameters A, n, C_0 and C_f also must be determined before the fatigue life can be computed. These parameters are used to describe the fatigue process and help predict fatigue life.

The parameter A is affected by mixture variables such as percent asphalt, asphalt hardness, and mixture density. The value of A is variable and is computed by using the equation

$$A = \frac{1}{K^n} \frac{dc}{dN} \quad (8)$$

The values of the non-dimensional parameters C_0 and C_f are determined during the fatigue tests, with C_f being based on the crack depth at failure and C_0 on the initial cracks and their sizes. Typical values for C_0 range from 0.025 to 0.1 for sand-asphalt and asphaltic concrete mixes, respectively.

The value of n is the slope of the line representing the crack growth rate, dc/dN , plotted against the stress intensity factor. The slope of this line increases as the elastic modulus of the foundation increases. An illustration of the relationship is shown in Figure 9.

By determining the parameters C_0 , C_f , and n, through a fatigue test, the fatigue life of a bituminous mix may be predicted for any load through the use of equations 6 and 7.

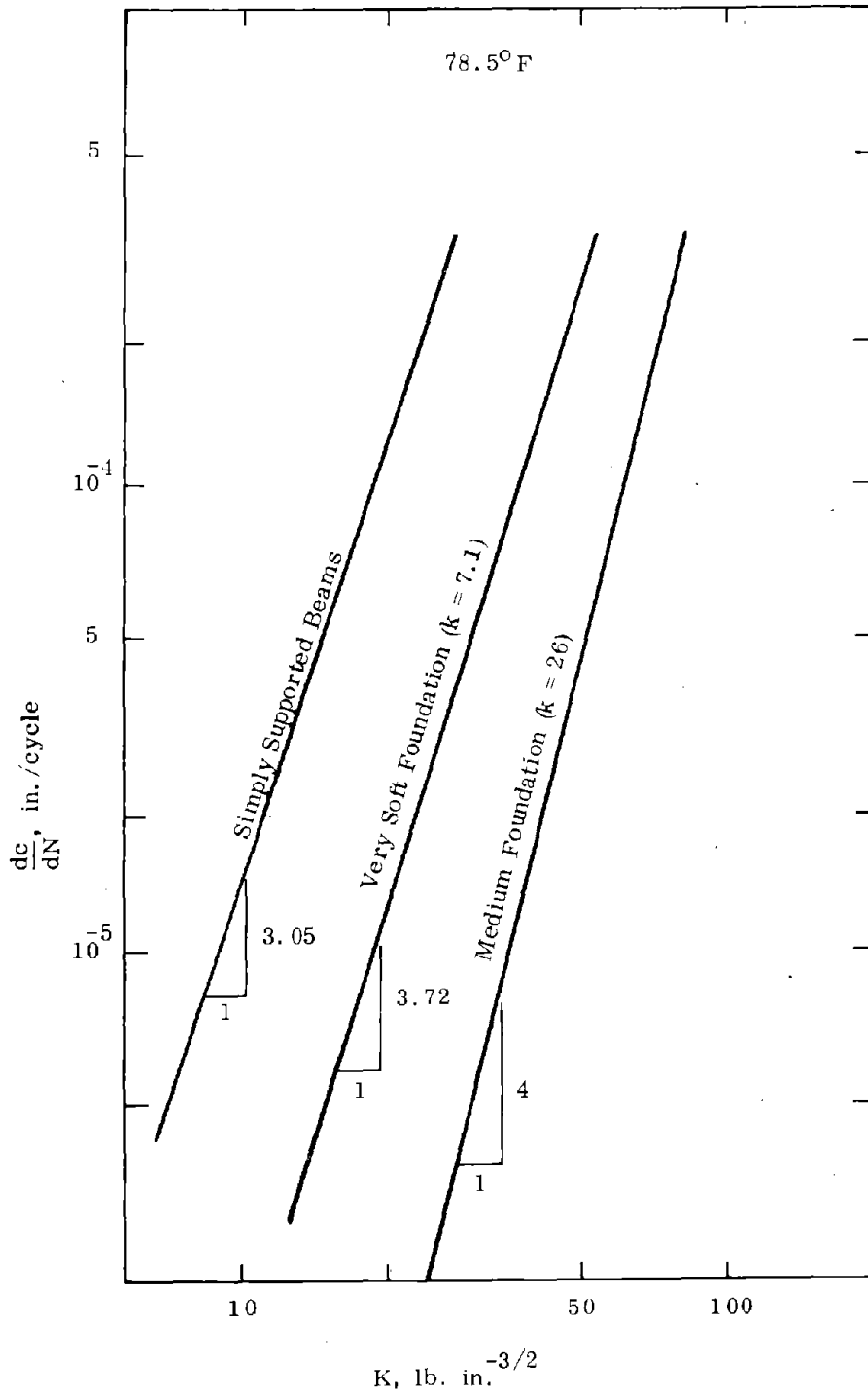


Figure 9. Comparison of rates of crack propagation in simply supported beams and beams on elastic foundation. (17)
 1 in. = 2.54 cm; 1 lb. in. = 0.113 mN).

Plate Specimen

A fatigue testing machine capable of testing a plate specimen under a sinusoidal load was developed by Jiminez.⁽¹⁴⁾ This machine, called the deflectometer flexure fatigue tester, is capable of testing both laboratory specimens and road samples. A special vibratory kneading compactor is used to make laboratory specimens 18 in. (45.7 cm) in diameter and between 1 in. (2.5 cm) and 5 in. (12.7 cm) thick.

Equipment

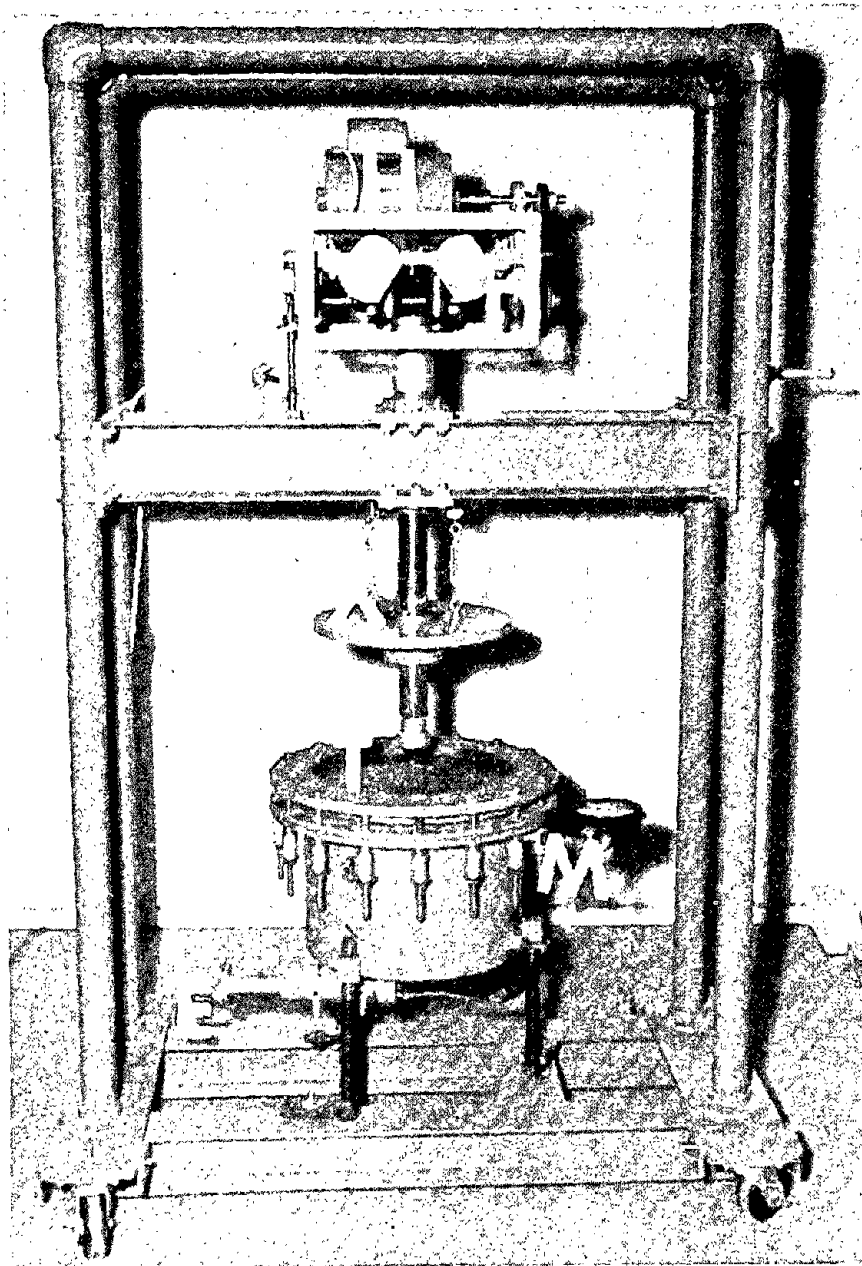
The test specimen is supported by the reaction unit shown in Figure 10. This unit consists of a metal chamber that contains oil and air and is covered by an airtight rubber membrane. The membrane provides support for the specimen by entering a controlled amount of air pressure into the chamber. The specimen is held in place along its circumference by a steel ring having an inside diameter of 14 in. (35.6 cm) and an outside diameter of 20 in. (50.8 cm). This ring is secured to the chamber by 16 bolt-spring units.

The specimen is loaded in the center using a load disk with a contact area 5 in.² (32.3 sq. cm). The loading system is designed to allow it to move with the deflection of the specimen. The total load applied to the specimen is fixed and comprises a 150-lb. (68.0 kg) dead load and a 130-lb. (59.0 kg) live load. The dead load is the weight of the motor and loading system acting on the specimen. The live load is applied in a sinusoidal form using counter-rotating eccentric masses. The live loading is applied at a frequency of 12 repetitions per second.

Data Collection

The deflectometer flexure fatigue tester uses only the controlled stress mode of testing. The data collected are limited to the number of loadings, support pressure, and deflection. The deflection is measured by dial extensometer gages which are read by the operator. The number of loadings is recorded by a counter driven by the shaft rotating the eccentric masses.

The initial deflection reading is taken after the first 1,000 loadings. The specimen reaches failure when a running plot of the deflections vs. number of loadings deviates from a straight line.



- A — Reaction unit supporting 18" diameter specimen
- D — Loading system of counter rotating eccentric masses
- E — Displacement pump
- H — Electric motor for loading system
- M — Pressure gage for reaction unit
- T — Specimen
- X — Ballast for dead load

Figure 10. Deflectometer flexure fatigue tester. ⁽¹⁴⁾

Analytical Methods

The deflectometer type of fatigue testing equipment is extremely limited because it is capable of using only a controlled stress mode of testing with a sinusoidal load pattern. Since only one loading can be placed on the specimen, a strain vs. fatigue life relationship cannot be developed. This test can give the data necessary for computing the dynamic modulus of elasticity using the total load, twice the repeated live load, the repeated midpoint deflection, and a support pressure of 1.5 psi (10.4 KPa).

Cylindrical Specimen

The use of cylindrical specimens in fatigue testing has been limited. Moore and Kennedy used a specimen 4 in. (10.2 cm) in diameter and 2 in. (5.1 cm) in height.⁽²²⁾

The testing equipment is the closed-loop electrohydraulic loading system with an indirect tensile loading head shown in Figure 11. The recording equipment is a light-beam oscillograph that records both the load and its corresponding deformation. The load is controlled by a strain gage type load cell and has a frequency of one cycle per second.

The use of this equipment has been directed toward testing and evaluating the effect of various material properties on fatigue life. The test data have been used in a multiple regression analysis to develop equations for estimating fatigue life. Variables such as asphalt content, asphalt cement type, mixing temperature, compaction temperature, and stress levels have been used in the regression analysis.

Trapezoidal Specimen

The trapezoidal specimens originally were used by Bazin and Saunier⁽¹⁵⁾ and then later by Coffman et al.⁽¹⁶⁾ The specimens can be either laboratory fabricated or taken from the pavement. They are then sawed into a trapezoidal shape.

The testing equipment consists of a closed-loop electrohydraulic system. The specimen is firmly connected to steel plates as shown in Figure 12, then bolted to the loading frame as shown in Figure 13. It is loaded through a pretensioned wire attached through the top plate. The C-shaped steel frame is attached to the closed-loop electrohydraulic system.

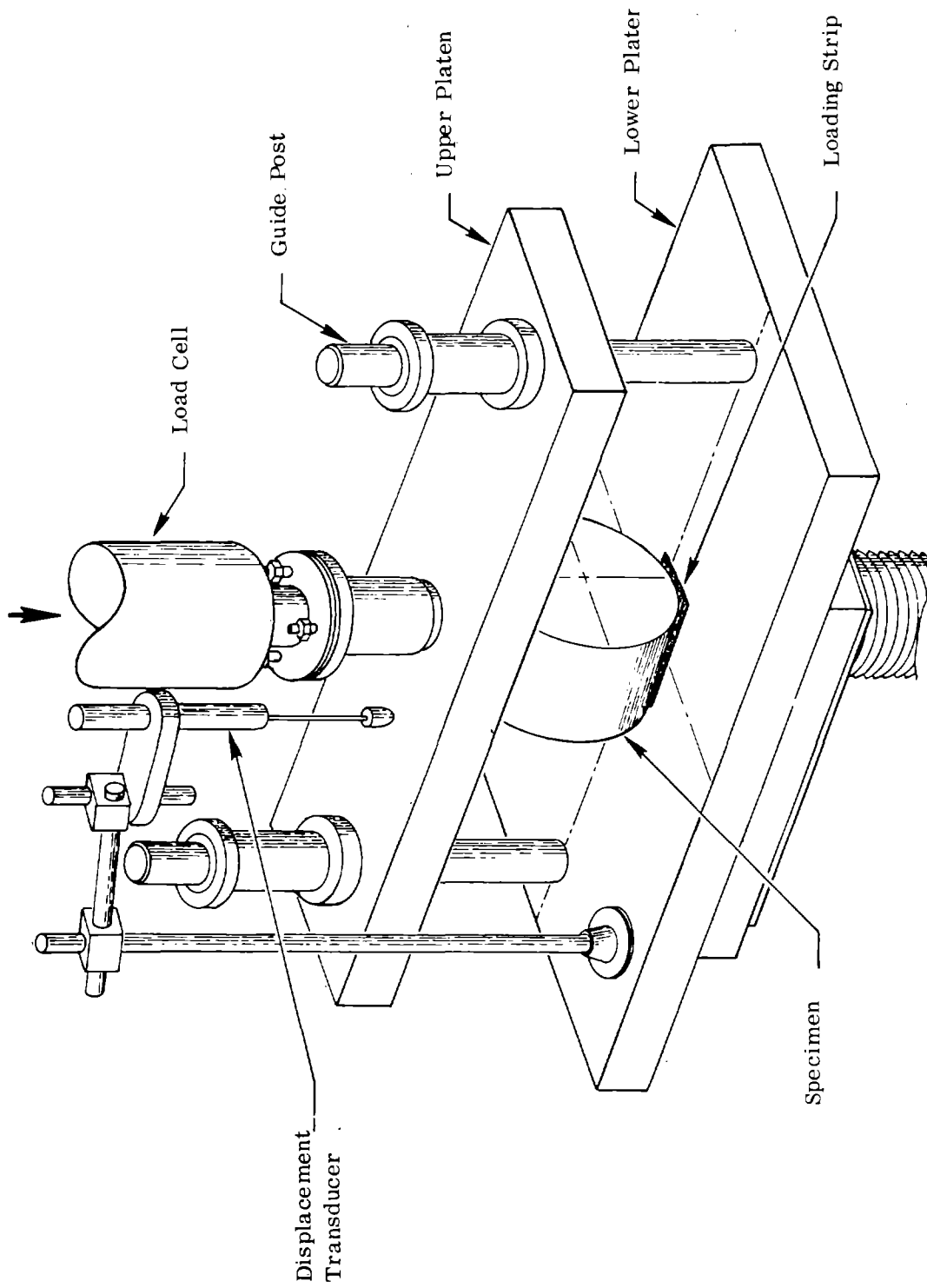


Figure 11. Loading head with rigid parallel platens. (23)

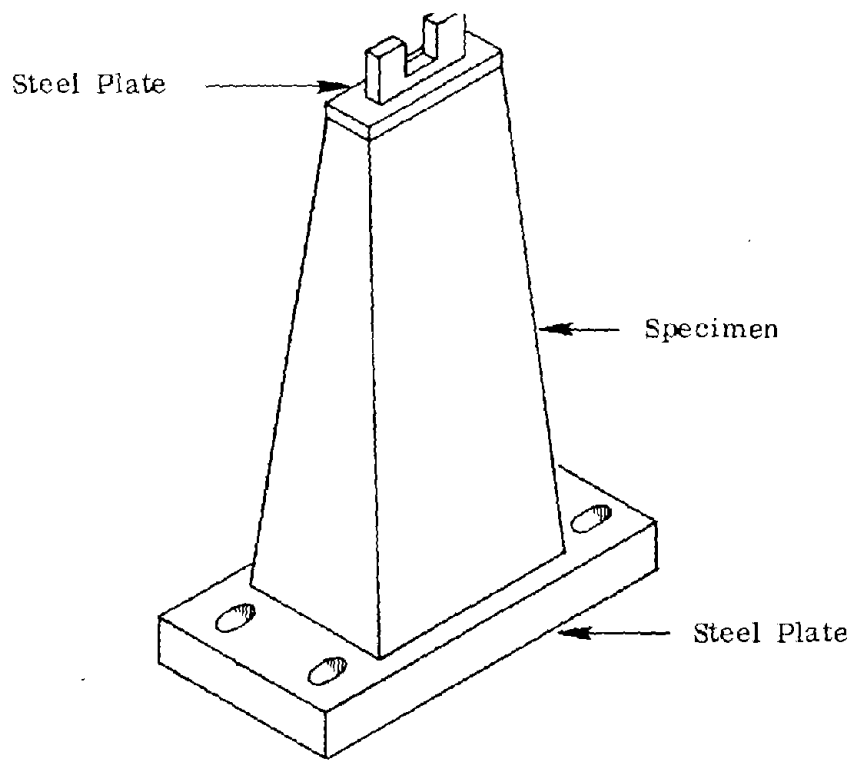


Figure 12. Trapezoidal specimen. (16)

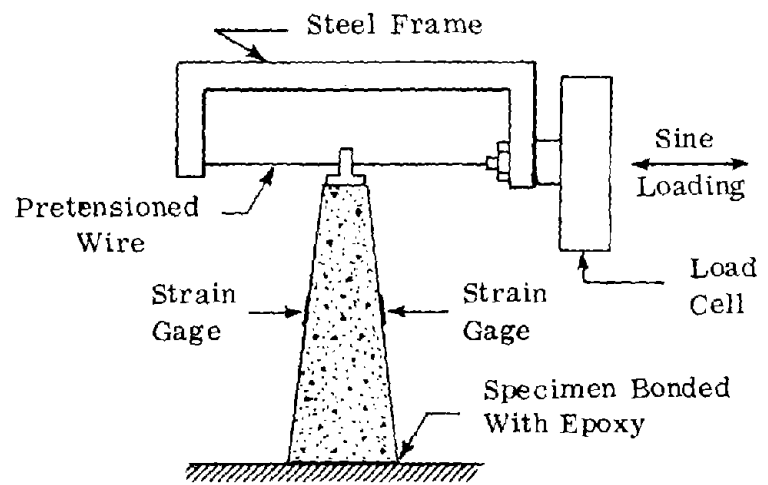


Figure 13. Trapezoidal specimen loading apparatus. (16)

The specimen is loaded under a controlled stress mode and a sinusoidal load pattern. Failure is monitored by using lines of conductive paint placed on the sloping faces of the trapezoid and connected to a galvanometer which detects the cracks and their magnitudes. The deflections are measured with a LVDT and recorded on an oscillograph.

From the data recorded, the relationship for predicting fatigue life by the least squares regression analysis, $N = K(1/\epsilon)^n$, mentioned previously can be developed.

Pell Specimen

A fatigue test method using a specimen of the shape shown in Figure 14 was developed by Pell.^(8,24) This specimen is unique because the diameter of its "neck" varies from 3 1/2 in. (8.9 cm) to 2 1/2 in. (6.4 cm). The metal specimen end fittings, shown in Figure 14, are placed on the specimen during its fabrication. The specimen is clamped in a vertical position using the chuck of the rotating type cantilever fatigue machine.

The loading is applied to the top bearings by a loading stirrup connected to weights, which places a constant bending stress on the specimen. The specimen is then rotated by the main shaft connected to the base of the testing machine. The rotation subjects the specimen to a sinusoidal loading. The maximum bending stress is developed in the neck of the specimen, and when fracture occurs the specimen will break completely in half. The motor driving the rotating shaft is a variable speed D.C. electric motor of 1.5 HP (1 HP = 750 W) capable of varying the loading frequency from 80 to 3,000 cycles per minute. The loading frequency used by Pell was 1,000 cycles per minute.

Pell used a controlled temperature bath of alcohol and water that enabled tests to be performed with temperatures controlled to an accuracy of $\pm 0.2^\circ\text{C}$ over a range of -5°C to $+30^\circ\text{C}$.

The data recorded during the test are the load applied to the specimen and the deflection of the specimen at the loading head. The deflection can be determined by measuring the movement of the loading wire from its initial unloaded position.

Again, the least squares regression analysis is used to relate strain to fatigue life by the equation $N = K(1/\epsilon)^n$.

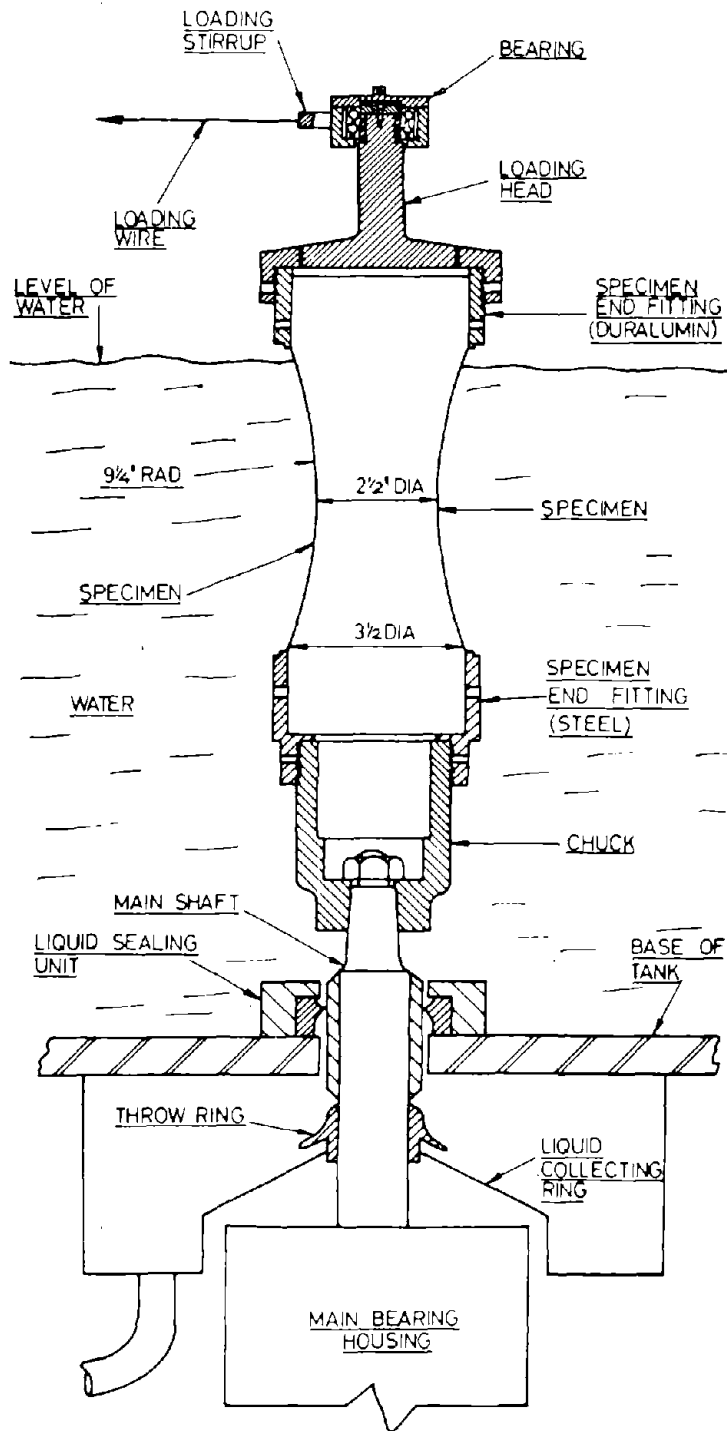


Figure 14. Pell Testing Apparatus. (24)
 (1 in. - 2.54 cm)

Evaluation of Test Methods

In evaluating the test methods, each was examined against the following criteria.

1. The capability of the method to perform both controlled stress and controlled strain modes of testing;
2. the capability of applying both simple and compound loadings;
3. the capability of varying the frequency of loading;
4. the capability of using various load patterns; and
5. the difficulty of fabricating the specimens.

Beam Specimen

The test methods used to test beam specimens — the air or pneumatic pressure system and the electrohydraulic systems — both use similar repeated-flexure apparatus. The control and loading mechanisms are also quite similar; each being capable of using controlled stress and controlled strain and simple and compound loading, and of varying the frequency of loading as necessary. The distinguishing characteristic is that the electrohydraulic system is capable of using any load pattern, while the pneumatic pressure system is limited to a block pattern. The fabrication of the specimen is relatively simple using the procedure outlined by ASTM Designation D3202-73 for the California Kneading Compactor.

Plate Specimen

The deflectometer test, used with a plate specimen, is capable of applying only a controlled stress mode. The testing mechanism applies a simple loading of constant magnitude and frequency. Since the magnitude and frequency are constant, the curve for predicting fatigue life cannot be developed. This test method is further limited by its inability to apply any load pattern other than sinusoidal. The fabrication of the specimens is difficult because of the size of the specimens and the type of compaction equipment necessary.

Cylindrical Specimen

This method of fatigue testing cylindrical specimens uses a 4 in. (10.2 cm) diameter specimen made under standard Marshall compaction procedures. The testing mechanism can place only compressive loads on the specimen and in a sinusoidal pattern. The test method is a controlled stress using simple loading. The frequency of loading can be varied, with high frequencies most often being used. Since there is no tensile force applied to the specimen, which would represent the elastic rebound of the pavement, the laboratory fatigue life values may not be comparable to roadway fatigue life values.

Trapezoidal Specimen

The trapezoidal specimen uses the electrohydraulic load and control system discussed under beam specimens. The testing mechanism is capable of performing controlled stress and controlled strain tests, applying simple and compound loadings, varying the frequency of loading, and using various load patterns. The major drawback of the test method is the difficulty of specimen fabrication and the placement of the specimen in the loading apparatus.

Pell Specimen

The Pell specimen is tested using the rotating cantilever machine. This machine is capable of producing a controlled stress mode under a sinusoidal loading pattern. The specimen can be tested under simple or compound loadings and at different frequencies. However, the odd shape of the specimen makes fabrication difficult.

Summary

In summary, the test method showing the greatest overall capability in fatigue testing is the electrohydraulic control system using a 3 in. x 3 in. x 15 in. (7.6 cm x 7.6 cm x 38.1 cm) beam specimen. This method is capable of performing all modes of testing desired.

CHAPTER III. LITERATURE REVIEW OF SIMPLE TEST METHODS

Purpose and Scope

This literature review examined simple test methods that possibly could be used to delineate the fatigue properties of asphaltic concrete. Because fatigue failure usually is caused by repetitions of tensile stresses and strains, it is logical that the simple test should provide for testing in a tensile mode. The findings from the literature search which follow concentrate on but are not limited to the items listed below.

1. Tensile testing.
2. Simplicity of sample preparation.
3. Utilization of laboratory and pavement samples.
4. Sensitivity of test method to —
 - A. aggregate shape, texture, and gradation;
 - B. mineral filler;
 - C. test temperature;
 - D. rate of deformation; and
 - E. asphalt content and grade.
5. Predictive capability of fatigue behavior.

Methods of Testing

Indirect Tensile Test

History of Development

The indirect tensile test was developed in 1953 by Carneiro and Barcellos of Brazil and Akazawa of Japan, working independently. It was developed for use in testing cylindrical concrete specimens by applying compressive loads along a diametrical plane through two opposite loading heads. This type of loading produces a relatively uniform stress which acts perpendicular to the applied load plane, and the specimen usually fails by splitting along the loaded plane.⁽²⁵⁾

Timoshenko and Goodier developed the theory showing stresses present in a circular disk when two equal and opposite forces act along the diametrical plane.⁽²⁶⁾ Figure 15

shows the stresses developed in a circular disk when the forces are applied.

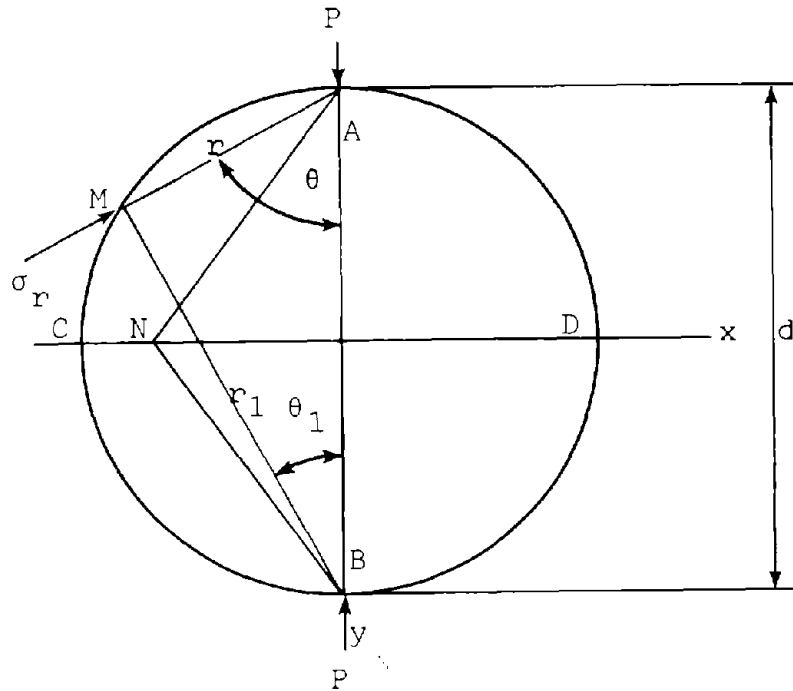


Figure 15. Stresses in a circular disk. (26)

The thickness of the plate is unity and the load, P , is assumed to be distributed uniformly over the unit thickness. Considering a situation where the disk is loaded only from the top, the stress, σ_r , at a point M can be determined by simple radial stress distribution. This simple compression stress is in the radial direction and can be computed by

$$\sigma_r = - \frac{2P}{\pi} \frac{\cos \theta}{r} \quad (9)$$

When two equal and opposite forces act on the disk, each force produces a simple radial stress distribution. Again using a point M , it would have two compressive forces acting on it in the directions r and r_1 . These forces are equal to

$$\frac{2P}{\pi} \frac{\cos \theta}{r} \quad \text{for } r \quad \text{and} \quad \frac{2P}{\pi} \frac{\cos \theta_1}{r_1} \quad \text{for } r_1.$$

Since r and r_1 are perpendicular to each other, it can be shown that

$$\frac{\cos \theta}{r} = \frac{\cos \theta}{r_1} = \frac{1}{d},$$

where d is the diameter of the disk. It can now be seen that the compressive forces acting in the direction of r and r_1 are equal and of magnitude

$$\frac{2P}{\pi d}$$

Timoshenko used this theory to develop equations for σ_x and σ_y along the horizontal diametrical axis. Similar relations for stresses in the indirect tensile test can be derived with equations developed by Frocht⁽²⁷⁾ using a system of rectangular stress coordinates.

Frocht used the theory of Timoshenko in his development of the equations. His equation for simple radial compressive stress was the same as Timoshenko's, except that he did not assume the thickness to be unity. Frocht's equation for σ_r is

$$\sigma_r = - \frac{2P}{\pi t} \frac{\cos \theta}{r} \quad (10)$$

where t is the thickness of the disk.

Using this equation for simple radial compressive stress and the system of rectangular stress components shown in Figure 16, Frocht developed the equations for stresses in the x and y directions at any point to be

$$\sigma_x = \sigma_r' \sin^2 \theta_1 + \sigma_r'' \sin^2 \theta_2 + \frac{2P}{\pi t d} \quad (11)$$

$$\sigma_y = \sigma_r' \cos^2 \theta_1 + \sigma_r'' \cos^2 \theta_2 + \frac{2P}{\pi t d} \quad (12)$$

By the substitution of various expressions into the equations, they can be simplified into the form

$$\sigma_x = \frac{-2P}{\pi t} \left(\frac{(R-y)x^2}{r_1^4} + \frac{(R+y)x^2}{r_2^4} - \frac{1}{d} \right) \quad (13)$$

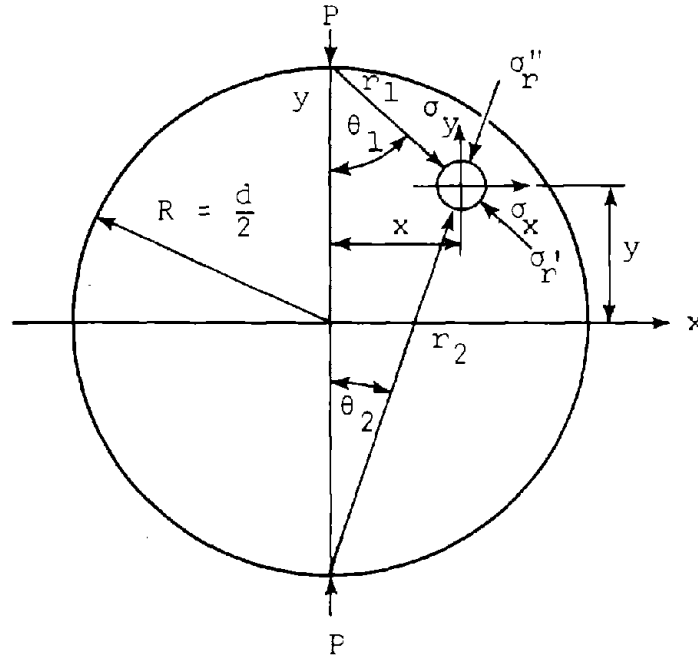


Figure 16. Notation for rectangular stress components. (27)

$$\sigma_y = \frac{-2P}{\pi t} \left(\frac{(R - y)^3}{r_1^4} + \frac{(R + y)^3}{r_2^4} - \frac{1}{d} \right) \quad (14)$$

The stresses developed on the horizontal diametrical plane by use of the above equations are shown in Figure 17. The equations for these stresses are

$$\sigma_x = \frac{2P}{\pi t d} \left(\frac{d^2 - 4x^2}{d^2 + 4x^2} \right)^2 \quad (15)$$

$$\sigma_y = \frac{-2P}{\pi t d} \left(\frac{4d^4}{(d^2 + 4x^2)^2} - 1 \right) \quad (16)$$

with σ_x being a tensile stress and σ_y being compressive.

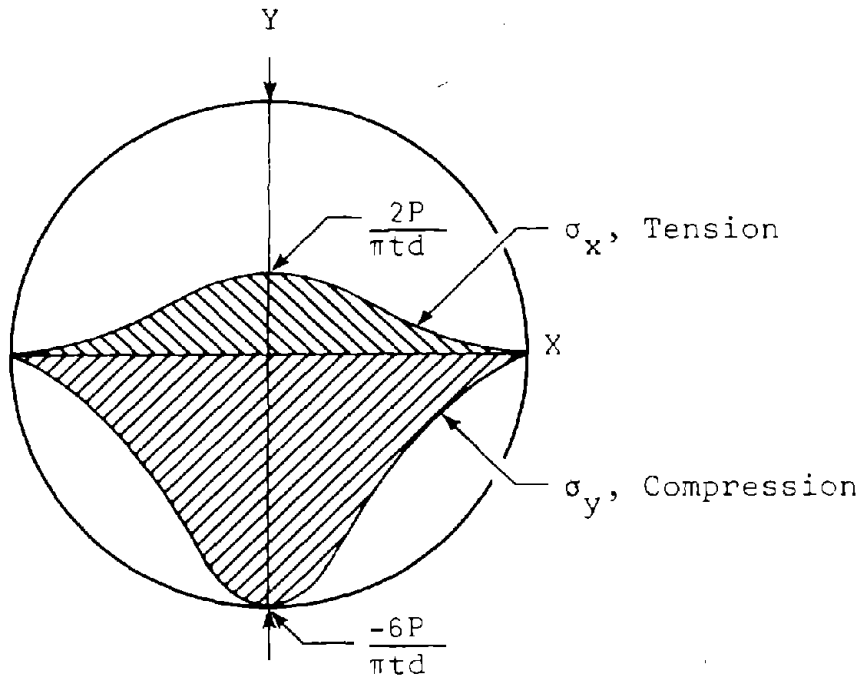


Figure 17. Stress distributions on x-axis. (25)

The stress distributions determined along the vertical y-axis through the use of equations 13 and 14 are shown in Figure 18. These equations can be simplified to be (25)

$$\sigma_x = \frac{2P}{\pi td} \quad (17)$$

$$\sigma_y = \frac{-2P}{\pi td} \left(\frac{2}{d - 2y} + \frac{2}{d + 2y} - \frac{1}{d} \right) \quad (18)$$

Variations from Theory

The theory that has been developed will give the exact solution for an idealized case. However, in testing asphalt, theoretical conditions will never be attained. Assumptions that were made during the development of the theory are: (25)

1. Homogeneity of asphaltic concrete,
2. Hooke's law is valid for asphaltic concrete,
and
3. point loading.

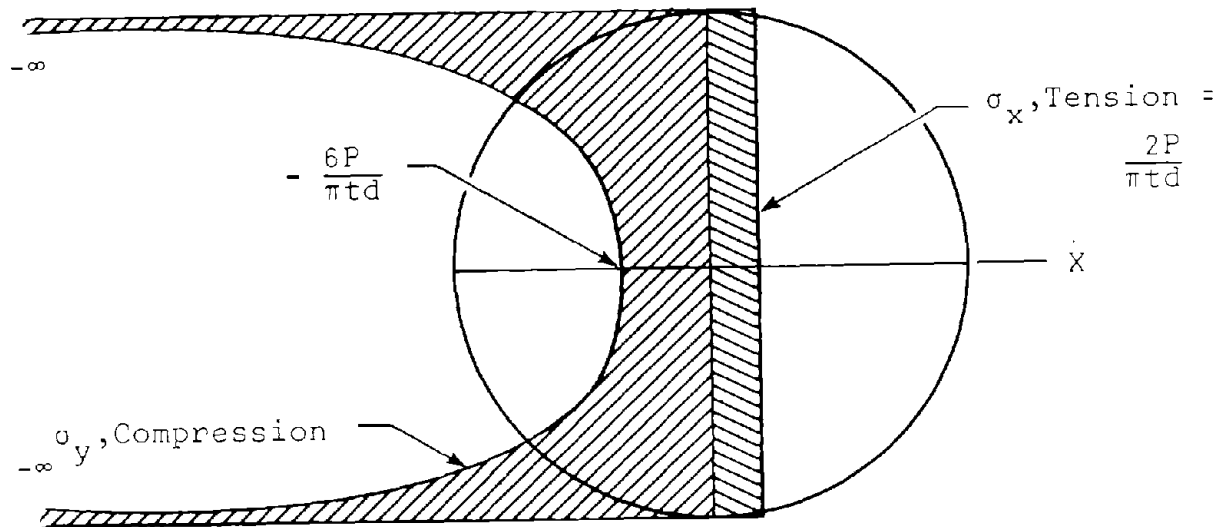


Figure 18. Stress distributions on y-axis. (25)

Since these assumptions are not valid for the indirect tensile testing of asphaltic concrete the variations have to be considered.

Bituminous materials are heterogeneous, which fact causes a less than ideal condition. The heterogeneity⁽²⁵⁾ of the material affects the stress distributions, however, the degree to which they do so has not been determined. Tests have shown that the heterogeneity of the material definitely affects the stress distributions, although the influence has been so small that the tests have been considered satisfactory for use.

Frocht's theory considers the material to be linearly elastic. This theory does not hold for bituminous materials tested at slow loading rates because they show a viscoelastic behavior. Heukelom and Klomp⁽²⁸⁾ have stated that Van der Poel defined the stiffness modulus of a viscoelastic material as time and temperature dependent. This is shown in Figure 19, which illustrates the effects of slow and fast loading rates.

When the asphalt is subjected to a slow loading rate, it behaves as a viscous material and flows under a constant load.⁽²⁹⁾ As the loading rate is increased, the material becomes more elastic, and is almost completely elastic at very fast loading rates.

When using slow loading rates in the indirect tensile test, the modulus of elasticity increases with increased

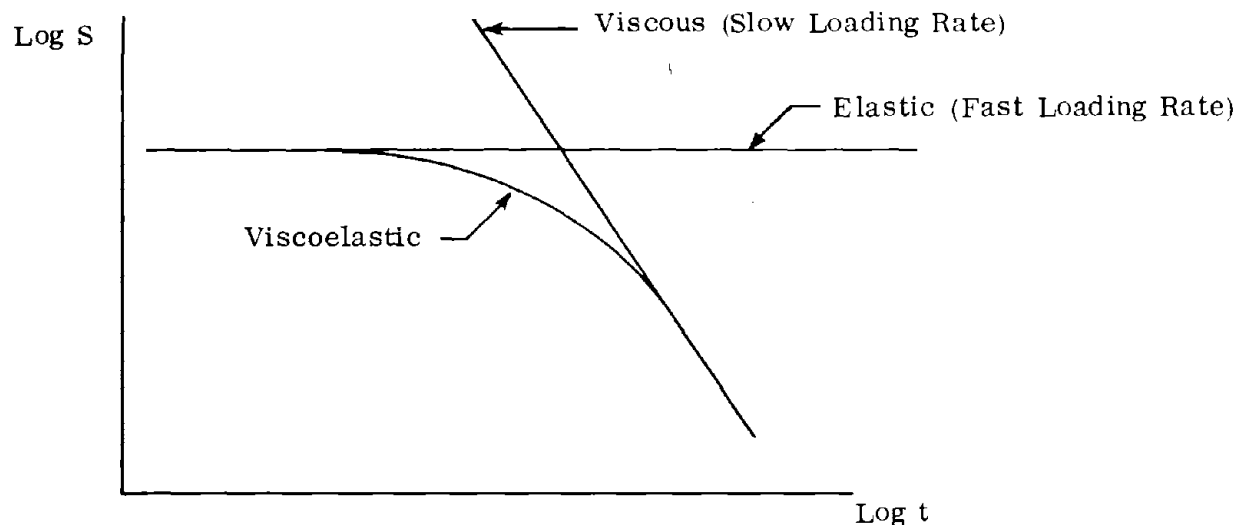


Figure 19. Stiffness modulus for asphalt as a function of the loading time. (28)

loading rates. The University of Texas⁽²⁹⁾ performed tests on asphalt specimens by varying the loading rates and recording the effect on the specimens. It was found that loading rates ranging from 0.05 in./min. (1.2 mm/min.) to 0.5 in./min. (12.7 mm/min.) caused a fairly fast increase in the modulus of elasticity as the rate was increased. For rates of 0.5 in./min. (12.7 mm/min.) up to 6 in./min. (152.4 mm/min.), the modulus of elasticity increased at a much slower degree with an increased loading rate.

The development of the indirect tensile theory assumed that bituminous materials obey Hooke's law; that is, that stress is proportional to strain.⁽²⁵⁾ However, this is not true, because the modulus of elasticity will decrease with increased stress. Wright felt that because of the non-elastic nature of the material, the more highly stressed parts of the specimen would be relieved by throwing the stress onto elements on which the stress was lower.⁽³⁰⁾ This in turn would cause an increase in the load required to break the specimen. Hudson and Kennedy felt that so long as the specimens failed in tension, the results obtained from the indirect tensile test were satisfactory for use.⁽²⁵⁾ However, for less brittle materials, such as asphaltic concrete in a warm state, the test did not give satisfactory results because the specimens failed in compression.

Frocht's theory also assumed that the loading was a point loading not spread evenly over a 1/2 in. (12.7 mm)

wide loading strip as is the case in the indirect tensile test. The stress components developed by the loading strips are shown in Figure 20.

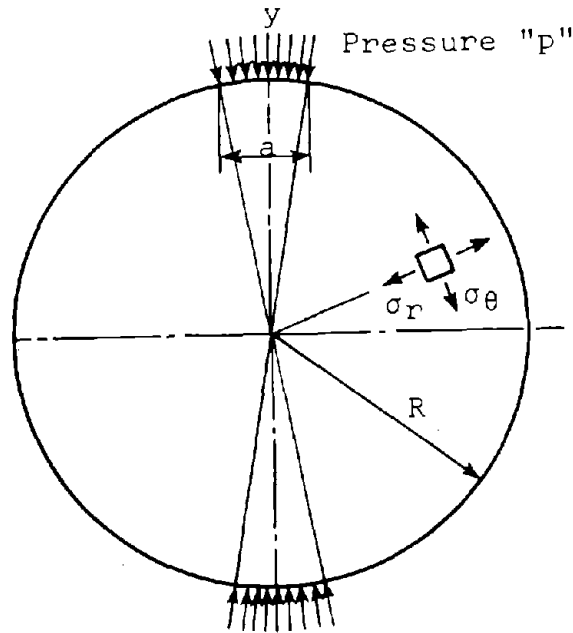


Figure 20. Stress components in specimen using loading strips.(29)

Hondros developed equations for the stresses along the principal diameters resulting from the use of loading strips.(31) He found that the stress distributions did vary from those caused by a point loading; however, the stresses at the center of the disk were the same for both point loading and the loading strips. The stress distributions produced when the loading heads are used are shown in Figure 21.(29) It can be seen that the σ_y stress goes from tension in the center to compression as it approaches the loading strips. Hondros states that the compressive stress along the y -axis is approximately twice that of the tensile stress.(31) Therefore, since asphalt can withstand considerable more compressive stress than tensile stress, the specimen will fail in tension.

In a report by Hadley, Hudson, and Kennedy, the effects of varying the properties of bituminous concrete on the indirect tensile strength and modulus of elasticity were discussed.(32) The values of tensile strength and modulus of elasticity were determined by using a regression analysis

by the gradation of the aggregate. For the fine materials the optimum asphalt content increased with increased compaction temperatures, whereas for the coarser materials the optimum asphalt content decreased as the compaction temperature increased. For the medium graded mixes the optimum asphalt content stayed nearly constant as the compaction temperature increased.

Equipment

The basic equipment needed for performing the indirect tensile test is a loading apparatus capable of applying compressive loads at a desired deformation rate,⁽²³⁾ the loading strips, and a means of measuring the applied load and the horizontal deformation of the specimen.⁽²³⁾

The loading apparatus should be capable of applying enough compressive load to cause the specimen to fail and also be capable of applying the load at a uniform rate.⁽²³⁾ There is no standard loading rate, although the rates most used are 1-inch per minute (25 mm/min.) or 2-inches per minute (50 mm/min.), depending upon the stiffness of the material. For stiff materials, slow loading rates are used.

The loading strips are generally 1/2 in. (12.7 mm) wide and have a curved face.⁽²³⁾ When loading the specimen it is necessary to keep the strips as nearly parallel as possible so as to eliminate any bending stresses. A guided loading device such as that shown in Figure 11 is used to keep the strips parallel. This device has upper and lower plates to which the strips are fixed. The lower plate has two guide rods which allow the upper plate to slide vertically and remain parallel to the lower plate.

The applied load can be measured by using a proving ring to indicate the compressive force if only the strength data are necessary.⁽³³⁾ The compressive force and compressive deformation can be recorded for each test by using instrumentation similar to that used for Marshall stability and flow tests. If simultaneous load and deformation data are desired, then a method of recording the load is necessary.

The horizontal deformation can be recorded by using two LVDT's or a specially designed transducer⁽³³⁾ with strain gages mounted on cantilever aluminum arms. Strip chart recorders should be used to record these measurements.

Test Procedure

The test procedure is outlined below. (23)

1. "Determine the height and diameter of the test specimen.
2. Calibrate the horizontal deformation device.
3. Center test specimen on loading head.
4. Bring upper platen of die set into light contact with test specimen. Monitor load on the x-y platen that is recording load versus vertical deformation.
5. Place horizontal deformation device in position with arms in light contact with specimen and lock arms in position.
6. Load specimen at a constant deformation rate and record load, vertical deformation, and horizontal deformation."

Generally, a Marshall specimen is used because its fabrication is quite simple and requires no special equipment. (33)

The maximum tensile stress at the center of the specimen may be determined by equation 16. For a 4-in. (101.6 mm) specimen this equation is

$$\sigma_{IT} = \frac{0.156 P_{fail}}{t} \quad (19)$$

Poisson's ratio, (32) is determined as

$$\nu = \frac{\int_{-r}^r \sigma_{ry} + R \int_{-r}^r \sigma_{rx}}{R \int_{-r}^r \sigma_{\theta x} + \int_{-r}^r \sigma_{\theta y}} \quad (20)$$

where

$$\int_{-r}^r \sigma_{ry} \text{ and } \int_{-r}^r \sigma_{rx} = \text{integration of radial stresses in the y and x directions, respectively}$$

$\int_{-r}^r \sigma_{\theta x}$ and $\int_{-r}^r \sigma_{\theta y}$ = integration of radial stresses in the x and y directions, respectively

$R = \frac{y}{x}$ is the least squares line of best fit between the vertical deformation, y, and the corresponding horizontal deformation, x, up to the load, P.

For a 4-in. (101.6 mm) specimen, Poisson's ratio can be simplified to

$$\nu = \frac{0.0673R - 0.8954}{-0.2494R - 0.0156} \quad (21)$$

The modulus of elasticity, E, can be determined by

$$E = \frac{P}{x_T} \left[\int_{-r}^r \frac{\sigma_{rx}}{P} \nu \int_{-r}^r \frac{\sigma_{\theta x}}{P} \right] \quad (22)$$

where $\frac{P}{x_T}$ is the least squares line of best fit between the load, P, and the total horizontal deformation, x, for loads up to 50% of the load, P_{max} , at which the first break point occurs in the load deflection curve (see Figure 22); and

$\int_{-r}^r \frac{\sigma_{rx}}{P}$ and $\int_{-r}^r \frac{\sigma_{\theta x}}{P}$ are the integration of the unit stresses σ_{rx} and $\sigma_{\theta x}$.

When testing a 4-in. (101.6 mm) specimen, the modulus of elasticity equation is reduced to

$$E = \frac{S_H}{t} (0.9976\nu + 0.2692) \quad (23)$$

where S_H is the horizontal tangent modulus $\frac{P}{x_t}$.

Possible Correlation of Indirect Tensile Test Data to Fatigue Test Data

In a study by Maupin of the Virginia Highway and Transportation Research Council,⁽³³⁾ the emphasis was on developing

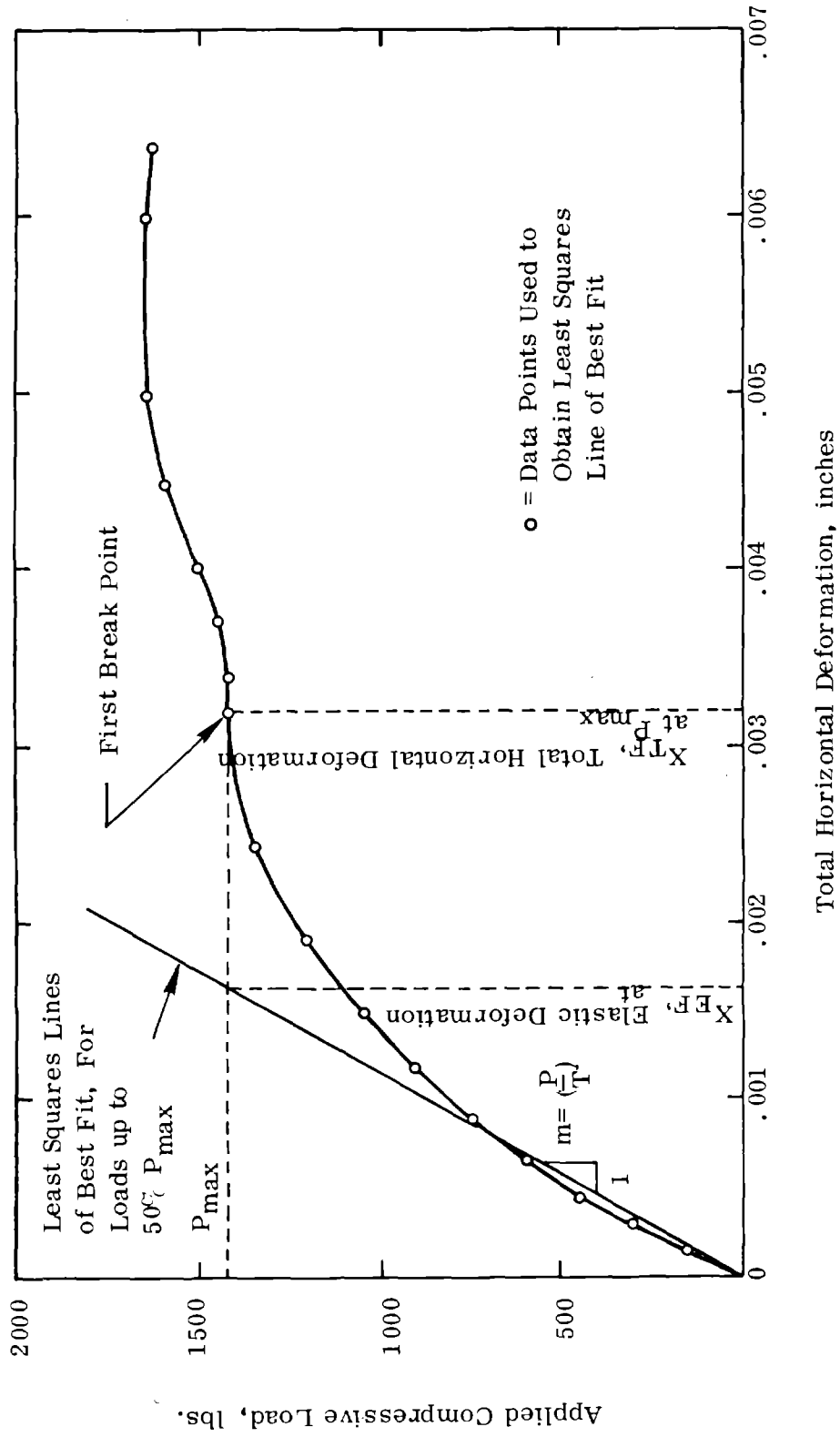


Figure 22. Generalized characterization of load-horizontal deformation data. (32) (1 lb. = 4.45 N; 1 in. = 25400 μ m).

a correlation between the indirect tensile stiffness and the fatigue life of specimens tested under the constant strain mode.

Maupin used the data from the indirect tensile test to plot a typical stress-strain curve. This curve was linear until about three-quarters of the failure stress was reached, and thereafter the strain increased at a greater rate than did the stress. The stiffness value used by Maupin was the stiffness at three-quarters of the tensile failure stress, which is defined by $S_{3/4} = 3/4 \sigma_{TF} / \epsilon_{3/4}$, where σ_{TF} is the tensile stress at failure and $\epsilon_{3/4}$ is the tensile strain at three-quarters failure stress.

The fatigue tests showed that stiffer mixes had shorter lives than flexible mixes when tested in the constant strain mode. Therefore, by being able to determine the stiffness of the asphaltic concrete from an indirect tensile test, it may be possible to determine fatigue life.

Marais⁽³⁴⁾ reported a tentative mix design of gap-graded bituminous surfacings in which the indirect tensile strength is used as a criterion for fatigue design. A strong correlation was developed between the indirect tensile strength and the service life for several mixes. The tentative mix design limits the maximum indirect tensile strength at 40°C (104°F) to 680 kn/m² (99 psi). Marais' work strongly supports the idea of using the indirect tensile test for fatigue design.

Resilient Modulus Indirect Tensile Test

A test method developed by Schmidt of the Chevron Research Company uses a loading apparatus capable of applying a light pulsating load across the vertical diameter of a Marshall specimen.⁽³⁵⁾ This load causes deformation across the horizontal diameter, which is measured by LVDT's.

The theory used in developing this test is the same as that used in the standard indirect tensile test, which uses a static loading. The major difference between the two tests is that Schmidt's test is nondestructive and obtains its resilient modulus by using a short duration dynamic load. The corresponding horizontal deformation caused by the vertical load can be recorded and the resilient modulus thus can be calculated. The equation used by Schmidt to determine the resilient modulus is

$$E = P (\nu + 0.2734) / t\Delta \quad (24)$$

where

P = dynamic load, lbs. (1 lb. = 4.45 N)

ν = Poisson's ratio

t = thickness of specimen, in. (1 in. = .0254 m)

Δ = total horizontal deformation, in. (1 in. = .0254 m)

This equation is the same as the one used for a static load, except for a minor deviation in the constants used.

The equipment used by Schmidt consists of an air supply control, a pneumatic load applicator, twin LVDT's, a recorder or readout, an electronic timing device, and a frame for holding the specimen. The loading apparatus is the pneumatic load applicator, which receives air pulses from an electrically activated solenoid. The pulses are applied every three seconds and are one-tenth of a second in duration.

Horizontal LVDT's are mounted to the specimen to measure its horizontal movement. This value is recorded on a strip chart.

Since Schmidt's dynamic loading better approximates fatigue test loading than does the standard indirect tensile test, it could possibly offer a better correlation to fatigue life. There has been no attempt at such a correlation but the possibility might be worth investigating.

Double Punch Test

The double punch test was developed by W. F. Chen as a method for determining the tensile strength of concrete.⁽³⁶⁾ Later Chen and Fang expanded the use of the test to determine the tensile strength of cohesive soils.⁽³⁷⁾ On the basis of the work of Chen and Fang, Jimenez decided that the double punch test was a promising method for testing asphaltic concrete.⁽³⁸⁾ His initial tests were made to measure the stripping or debonding of asphalt from aggregate.

The double punch test is performed by centrally loading a cylindrical specimen on the top and bottom surfaces with cylindrical steel punches.⁽³⁸⁾ A standard Marshall specimen is suitable for the test. The loading by the punches causes cones to be developed in the specimen as shown in Figure 23. The penetration of the cores causes the specimen to split along the weakest radial plane.

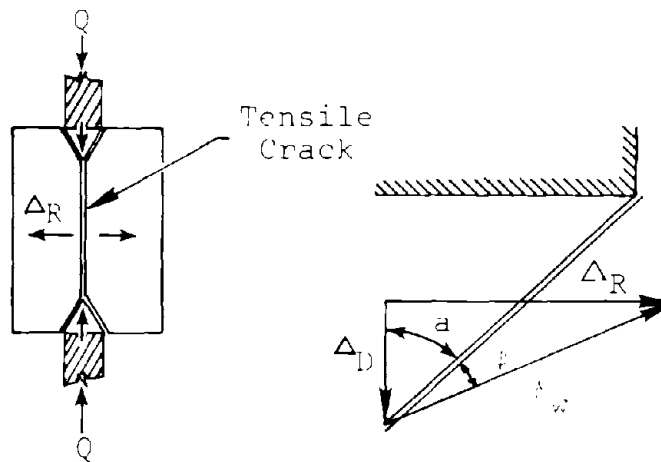


Figure 23. Failure mechanism of double punch test.⁽³⁸⁾

The double punch test has been compared to the indirect tensile test for repeatability and the relationship between the average stresses obtained for two aggregate gradations.⁽³⁸⁾ It has proved to have better repeatability than the indirect tensile test, and the average stresses obtained with it are nearly equal to those obtained from the indirect tensile test. Jimenez feels that the double punch test is simpler to perform, and the stress analysis does not have to be adjusted for the area of the loaded surface.

The test is performed by centering the specimen in the bottom punch.⁽³⁸⁾ The punches are 1-in. (25.4 mm) in diameter steel rods perfectly aligned one over the other. The upper punch is lowered until contact is made with the specimen. The specimen is then loaded at a rate of 1.0 inch (25 mm) per minute) until failure.

The tensile strength⁽³⁸⁾ is computed by:

$$\sigma_T = \frac{P}{\pi (1.2 bh - a^2)} \quad (25)$$

where:

σ_T = tensile stress, psi (Pa)

P = maximum load, lb. (N)

a = radius of punch, in. (mm)

b = radius of specimen, in. (mm)

h = height of specimen, in. (m)

Jimenez has developed a method of computing the modulus of elasticity. By use of the measured values of mid-height radial displacements and vertical load and Table 1, the modulus of elasticity may be computed.

The double punch test is relatively new as regards asphaltic concrete testing, and no work has been reported on the effects of the various properties of the mix on the tensile strength or modulus of elasticity.

Cohesimeter Test

Another means used for finding the tensile properties of asphalt is the cohesimeter test. It was developed by Hveem of the California Highway Department for use in designing asphaltic mixtures and pavements. (39)

The test is performed on a standard Marshall specimen (4-in. diameter x 2.5-in. height) (101.6 mm diameter x 63.5 mm height) that has been heated in a 140°F (60°C) oven for approximately two hours prior to testing.

The specimen is placed in the cohesimeter as shown in Figure 24. The cohesimeter is calibrated so that the lead shot used to load the specimen will flow into the shot receiver at a rate of 1800 ± 20 grams per minute. The thermostatically controlled heater is adjusted to maintain a 140°F ± 2°F (60°C ± 1°C) temperature in the cabinet. Once the specimen is clamped into position, the release pin is pulled to allow the shot to flow into the receiver. The shot is allowed to flow until the specimen breaks. However, if the specimen fails to break after the loading arm has moved 1/2-in. (12.7 mm) vertically, the loading is stopped. The shot accumulated in the shot receiver is then weighed to the nearest gram and recorded as shot weight.

From the test described above, the cohesimeter value may be determined by

$$C = \frac{L}{W (.20H + 0.044H^2)} \quad (26)$$

where

C = cohesimeter value (grams per inch (25.4 mm) width corrected to a 3-in. (76.2 mm) height)

Table 1

COEFFICIENTS FOR MODULUS OF ELASTICITY
 BY U. OF A. DOUBLE PUNCH TEST
 (Source: R. A. Jimenez)
 Basic Conversion Unit: 1 in. = 2.54 cm

Poisson's Ratio = 0.35 and Punch Diameter = 1.00 in.

$$E_D = \frac{K P}{d}$$

E_D = Dynamic modulus of elasticity, psi (Pa)

P = Repeated vertical load, lb. (N)

d = Repeated radial displacement at mid-height, in. (mm)

K = Coefficient from table below, 1/in. (1/m)

Specimen Height, in.	Specimen Diameter, in.					
	3.0	3.2	3.4	3.6	3.8	4.0
1.5	.213	.210	.206	.201	.197	-
2.0	.235	.240	.243	.245	.245	.244
2.5	.218	.233	.245	.256	.264	.271
3.0	.181	.200	.219	.236	.252	.267
3.5	.139	.158	.179	.199	.219	.239
4.0	.100	.117	.137	.157	.178	.199
4.5	-	-	-	-	-	.157
5.0	-	-	-	-	-	.116

L = weight of shot in grams
 W = diameter or width of specimen in inches
 H = height of specimen in inches

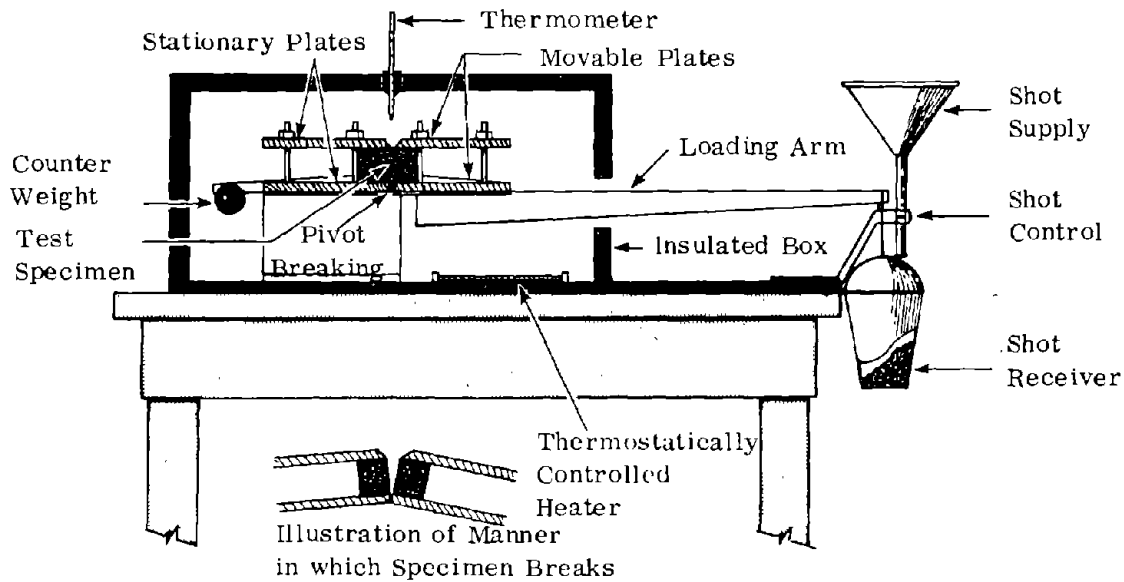


Figure 24. Hveem cohesiometer. (40)

In two experiments performed by Hadley, Hudson, and Kennedy, (41) the values from the indirect tensile test were compared to those of the cohesiometer test. The variables and design for the two experiments are shown in Figure 25.

The study was to establish through a linear regression analysis whether a correlation existed between the modulus of elasticity, Poisson's ratio, and tensile strength of the indirect tensile test, and the cohesiometer value. The correlation of the variables was classified as -

1. no correlation,
2. a trend, and
3. an acceptable correlation.

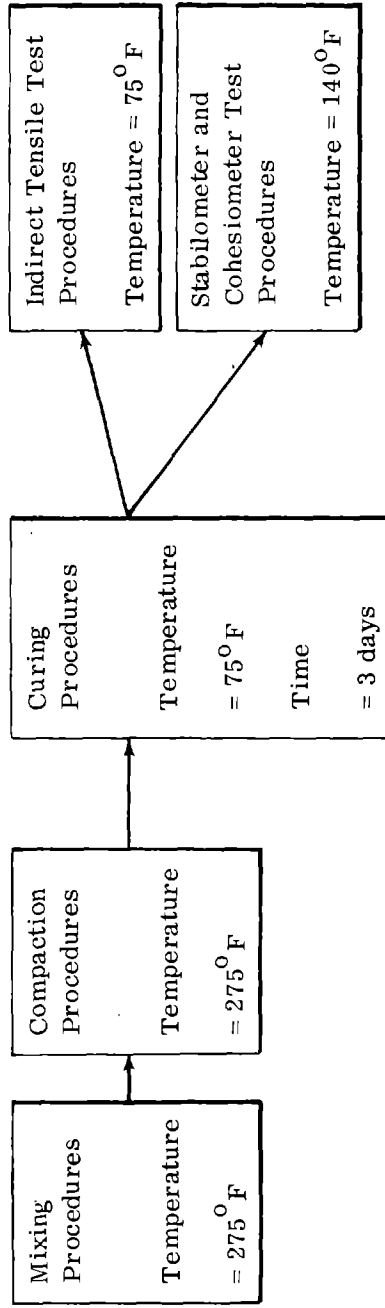
A relationship was classified as no correlation when the variables were independent of each other. A weak relationship was said to exist between two variables when an increase in one resulted in a general increase or decrease in the other. An

PREPARATION SPECIMEN

Experiment 1

Mix Variables

- Aggregate Type
- Aggregate Gradation
- Asphalt Content



Experiment 2

Mix Variables

- Asphalt Viscosity
- Aggregate Type
- Asphalt Content
- Aggregate Gradation

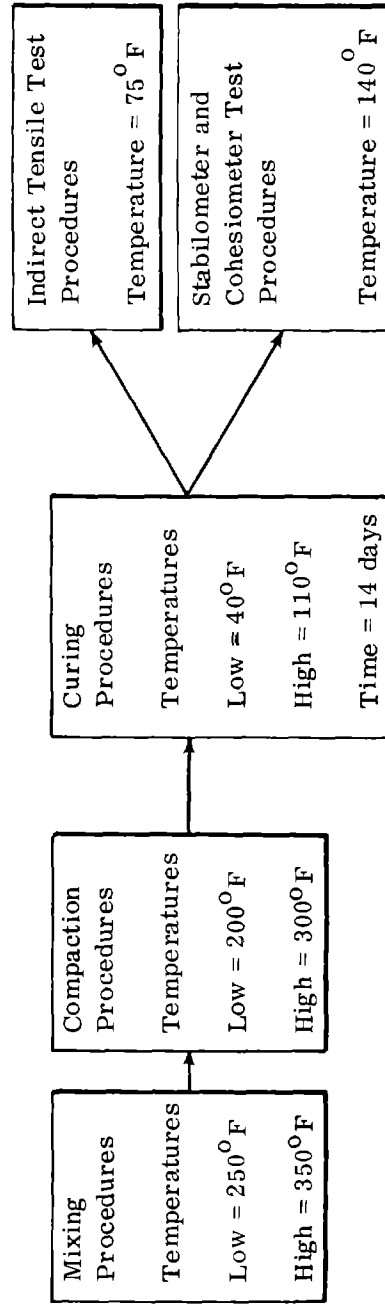


Figure 25. Experimental approach to correlation analysis. (41)

$$\left(^\circ\text{C} = \frac{5}{9} (^\circ\text{F} - 32) \right)$$

acceptable degree of correlation was assumed when one variable could be predicted from a second with a relatively high degree of reliability.

The results obtained from the experiments are shown in Table 2. It can be seen that when the results are combined no correlation exists between the Poisson's ratio and the cohesiometer value, but an acceptable correlation exists between the tensile strength and the cohesiometer value and the modulus of elasticity and the cohesiometer value.

It was generally felt that even though the predicted value for the modulus of elasticity was acceptable, the test would not provide accurate values of Poisson's ratio that might be needed later.

Jimenez,⁽³⁸⁾ when searching for a simple tensile test for detecting the stripping or debonding of asphalt, stated that his prior experiences with the cohesiometer were not particularly good.

Hudson and Kennedy do not recommend the test because of the nonuniform and undefined stress distribution which exists across the specimen and the fact that the maximum tensile stress occurs at the outer surface.⁽²⁵⁾ This latter condition accentuates the effect of surface irregularities and may result in low indicated values of tensile strength.

Direct Tension

The direct tension test is simple in theory and application.⁽²⁵⁾ It is performed by applying a direct axial tensile force to a specimen and measuring the stress-strain characteristics of the material.

The results⁽⁴²⁾ are in the form of the tensile force and the corresponding deformation of the specimen due to that force. The deformation can be measured by using dual LVDT's connected to a recorder. From this test, the tensile strength and maximum elongation of the specimen can be computed. An important item to note is that the axis of failure must be outside of the elongation measuring area or the recorded elongation would be far too high.

The problems that arise with this test lie with the caliber of equipment needed to obtain satisfactory test results. One of the basic requirements in choosing a simple test method is that the method be simple and that the equipment can be purchased at relatively little cost. When using

Table 2

PARAMETERS USED IN CORRELATION ANALYSIS

<u>Variables</u>	<u>Correlation Coefficient r</u>	<u>Does Correlation Exist?</u>	<u>95% Confidence Bands About</u>		<u>Slope Ratio</u>	<u>Coefficients of Variation, %</u>	<u>Acceptable Correlation</u>
			<u>Correlation Coefficient</u>	<u>Correlation Coefficient</u>			
Elasticity and cohesionmeter value	.7238	Yes	$.356 \leq r \leq .898$		1.9	19, 13	Yes
Poisson's ratio and cohesionmeter value	.4109	No					
Tensile strength and cohesionmeter value	.6185	Yes	$.177 \leq r \leq .853$		2.6	15, 14	No
EXPERIMENT 2 ⁽⁴¹⁾							
Elasticity and cohesionmeter value	.8069	Yes	$.593 \leq r \leq .905$		1.5	29, 26	Yes
Poisson's ratio and cohesionmeter value	-.6411	Yes	$-.337 \leq r \leq .824$		2.4	57, 34	No
Tensile strength and cohesionmeter value	.8580	Yes	$.705 \leq r \leq .935$		1.4	21, 23	Yes

relatively inexpensive test equipment, two severe difficulties that arise are the gripping of the specimen and application of a pure tensile load.

The cylindrical specimen⁽²⁵⁾ is secured by cementing a semicircular loading head to the outer circumference of the specimen as shown in Figure 26. This method reduces the effect of planes of weakness caused by compaction by layers and also is convenient.

The rectangular specimen,⁽⁴³⁾ a 1.5 in. x 1.5 in. x 4.5 in. (38.1 mm x 38.1 mm x 114.3 mm) beam, is fastened with epoxy to the loading heads. This method also reduces the possibility of failure on a weak plane caused by the compaction by layers.

The test is performed with the assumption that only pure tension is applied to the specimen.⁽⁴³⁾ However any misalignments of the loading heads will introduce bending stresses and cause errors in the test results. The application of a pure tensile force is very difficult and time-consuming.

The use of good testing equipment helps to alleviate this problem to a certain degree. A testing system which uses a universal joint for each loading head is shown in Figure 27.⁽⁴³⁾ Epps and Monismith used an electrohydraulic closed loop testing system capable of applying a constant rate of deformation.

Another problem that is encountered with the direct tensile test occurs in the evaluation of the test results. It is normally assumed by engineers that the stress is uniformly distributed across the central cross section. However a report by Mitchell states that the maximum stress on the central cross sectional plane was about 1.75 times larger than the average stress.⁽⁴⁴⁾

Hudson and Kennedy state that "In view of these difficulties and uncertainties it is felt that the direct tensile test has limited application and that the test results obtained by this method are questionable."⁽¹⁾

Flexural Beam Test

The flexural beam test is simple to perform.⁽²⁵⁾ It is preferred by some engineers because of its similarity to the field loading of a pavement. This test, like the cohesiometer test, can be characterized as being more of a bending test than a tensile test. The beam is loaded one of two ways:

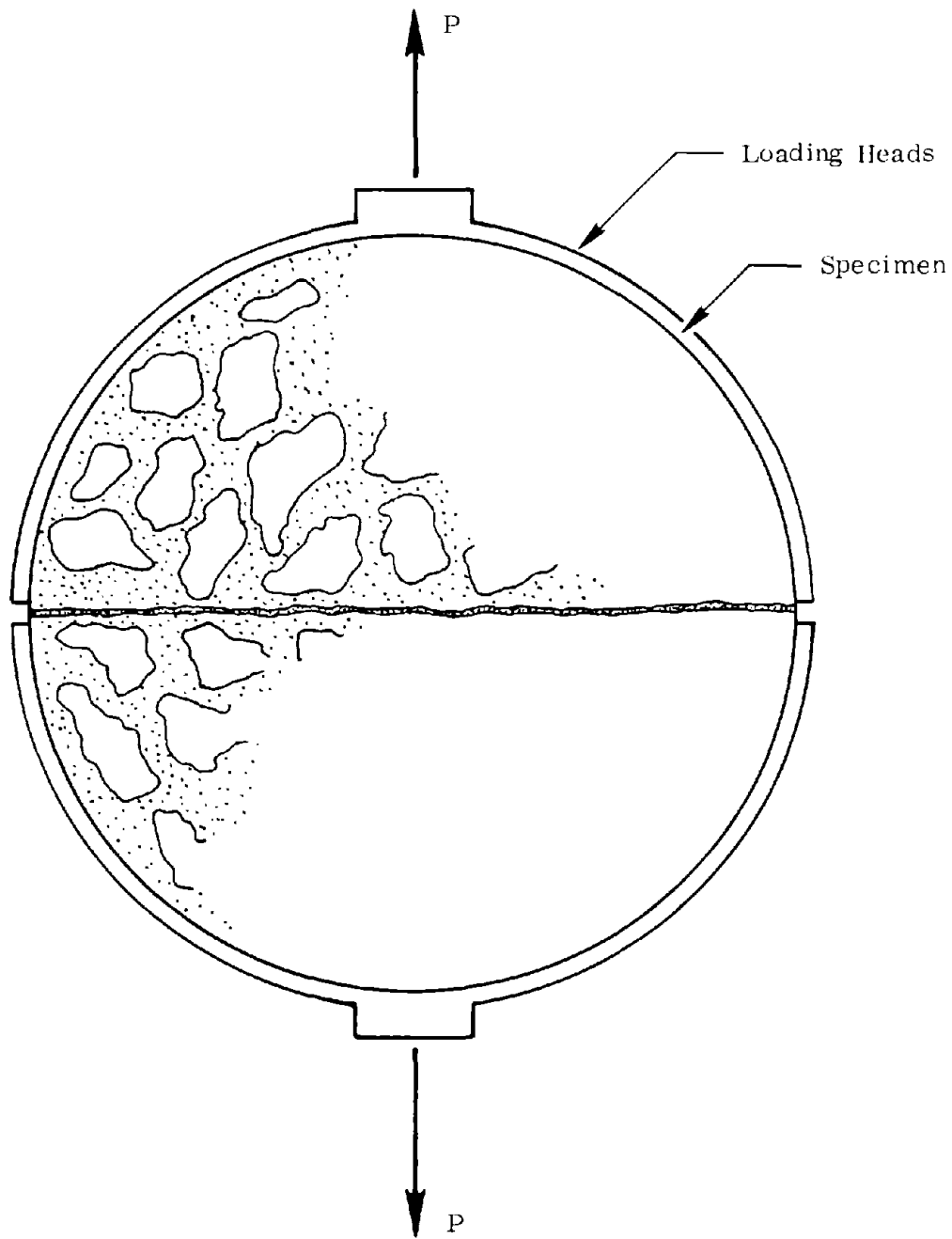


Figure 26. Diametrical direct tensile test. ⁽²⁵⁾

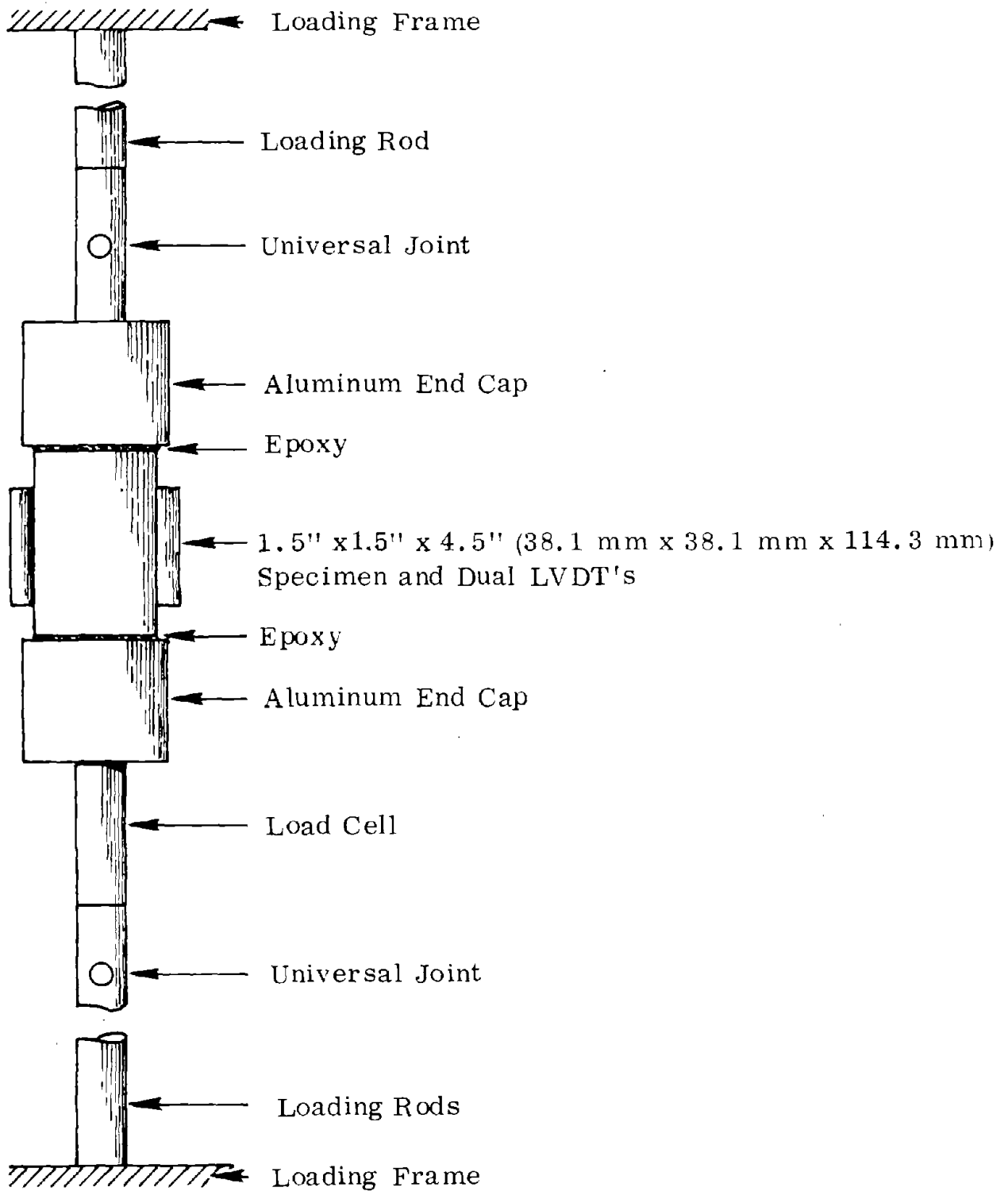


Figure 27. Direct tension testing apparatus. ⁽⁴⁵⁾

the load is applied in two equal concentrated forces on third points of the beam, or it is applied as one concentrated force at the midpoint of the beam.

The beam is tested by placing it in a frame with the ends simply supported and loading it at the centerline under a constant rate of deformation.⁽⁴⁵⁾ The load and the deflection of the beam can be obtained directly from the test.

The tensile strength of the beam can be found by the equation

$$S_R = \frac{Mc}{I} \quad (27)$$

where

M = moment in inch pounds (Nm)

c = one-half depth of the beam in inches (m)

I = moment of inertia in inches⁴ (m⁴)

This formula assumes that the stress is proportional to the distance from the neutral axis, which means there is a linear stress-strain relationship in the tested material.⁽²⁵⁾ This relationship is not valid for asphalt and is very much in error at failure. The use of this formula will usually give a higher tensile strength at failure than the actual strength.

Using the values of load and deflection from the test, the modulus of elasticity, often called the stiffness modulus, S_f , can be determined by⁽⁴⁵⁾

$$S_f = \frac{\Delta PL^3}{48 \Delta f I} \quad (28)$$

where

ΔP = change in load applied in lbs. (N)

L = span in inches (mm)

Δf = deflection corresponding to P in inches (mm)

I = moment of inertia in inches⁴ (mm⁴)

In flexural beam tests performed by Bushy and Rader,⁽⁴⁵⁾ beams containing asphalts of three penetration grades — 200/300, 85/100, and 40/50 — were tested at a temperature of

25°F (-4°C). The stiffness moduli of beams containing the different grades had coefficients of variation of 13.0%, 23.1%, and 21.5%, respectively. The coefficient of variation could be expected to increase when higher testing temperatures are used.

Hudson and Kennedy felt that the flexural beam test had the same shortcomings that the cohesiometer test had.⁽²⁵⁾ The major criticisms, as discussed earlier for the cohesiometer test, are the nonuniform and undefined stress distributions that occur during loading and the fact that the maximum tensile stress occurs at the outer surface, where surface irregularities affect results.

Sonic Test

Freeme and Marias revealed a correlation between bulk modulus as determined by ultrasonic sound wave measurements and the K value that appears in the fatigue equation, $N_f = K (1/\epsilon)^n$, for constant strain fatigue tests (see Figure 28).⁽⁴⁶⁾ Their work indicates a possibility of using ultrasonic methods to predict the fatigue life of bituminous mixtures.

Although ultrasonic equipment is not generally available, many agencies use a sonic device which is commercially available at reasonable cost to obtain freeze-thaw data on portland cement concrete specimens. Leslie and Cheesman⁽⁴⁷⁾ found a good correlation between the sonic moduli and the ultrasonic moduli (bulk modulus) for 300 concrete beams; therefore, it may be possible to use the sonic device to predict K for bituminous mixtures.

Summary and Evaluation of Test Methods

Table 3 lists and rates the simple test methods according to their prospective usefulness in predicting the fatigue life of asphaltic concrete mixtures. The methods were rated according to the characteristics discussed below.

1. Simplicity of sample preparation and testing equipment — Can the method utilize specimens that are currently used in design procedures, and, if not, will new sample preparation and testing techniques be simple? An ideal specimen would be a cylindrical one, such as the Marshall and Hveem, which is used in the other design procedures. Also the cylindrical specimen can be obtained from the pavement with simple coring equipment.

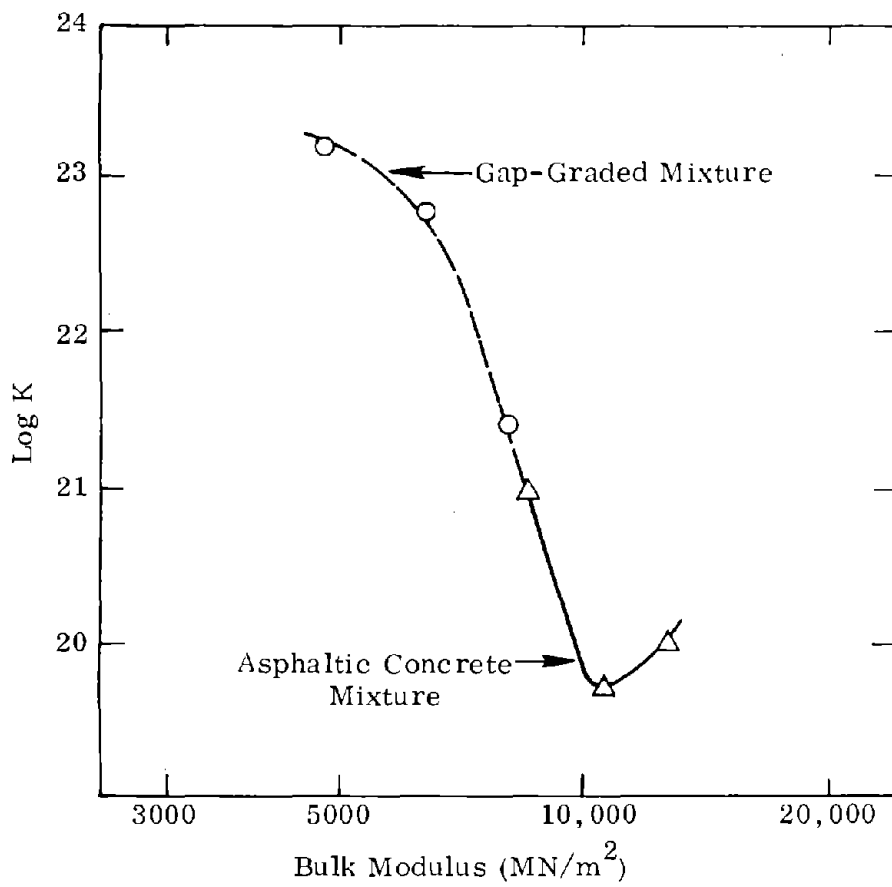


Figure 28. Variation of log K with bulk modulus.

Table 3

RATING SIMPLE TEST METHODS

Test	Simplicity of Sample Preparation and Test Equipment	Yield Accurate Desirable Information (stress, strain, modulus)	Correlated with Fatigue	Average Rating
Static Indirect Tensile Test	9	8	8	8.3
Resilient Modulus Test	8	8	-	8.0
Double Punch Test	9	8	-	8.5
Cohesimeter Test	9	4	-	6.5
Direct Tension Test	4	9	-	6.5
Flexure Test	7	7	-	7.0
Sonic Test	8	6	8	7.3

Rating scale: 0- least desirable 10- most desirable.

Testing equipment should be relatively inexpensive and easy to operate so that tests could be performed in conventional mix design laboratories. If the equipment is expensive and requires extensive training for personnel, it is very unlikely that it could be used on a routine basis for mix design.

2. Accurate desirable information — Although it is not known exactly what type of information is necessary to predict fatigue behavior, investigations have alluded to the type of data that may be useful. It has been shown that fatigue is related to stiffness, therefore a stiffness or modulus measurement may prove useful. Marais proposes using strength or stress criteria to control fatigue behavior, therefore, this measurement may be useful. Strain measurement would possibly be another useful item.

Not only must the test method yield desirable information but the data must be accurate and not excessively variable.

Recently developed pavement design procedures require the moduli of the individual pavement layers, therefore, if the asphalt modulus could be obtained from the same test it would be an additional benefit.

3. Correlation with fatigue — Since the correlation of a simple test with fatigue characteristics is the object of this project it is obvious there has not been a great deal of work in this area. However, there have been several studies that yielded correlations of fatigue and simple test results. These studies were mentioned previously.

If a test has already been correlated with fatigue to some degree this is certainly in its favor.

The sensitivity of the test methods to testing conditions and mixture characteristics was surveyed. The static indirect tensile test, resilient modulus test, cohesiometer test, and direct tension test were found to be sensitive to most of the desired factors.

The other test methods have not been researched as extensively, therefore, not as much information is available on their sensitivity.

According to Table 3 the rating would be:

1. Double Punch

2. Static Indirect Tensile
3. Resilient Modulus
4. Sonic
5. Flexure
6. Direct Tension
7. Cohesiometer

It was proposed that four simple test methods would be selected for laboratory testing. The sonic test was added at the last moment because it can be performed on the fatigue specimens, and thus, no additional specimens need to be fabricated. Therefore, the simple test methods proposed for laboratory study are the double punch, static indirect tensile, resilient modulus, flexure, and sonic.

CHAPTER IV. LABORATORY INVESTIGATION OF SIMPLE TEST METHODS

Objective and Scope

The objective of the laboratory investigation was to determine the best available simple test method for use in predicting the fatigue life of asphaltic concrete. To achieve this objective the following research was planned.

1. Fatigue testing of five bituminous concretes in constant stress and constant strain flexural modes.
2. Simple testing of five bituminous concretes using four of the most promising simple tests.
3. Correlation of simple laboratory test results with fatigue test results.

General Approach

Five mixes were tested using the two fatigue modes and four simple test methods. An additional simple test method (sonic) was added because no extra specimens had to be made and testing equipment was available.

Fatigue curves were obtained for each mix in both the constant stress and constant strain modes in the form of equations (4) and (5).

The simple test results obtained were strength, strain, deformation, and stiffness. These values were correlated with K and n from the fatigue relationships. Also simple test results were correlated with the stress at one cycle obtained from the fatigue relation $N_f = K_1 (1/\sigma)^{n_1}$ for constant stress fatigue tests.

Materials

The five mixes used in the tests, selected from throughout the United States, represent a variety of asphalt cements and aggregates and yielded the desired wide range of stiffness values.

An attempt was made to maintain all air voids at approximately the same level so that the number of laboratory tests could be kept to a reasonable number.

After testing the five original mixes it was decided to test two additional ones for verification of the preliminary results. Some of the mixes have been or are expected to be tested in fatigue by other agencies. The Pennsylvania mix was evaluated in a test track at Penn State University and tested in laboratory fatigue by the Asphalt Institute. A California mix with identical gradation and aggregates was tested by Monismith;⁽²⁰⁾ however, because of the unavailability of the original asphalt cement, a similar asphalt cement was substituted.

Tables 4, 5, and 6 list the mixtures, mix designs, and asphalt cement properties.

Table 4
 ASPHALTIC CONCRETE MIXTURES

Source	Aggregate Type	Asphalt Cement
California	crushed granite	AR-40
Utah	Basalt-sandstone & limestone	85-100 pen.
Ohio	gravel and natural sand	AC-20
Pennsylvania	limestone	85-100 pen.
Virginia #1	crushed granite & natural sand	AC-20
Virginia #2*	crushed granite & natural sand	50-60 pen.
Virginia #3*	crushed granite & natural sand	120-150 pen.

*Additional mixtures

Table 5

MIX DESIGNS

Sieve	Pennsylvania	Ohio	Utah	California	Virginia #1 AC-20	Virginia #2 50-60 pen.	Virginia #3 120-150 pen.
	% Passing						
3/4			100.0				
1/2	100.0	100.0	93.0	100.0	100.0	100.0	100.0
3/8	97.0	95.0	85.0	87.0	95.0	95.0	95.0
4	63.7	60.0	62.0	64.0	58.0	58.0	58.0
8	44.3	46.0	47.5	50.0	41.0	41.0	41.0
16	26.6		36.0	37.0			
30	18.0			26.0	19.0	19.0	19.0
50	12.0	12.5	22.5	19.0	11.0	11.0	11.0
100	7.2			11.0			
200	4.8	7.0	3.2		5.0	5.0	5.0
Asphalt Content, % (by weight)	5.5	5.5	6.8	5.7	5.8	5.7	5.7
Marshall Stability (lbs.)	----	1740	1700	2185	1860	2290	2125
Voids Total Mix (%)	2.0	2.5	1.9	2.1	2.0	2.3	2.2

Table 6

ASPHALT CEMENT PROPERTIES

Mix Identification	Pennsylvania	Ohio	Utah	California	Virginia AC-20	Virginia 50-60 pen.	Virginia 120-150 pen.
Original Asphalt Cement							
Specific gravity	1.033	1.020	1.012	1.027	1.018	1.038	1.024
pen., 77°F, mm	97	83	89	196	70	62	116
Viscosity, 140°F *poises	2254	2254	814	776	2293	5540	1340
Viscosity, 275°F *cSt	490	479	239	289	424	734	351
ductility, 77°F, cm	150+	150+	150+	100	150+		
Asphalt Cement Recovered from Beam Specimens							
pen., 77°F, mm	56	66	53	135	46	48	74
Viscosity, 140°F, *poises	4232	3374	948	1168	4398	7631	2137
Viscosity, 275°F, *cSt	668	568	250	362	507	855	448
ductility, 77°F, cm	105+	105+	105+	105+	105+		

* Average of tests by FHWA and VHTRC.

Note: Fingerprinting and sliding plate viscosities included in Appendixes A and B.

Testing Scheme

Each of the five original mixtures was tested in constant stress fatigue, constant strain fatigue, and by five simple test methods. Also, the two additional Virginia mixtures using 50-60 pen. and 120-150 pen. asphalt cement were tested in constant stress fatigue and by each of the simple test methods. Each fatigue test series required ten specimens per mixture plus one specimen as a control. The control specimens (Virginia AC-20 mixture) were tested with each mixture and compared to the regular Virginia fatigue series to ensure that testing conditions, results, etc. did not change during the testing period. If the control specimen test results differed significantly from the Virginia (AC-20) mixture results that particular series would be suspect.

Each of the simple test methods, with the exception of the resonant frequency and pulse velocity required eight specimens per mixture and two Virginia control specimens. The control results were compared to the regular Virginia results to verify the uniformity of test results. Resonant frequency and pulse velocity moduli tests were performed on each beam before fatigue tests were performed. Table 7 summarizes the number of tests that were performed, and Table 8 lists the average mixture properties for each series of test specimens.

Testing Methods

Fatigue Tests

Fatigue tests were performed on 3 in. (7.6 cm) x 3 in. (7.6 cm) x 15 in. (38.1 cm) sawed beam specimens. The specimens were prepared according to ASTM Designation D 3202-73, "Preparation of Bituminous Mixture Beam Specimens by Means of the California Kneading Compactor."

An electrohydraulic closed loop test system was used to apply fatigue loadings to the beam specimens. Loading was applied at approximately third points on the simply supported beams as illustrated in Figure 29. Controlled stress tests were conducted by applying haversine loadings of 0.1 second duration separated by 0.4 second rest period. It was necessary to apply a negative load to the beam to return it to the zero position after each loading. Failure was defined as the collapse of the beam. The maximum tensile stress and strain and the stiffness were computed by:

$$\sigma = \frac{Mt}{2I} \quad (29)$$

Table 7

NUMBER OF REQUIRED TESTS

Mix Designation	Fatigue Tests		Simple Tests					
	Constant Stress	Constant Strain	Indirect Tensile **	Punch **	Resilient Modulus **	Flexure **	Resonant Frequency	Pulse Velocity
California	11*	11*	10	10	10	10	22	22
Utah	11*	11*	10	10	10	10	22	22
Ohio	11*	11*	10	10	10	10	22	22
Pennsylvania	11*	11*	10	10	10	10	22	22
Virginia #1 AC-20	10	10	10	10	10	10	22	22
Virginia #2 50-60 pen.	11*	-	10	10	10	10	11	11
Virginia #3 120-150 pen.	11*	-	10	10	10	10	11	11
Total	76	54	70	70	70	70	132	132

*includes 1 control beam

**each set includes 2 control specimens

Table 8

AVERAGE MIXTURE PROPERTIES

Mixture	Test Series	Voids Total Mix % VTM	Voids Mineral Aggregate % VMA	Voids Filled With Asphalt % VFA
California	Fatigue-Constant Stress	2.5	16.6	85.2
	Fatigue-Constant Strain	2.4	16.5	85.8
	Flexure	2.6	16.7	84.7
	Resilient Modulus	2.3	16.5	85.9
	Punch	2.2	16.4	87.0
	Indirect Tensile	2.1	16.3	87.0
Utah	Fatigue-Constant Stress	2.3	17.4	89.5
	Fatigue-Constant Strain	1.7	17.3	90.0
	Flexure	2.1	17.6	87.9
	Resilient Modulus	1.6	17.2	90.8
	Punch	1.5	17.1	91.2
	Indirect Tensile	1.5	17.3	91.4
Ohio	Fatigue-Constant Stress	4.1	16.6	75.4
	Fatigue-Constant Strain	3.9	16.5	76.3
	Flexure	4.1	16.6	75.3
	Resilient Modulus	2.1	14.9	85.9
	Punch	1.4	14.4	89.6
	Indirect Tensile	2.0	14.8	86.5
Pennsylvania	Fatigue-Constant Stress	3.5	16.5	78.6
	Fatigue-Constant Strain	3.7	16.6	77.8
	Flexure	3.7	16.7	77.6
	Resilient Modulus	2.1	15.2	86.5
	Punch	1.3	14.6	91.0
	Indirect Tensile	1.4	14.6	90.4
Virginia (AC-20)	Fatigue-Constant Stress	3.9	17.6	77.6
	Fatigue-Constant Strain ³	3.9	17.6	77.7
	Flexure	3.9	17.6	77.8
	Resilient Modulus	2.5	16.4	84.6
	Punch	2.1	16.1	86.7
	Indirect Tensile	2.5	16.4	84.6
Virginia (50-60 pen.)	Fatigue-Constant Stress	3.9	17.4	77.7
	Flexure	3.8	17.3	78.0
	Resilient Modulus	2.7	16.3	83.6
	Punch	2.3	16.0	85.9
	Indirect Tensile	3.0	16.6	82.1
Virginia (120-150 pen.)	Fatigue-Constant Stress	3.8	17.3	78.0
	Flexure	3.8	17.3	77.9
	Resilient Modulus	2.0	15.7	87.4
	Punch	2.1	15.8	86.7
	Indirect Tensile	2.3	16.0	85.6

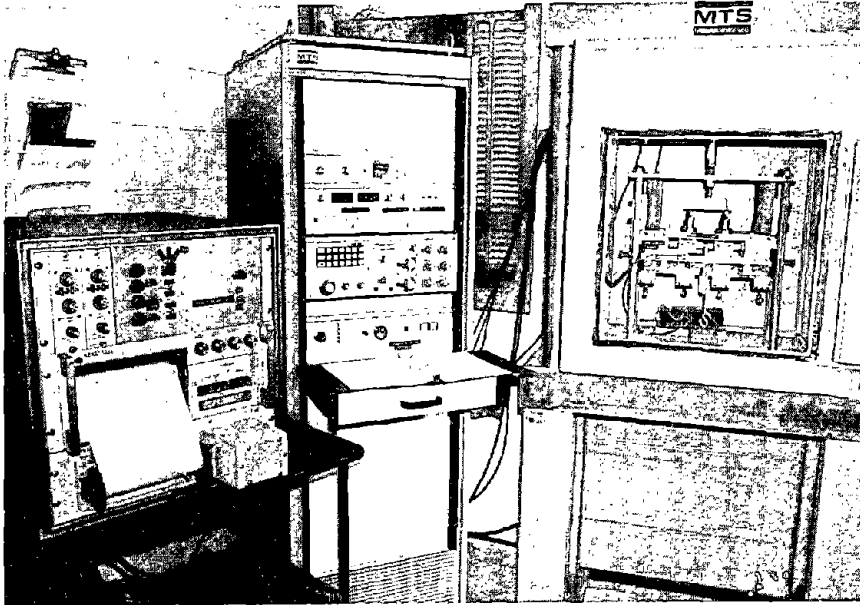


Figure 29. Fatigue test.

$$\epsilon = \frac{12td}{3\ell^2 - 4a^2} \quad (30)$$

$$E = \frac{Pa(3\ell^2 - 4a^2)}{48 Id} \quad (31)$$

where

- σ = maximum tensile stress, psi (Pa)
- ϵ = maximum tensile strain, in./in. (mm/mm)
- E = flexural stiffness, psi (Pa)
- P = applied load, lb. (N)
- M = maximum bending moment, in. · lb. (m · N)
- I = beam moment of inertia, in.⁴ (m⁴)
- t = depth of beam, in. (m)
- d = centerline deflection, in. (m)
- ℓ = length between \mathcal{Q} of end supports (m)
- a = distance between \mathcal{Q} of end support and nearest third point load (m)

The deflection, d , was monitored with an LVDT attached to the neutral axis of the beam at the centerline. The flexural stiffness was calculated from the load and deflection after approximately 200 cycles.

Constant strain fatigue tests required repetitions of haversine waveform centerline deflections. The deflection was monitored continuously to ensure a constant repetition. Failure was defined as a one-third reduction of the initial stiffness.

All fatigue tests were performed at room temperature 72°F (22°C) and a controlled air temperature cabinet was available if the room temperature varied more than $\pm 1^\circ\text{F}$ ($\pm 0.5^\circ\text{C}$).

Indirect Tensile Test

The indirect tensile test was performed using the procedure reported by Anagnos and Kennedy.⁽²³⁾ Test specimens 2.5 in. (6.4 cm) thick x 4 in. (10.2 cm) diameter were compacted and then tested in the apparatus shown in Figure 30. Curved steel loading strips 0.5 in. (1.3 cm) wide and with a 2 in. (5.1 cm) radius were used. The horizontal deformation was measured with two LVDT's wired so that the outward deformation was additive and it was recorded on a visicorder oscillograph.

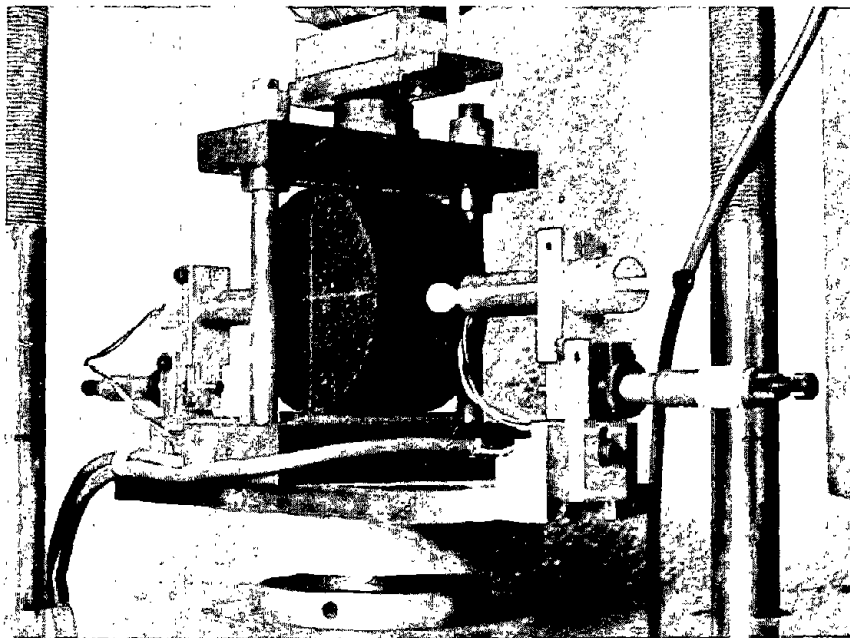


Figure 30. Indirect tensile test.

The load was applied at a vertical deformation rate of 2 in. (5.1 cm) per minute. A proving ring equipped with a LVDT was used to monitor the applied load on the visicorder oscillograph. The vertical deformation was computed using the deformation rate of the testing machine and the elapsed time during the test.

A typical test recording of load and deformation is shown in Figure 31. Equations 18, 20, and 22 were used to compute the tensile strength, σ_{IT} , Poisson's ratio, ν , and stiffness, E_{IT} , respectively.

Punch Test

The punch test was similar to that used by Jimenez.⁽³⁸⁾ The 2.5 in. (6.4 cm) thick x 4 in. (10.2 cm) diameter specimen was centered between 1 in. (2.5 cm) diameter punches (Figure 32). The specimen was then compressed between punches at the rate of 2 in. (5.1 cm) per minute.

The load, horizontal deformation, and vertical deformation were recorded as described under the previous section. The horizontal deformation was measured in only one direction. A typical test recording is illustrated in Figure 33.

The tensile strength, σ_T , was computed by equation 24.

The relationship $E = \frac{KP}{d}$ (48) was used to calculate the stiffness, E , as measured by the punch test where

P = load, lbs. (N)

d = radial displacement, in. (m)

K = constant depending on specimen dimensions, 1/in. (1/m)
(Table 1)

This relationship was originally intended to calculate dynamic stiffness but also should apply to tests at slow loading rates, 2 in. (5.1 cm)/min.

Resilient Modulus

The resilient modulus test was performed on a 2.5 in. (6.4 cm) thick x 4 in. (10.2 cm) diameter specimens made on the California kneading compactor. The stiffness, i.e. modulus, of the specimen was obtained by applying a dynamic diametral load and measuring the perpendicular diametral deformation as in the indirect tensile test.

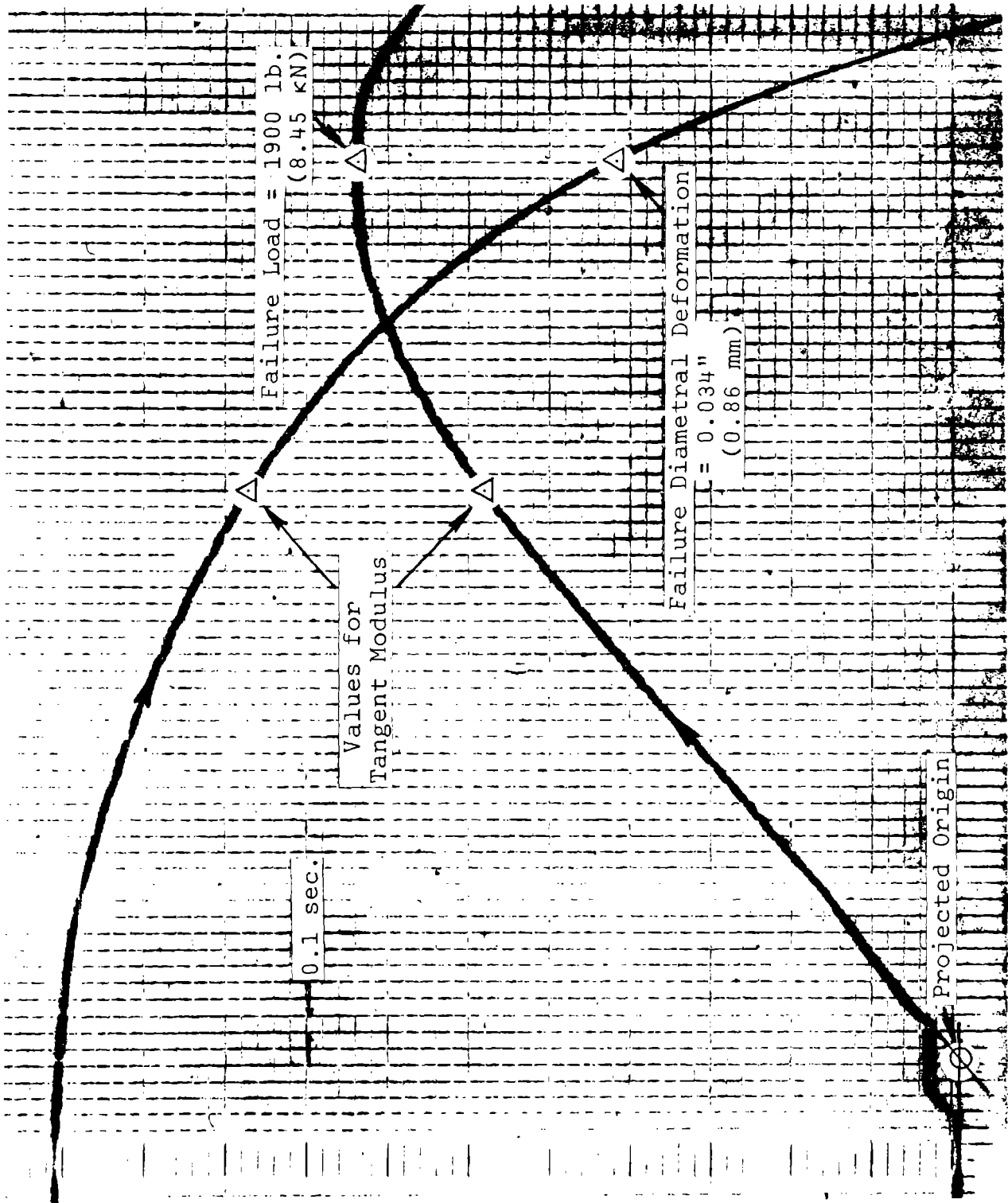


Figure 31. Typical indirect tensile test recording.

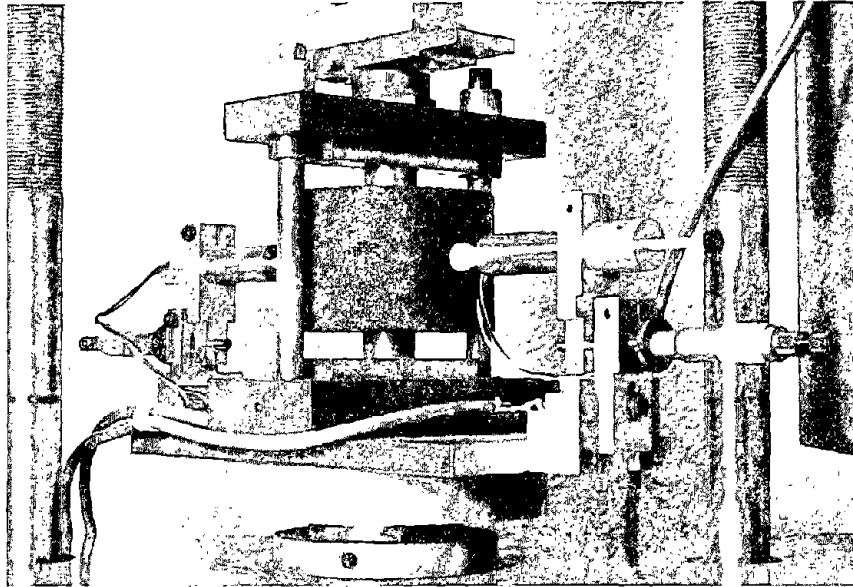


Figure 32. Punch test.

The test was performed utilizing equipment developed by R. J. Schmidt⁽³⁵⁾ (Figure 34), although other equipment capable of applying small dynamic loads and measuring small deformations could be used.

The same load (43.1 lb.) (192 N), corresponding to approximately a 3 psi (20.6 K Pa) tensile stress level, was applied for 0.1 sec. to all specimens, and the resilient modulus was determined by equation 23. Poisson's ratio was assumed as 0.3 for the computations.

Eight individual measurements 90° apart were made on each specimen.

Flexure Test

The flexure tests were performed on 3 in. (7.6 cm) x 3 in. (7.6 cm) x 7.5 in. (19 cm) sawed beams. The beams were prepared by ASTM Designation 3202-73 and cut to the proper size. Each beam made by the above procedure yielded two beams for testing.

During testing the beam was simply supported on 1.5 in. (3.8 cm) wide strips and loaded at midspan at a 2 in. (5.1 cm)/min. deformation rate on a 1 in. (2.5 cm) wide strip (Figure 35). The vertical deformation at midspan and the load were recorded, and the failure strength and stiffness were computed by equations (27) and (28), respectively.

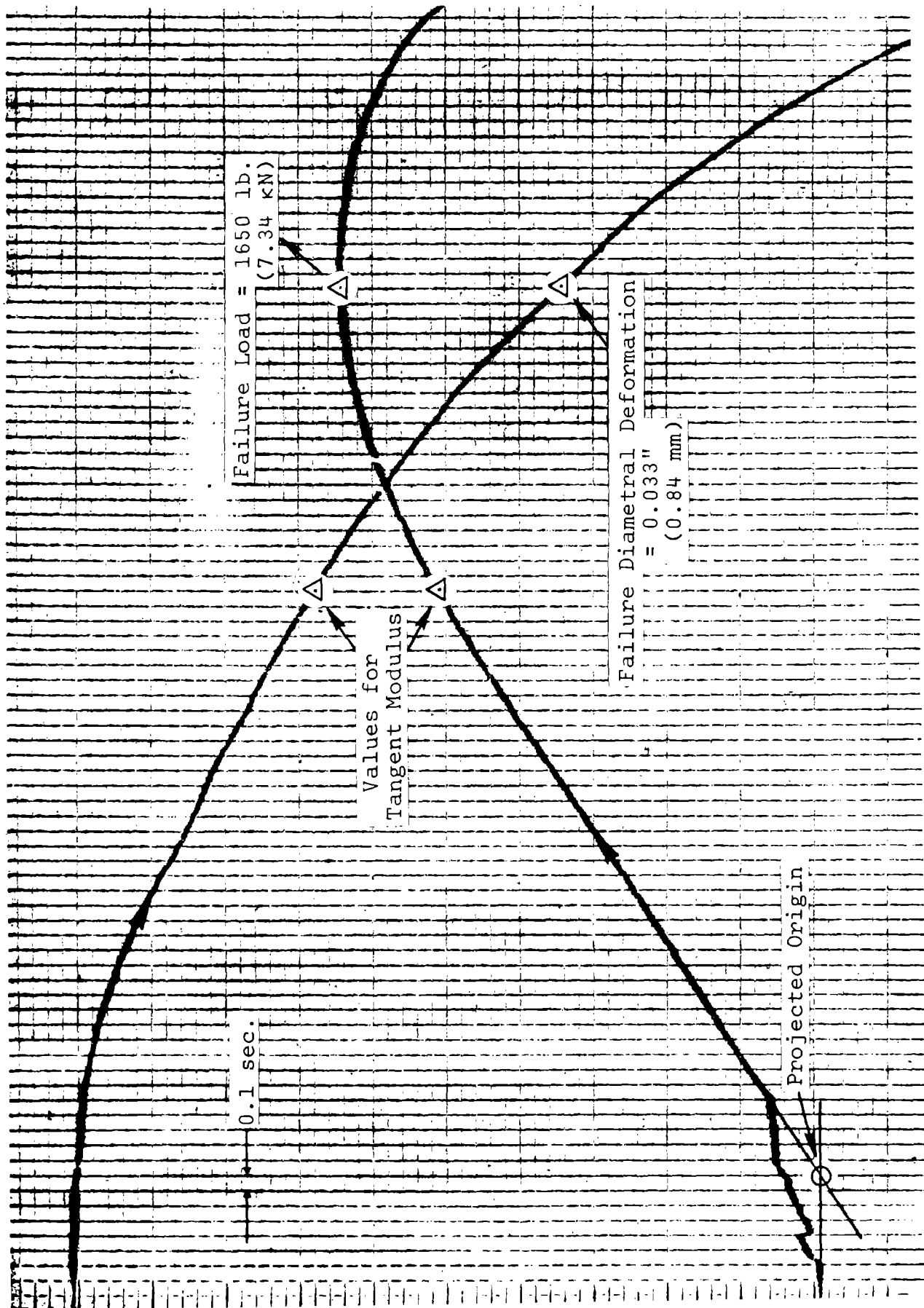


Figure 33. Typical punch test recording.

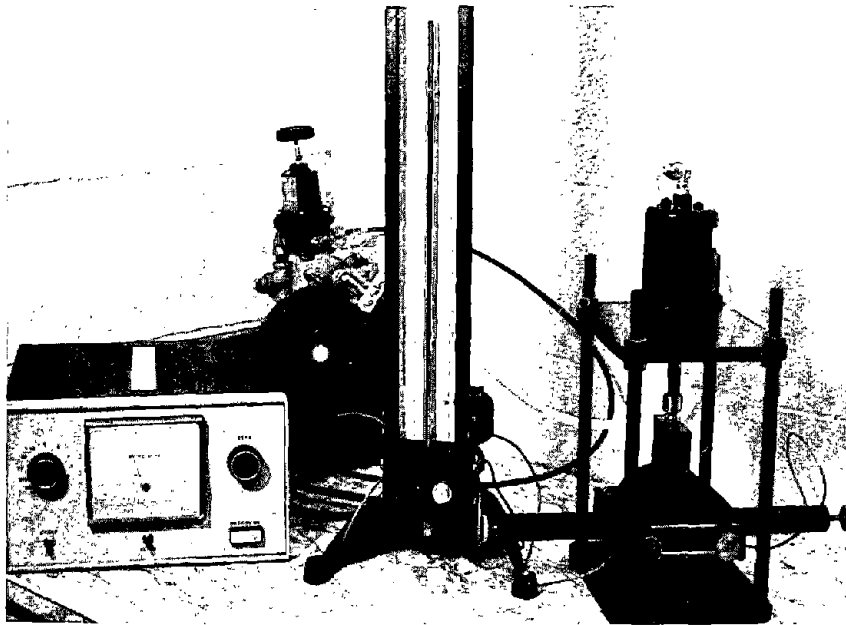


Figure 34. Resilient modulus test.

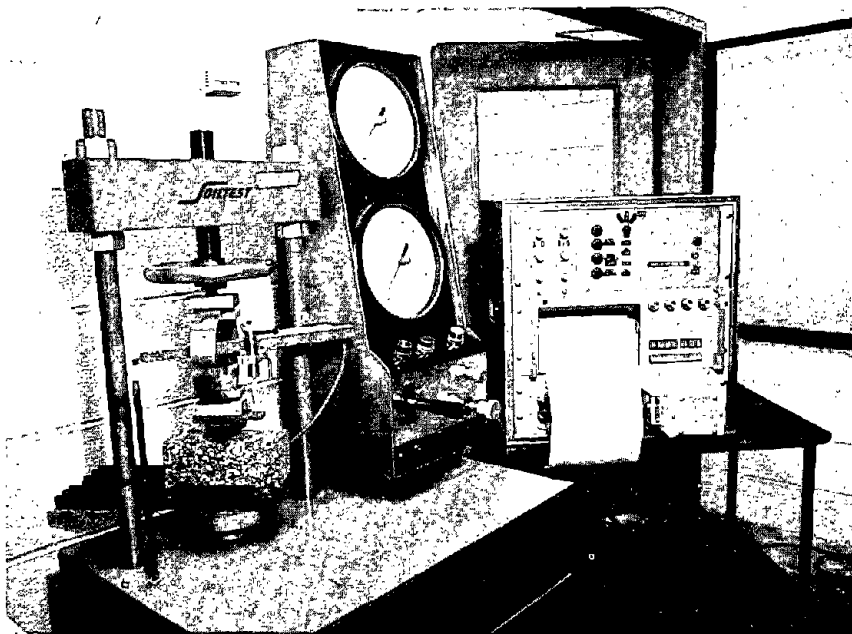


Figure 35. Flexure test.

A typical test recording is shown in Figure 36.

Resonant Frequency Tests

Resonant frequency tests were performed on each fatigue specimen in accordance with the method given in ASTM C 215-60 entitled "Standard Method of Test for Fundamental Transverse, Longitudinal and Torsional Frequencies of Concrete Specimens." The equipment consisted of the basic components of a driving circuit, a pickup circuit, and a specimen support conforming to the ASTM specifications (Figure 37).

The fatigue specimen was tested prior to being placed in the closed loop fatigue tester. The specimen was positioned on the tester so that the transverse resonant frequency was obtained. Using the resonant frequency, a value for dynamic Young's modulus was calculated from the equation

$$E = cwn^2 \quad (32)$$

where

w = weight of the specimen, lb. (N)

n = fundamental transverse frequency, Hz.

$c = 0.00245 * \left(\frac{L^3 T}{bt^3} \right)$ *Replace constant with .0964 for metric.

L = length of specimen, in. (m)

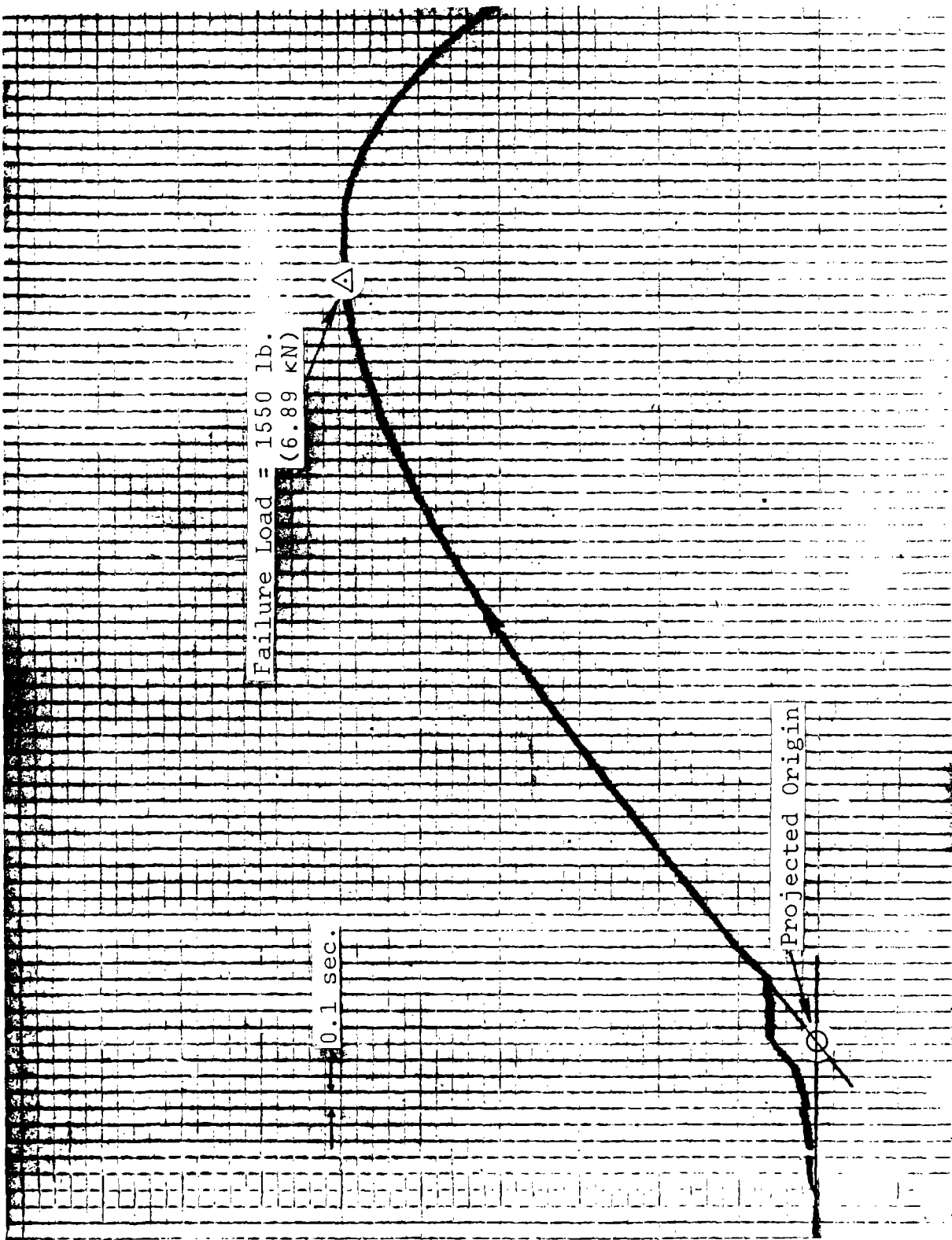
d = diameter of cylinder, in. (m)

t, b = dimensions of cross section of prism, in. (m)
t being in the direction in which it is driven

T = a correction factor which depends on the ratio of the radius of gyration, K ($K = t/3.464$) to the length of the specimen, L, and on Poisson's ratio.

Pulse Velocity Tests

Pulse velocity tests were conducted on the fatigue specimens prior to fatigue testing. The test was developed using the theory that the velocity at which a pulsating sound travels through a medium is related to the modulus of elasticity of the medium. By measuring the velocity of the sound, relationships were developed which could be used to obtain a



Reproduced from
best available copy.

Figure 36. Typical flexure test recording.

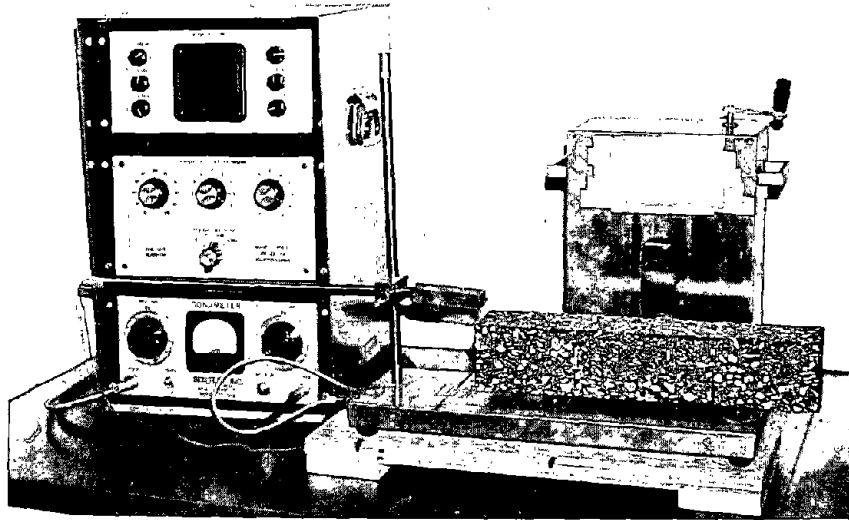


Figure 37. Resonant frequency test.

value of dynamic Young's modulus of elasticity.⁽⁴⁷⁾

The equipment (Figure 38) used is capable of generating ultrasonic energy that supplies pulsed energy to a transducer. A second transducer detects, amplifies, and displays the signal after it has passed through the medium. The instrument contains a time standard and measuring system for measuring the elapsed time of the sound wave passing through the medium to an accuracy of one-half microsecond.

With the measured value of time and the distance the pulse must travel, the velocity of the pulse traveling through the medium can be determined. The dynamic Young's modulus of elasticity can be completed using a relationship developed by Leslie and Cheesman.⁽⁴⁷⁾

$$E = 0.000216 V^2 d \frac{(1 + \nu)(1 - 2\nu)}{(1 - \nu)} \quad (33)$$

where

E = dynamic Young's modulus of elasticity, psi (Pa)

V = pulse velocity, ft./sec. (m/sec)

d = unit weight, lb./ft.³, (Kg/m³)

ν = Poisson's ratio

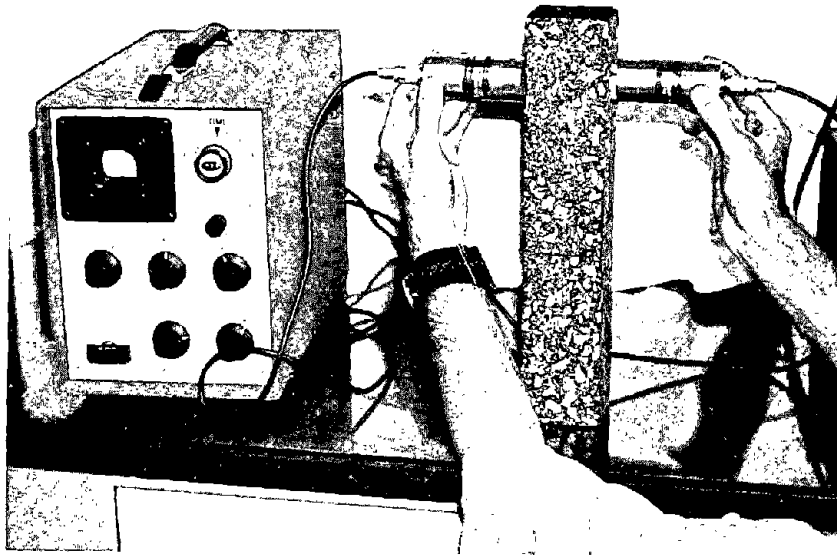


Figure 38. Pulse velocity test.

Results

Fatigue Tests

Constant strain fatigue tests were performed on five mixes and constant stress fatigue tests on seven mixes.

Figure 39 shows the results of the constant stress tests plotted as fatigue life versus the maximum bending stress, which occurs on the lower beam surface between loading clamps; and Table 9 lists the constants K and n for the relationships of stress and strain versus cycles to failure. The Utah and California mixes produced the steepest plots and the Virginia mixes with 120-150 pen. and 50-60 pen. asphalt cement produced the flattest. Although the slopes were equal, the California mix had a lesser fatigue life than did the Utah mix at the same stress level because the Utah mix was much stiffer. The Virginia (AC-20), Pennsylvania, and Ohio plots had approximately the same slope; however, the Ohio curve was shifted to the left because of the mixes' shorter fatigue life at the same stress level. It can be observed, as was expected, that the Virginia mix with low penetration asphalt cement (50-60 pen.) had a longer fatigue life than the mix with high penetration (120-150 pen.) asphalt cement.

Figure 40 shows the results of the constant stress fatigue tests plotted as fatigue life versus the initial maximum bending strain, which occurs on the lower beam surface between loading clamps at 200 cycles of load application.

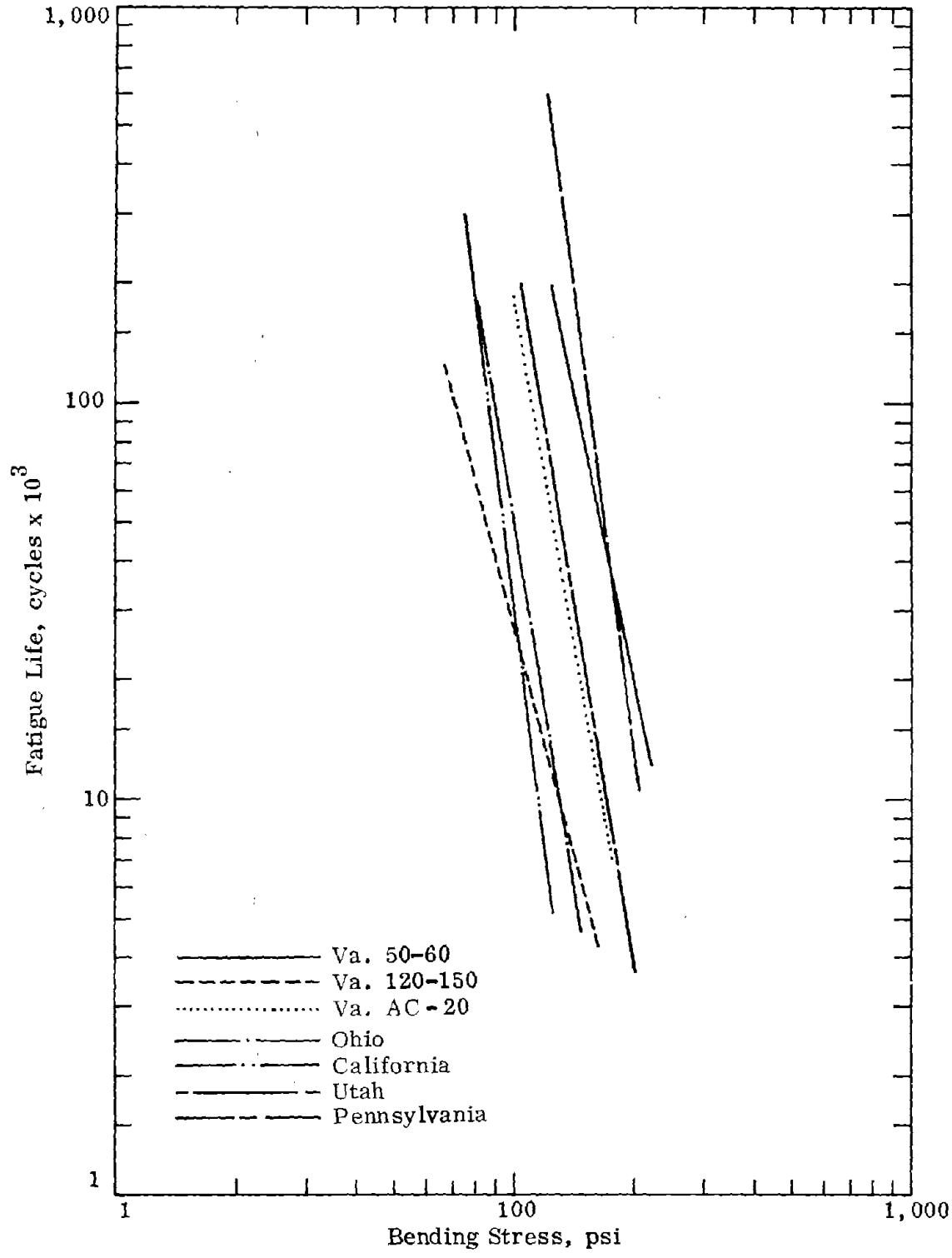


Figure 39. Constant stress tests — fatigue life vs. maximum bending stress. 1 psi = 6890 Pa.

Table 9

CONSTANT STRESS FATIGUE RELATIONSHIPS

Mix	$N = K_1(1/\sigma)^{n_1}$		$N = K_2(1/\epsilon)^{n_2}$	
	K_1	n_1	K_2	n_2
Virginia (AC-20)	1.0×10^{17}	5.9	2.8×10^{-8}	3.9
Virginia (50-60 pen.)	2.6×10^{15}	4.8	2.7×10^{-4}	2.6
Virginia (120-150 pen.)	2.3×10^{14}	4.9	8.5×10^{-2}	1.9
Pennsylvania	4.3×10^{17}	6.1	1.0×10^{-6}	3.6
Ohio	1.0×10^{17}	6.2	7.0×10^{-4}	2.5
Utah	2.6×10^{21}	7.5	9.5×10^{-9}	4.1
California	6.5×10^{20}	8.1	6.4×10^{-7}	3.8

Of the seven mixes, the California mix yielded the greatest fatigue life in the range of 10,000 to 200,000 cycles at the same strain level. Also, the least stiff Virginia mix, that containing the 120-150 penetration asphalt cement, had the greatest fatigue life of the three Virginia mixes at the same strain level in the range of 10,000 to 150,000 cycles.

Figure 41 illustrates the results of the constant strain fatigue tests plotted as fatigue life versus the maximum bending strain, and Table 10 lists the constants for these curves. The curves appear to converge at approximately one million cycles, with the exception of the curve for the Ohio mix. A similar type of convergence was reported by Monismith for mixtures with different stiffnesses. The slopes ranged from 2.1 for the Ohio mix to 4.4 for the Virginia (AC-20) mix.

Figure 42 illustrates the fatigue results of the constant strain tests plotted as fatigue life versus the initial bending stress, which was monitored at 200 cycles of load application. The Utah and Virginia curves were steeper than the Ohio, California and Pennsylvania curves. The slopes ranged from $n = 5.2$ for the Utah mix to $n = 2.5$ for the Ohio mix.

The linear regression correlation coefficients were generally higher for the constant stress tests than for the constant strain tests; however, the standard errors of estimate

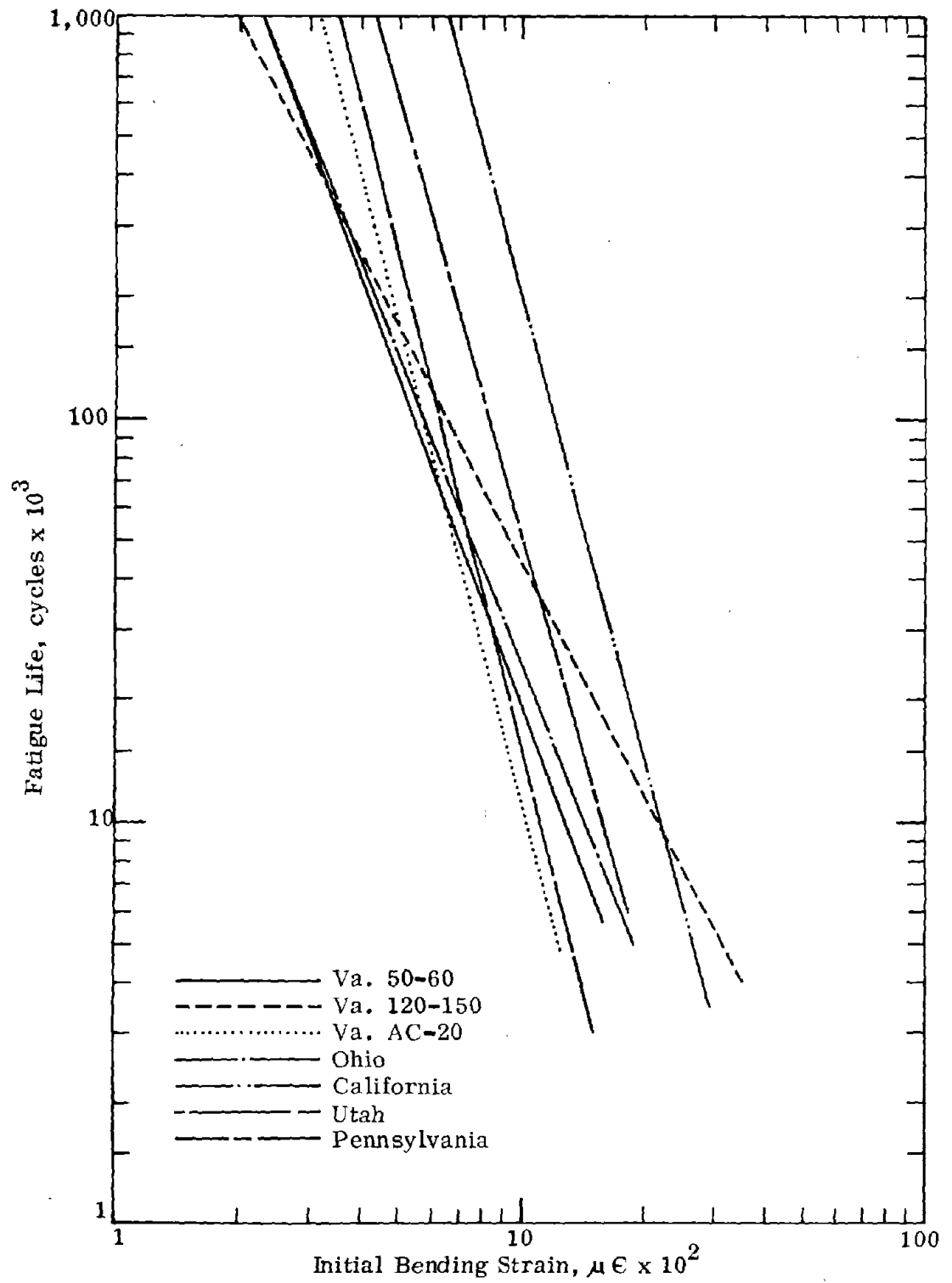


Figure 40. Constant stress tests — fatigue life vs. initial maximum bending strain.

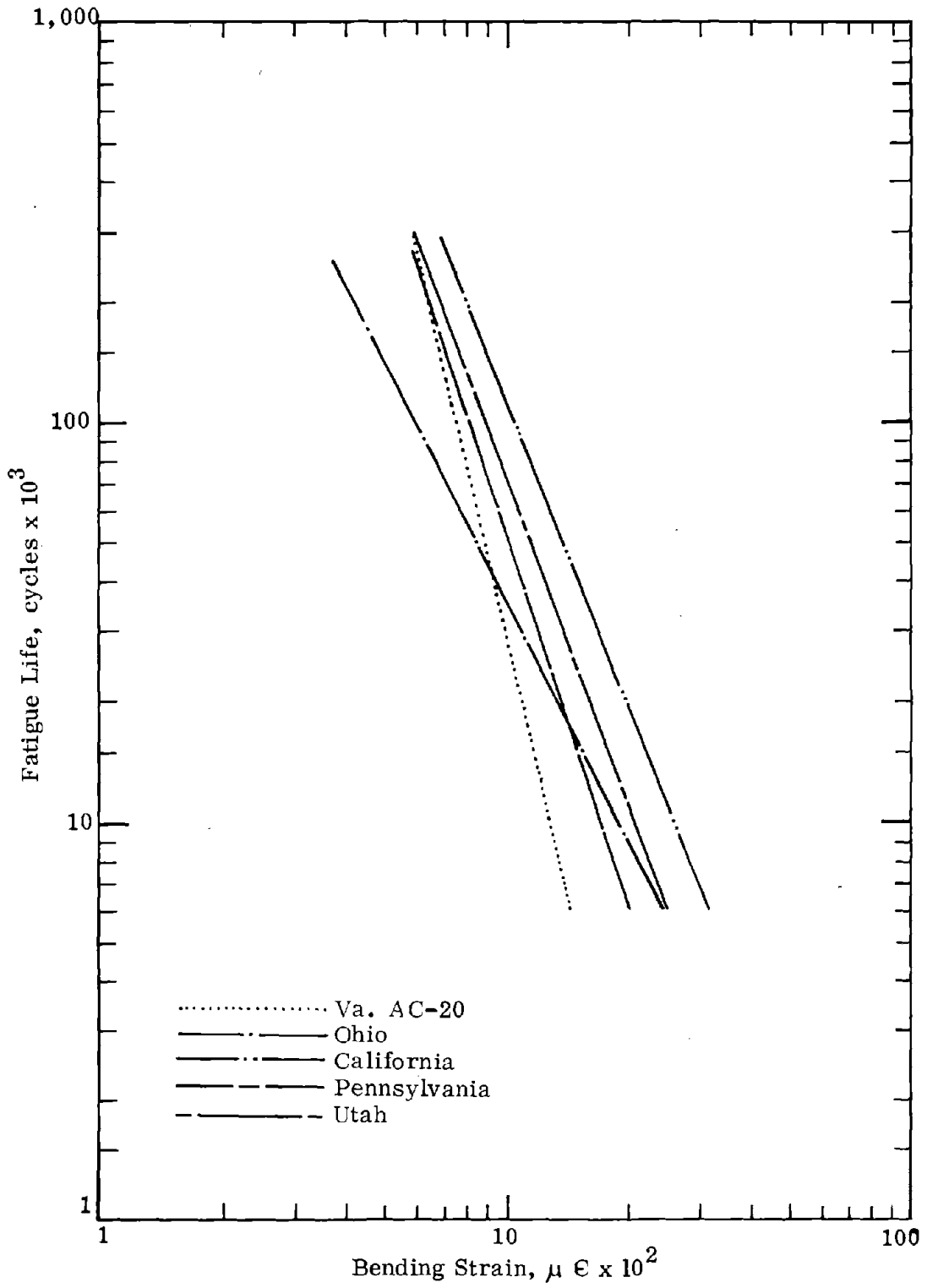


Figure 41. Constant strain tests — fatigue life vs. maximum bending strain.

were approximately equal for both constant stress and constant strain regressions, which indicated that the tests predict fatigue life equally well.

Table 10

CONSTANT STRAIN FATIGUE RELATIONSHIPS

Mix	$N = K_1(1/\sigma)^{n_1}$		$N = K_2(1/\epsilon)^{n_2}$	
	K_1	n_1	K_2	n_2
Virginia (AC-20)	2.0×10^{13}	4.0	2.3×10^{-9}	4.4
Pennsylvania	1.7×10^{10}	2.6	3.9×10^{-4}	2.8
Ohio	8.1×10^9	2.5	2.3×10^{-2}	2.1
Utah	4.6×10^{16}	5.2	2.4×10^{-5}	3.1
California	3.1×10^{10}	2.9	5.2×10^{-3}	2.4

Simple Tests

The results of the simple tests include failure stress, stiffness and deformation. Trends are examined for these results within and between the different mixtures. Low coefficients of variation would be beneficial if the test property is used to estimate fatigue life.

Indirect Tensile Test

The failure stress ranged from 71 psi (0.49 M Pa) to 160 psi (1.1 M Pa) (Table 11) for the California mix and Virginia mix with 50-60 pen. asphalt cement, respectively. The failure stresses of the Virginia mixes were 104 psi (0.717 M Pa), 124 psi (0.855 M Pa), and 160 psi (1.10 M Pa) for Virginia (120-150 pen.), Virginia (AC-20) and Virginia (50-60 pen.), respectively. These results are logical because failure stress increases as asphalt cement stiffness increases. The average coefficient of variation for eight specimens was 7%.

There was not a well-defined trend for the failure horizontal deformation. The deformations of the mixes with 50-60 pen. and 120-150 pen. asphalt cements were approximately equal,

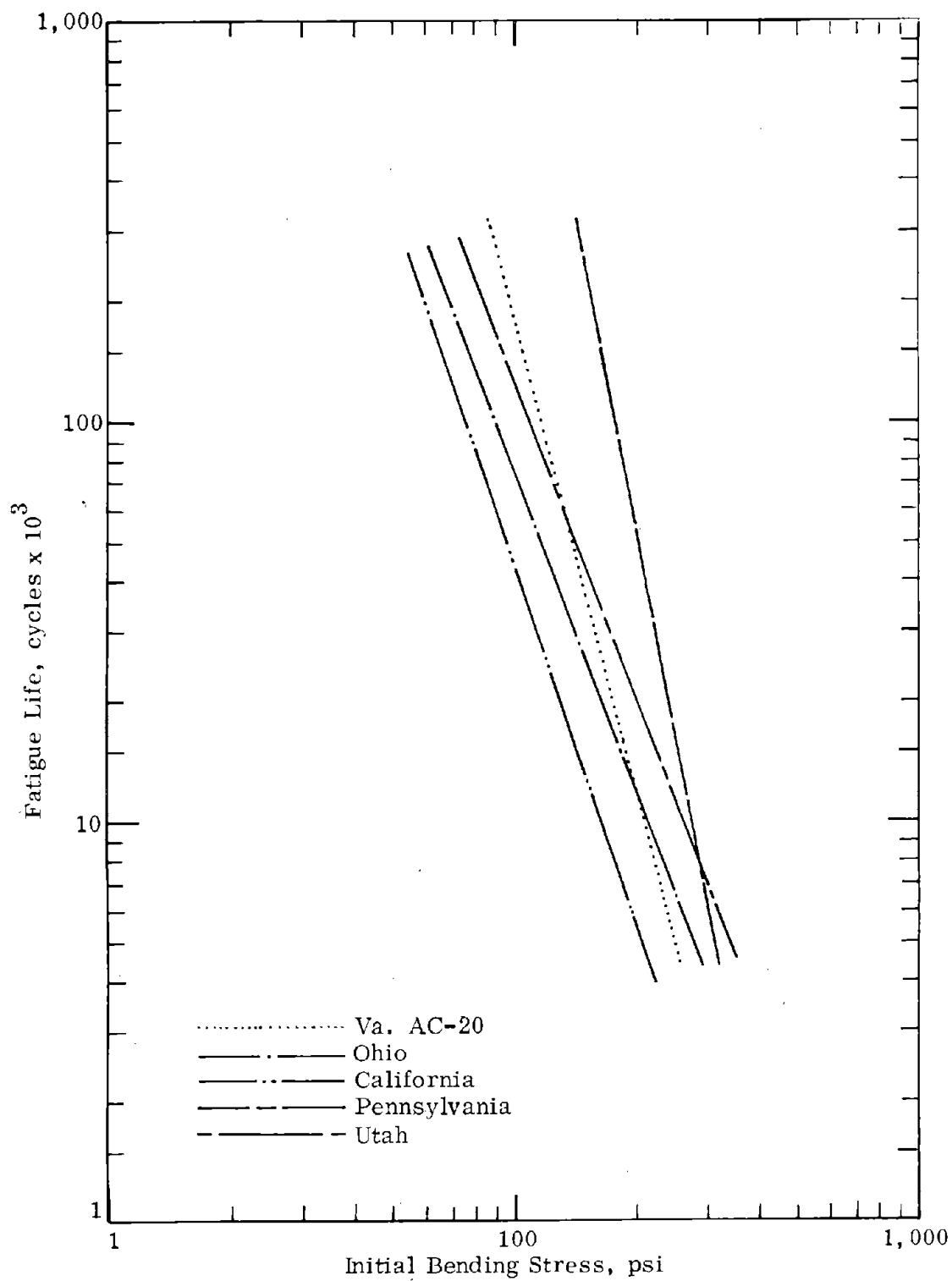


Figure 42. Constant strain tests — fatigue life vs. initial maximum bending stress. 1 psi = 6890 Pa.

Table 11

INDIRECT TENSILE TEST RESULTS

Mix	Failure Stress psi		Failure Horizontal Deformation - in.		Failure Vertical Deformation-in.		Failure Modulus-psi		Tangent Modulus-psi	
	Avg.	C. V.*	Avg.	C. V.*	Avg.	C. V.*	Avg.	C. V.*	Avg.	C. V.*
California	71	6	0.035	8	0.149	4	10,900	8	13,500	8
Ohio	94	4	0.034	4	0.172	5	12,500	6	15,800	9
Utah	106	9	0.043	8	0.210	4	11,500	13	17,200	19
Pennsylvania	98	5	0.039	7	0.193	3	12,000	6	17,800	10
Virginia (AC-20)	124	7	0.034	6	0.181	4	15,700	8	19,700	13
Virginia (50-60 pen.)	160	5	0.030	18	0.198	3	18,200	5	22,000	3
Virginia (120-150 pen.)	104	11	0.029	6	0.153	5	15,500	7	18,700	7
Average	---	7	---	8	---	4	---	8	---	10

*Coefficient of variation, %
 Note: 1 in. = 25.4 mm; 1 psi = 6890 Pa.

which was unexpected because of different physical properties.

The failure vertical deformation generally was higher for stiff mixes, ranging from 0.149 in. (3.78 mm) for the California mix to 0.210 in. (5.33 mm) for the Utah mix. The same trend occurred in the three Virginia mixes with different stiffnesses. The average coefficient of variation was 4% for eight tests.

The failure modulus and tangent modulus had the same trends although the tangent modulus was higher than the failure modulus. Both moduli ranked the California mix as least stiff and the Virginia mix with 50-60 pen. asphalt cement as most stiff. Also the Virginia mixes with different asphalt cements were ranked in the same order. The coefficients of variation were 8% and 10% respectively for the failure modulus and tangent modulus.

Punch Test

The failure strength ranged from 74 psi (0.51 M Pa) for the California mix to 136 psi (0.938 M Pa) for the Virginia mix with 50-60 pen. asphalt cement (Table 12). Also the failure strength of the three Virginia mixes was indicative of the type of asphalt cement in each mix. The coefficient of variation was 7%.

There was no apparent trend of diametral deformation with stiffness or strength.

The failure vertical deformation trended toward low values for less stiff mixes and high values for stiffer mixes. The same trend was apparent for the Virginia mixes.

The failure modulus and tangent modulus did not appear to be good indicators of the true stiffness. It was difficult to determine the tangent modulus because the stress curves were not linear, especially those for the Utah mix. The moduli coefficients of variation were high: 13% for the failure modulus and 23% for the tangent modulus.

Resilient Modulus

The resilient modulus is a measure of dynamic stiffness in indirect tension. The results (Table 13) in descending order of stiffness were: Virginia (50-60 pen.), Virginia (AC-20), Ohio, Utah, Pennsylvania, and California. Coefficients of variation ranged from 7% to 16%.

Table 12

PUNCH TEST RESULTS

Mix	Failure Stress psi		Failure Diametral Deformation-in.		Failure Vertical Deformation-in.		Failure Modulus-psi		Tangent Modulus-psi	
	Avg.	C. V.*	Avg.	C. V.*	Avg.	C. V.*	Avg.	C. V.*	Avg.	C. V.*
California	74	9	0.044	7	0.191	5	14,600	15	23,700	14
Ohio	107	5	0.040	6	0.238	3	25,400	10	78,300	27
Utah	87	6	0.050	6	0.311	4	16,600	7		
Pennsylvania	104	6	0.047	9	0.260	6	20,000	12	67,100	28
Virginia (AC-20)	119	8	0.041	10	0.235	4	26,600	17	51,500	24
Virginia (50-60 pen.)	136	6	0.039	12	0.246	2	31,900	17	52,700	23
Virginia (120-150 pen.)	96	6	0.036	11	0.191	4	24,000	15	42,400	19
Average		7		9		4		13		23

* Coefficient of variation, %
 Note: 1 in. = 25.4 mm; 1 psi = 6890 Pa

Table 13

RESILIENT MODULUS RESULTS

Mix	Resilient Modulus, psi	Coefficient of Variation, %
California	92,000	9
Ohio	201,000	8
Utah	194,000	7
Pennsylvania	166,000	9
Virginia (AC-20)	233,000	16
Virginia (50-60 pen.)	321,000	12
Virginia (120-150 pen.)	124,000	12

Note: 1 psi = 6,890 Pa

Flexure Test

The failure stress (Table 14) ranged from 335 psi (2.31 M Pa) for the California mix to 722 psi (4.98 M Pa) for the Virginia mix with 50-60 pen. asphalt cement. The failure stress of the Virginia mixes was in the expected relative order of 722 psi (4.98 M Pa) for the Virginia (50-60 pen.) mix, 637 psi (4.39 M Pa) for the Virginia (AC-20) mix, and 444 psi (3.06 M Pa) for the Virginia (120-150 pen.) mix. The average coefficient of variation was 8%.

The failure deformation ranged from 0.146 in. (3.71 mm) for the California mix to 0.193 in. (4.90 mm) for the Virginia mix with 50-60 pen. asphalt cement. Similarly, the deformation was higher for the Virginia mixes with stiffer asphalt cement. The average coefficient of variation for failure deformation was 4%.

The failure modulus ranged from 4,940 psi (34.1 M Pa) for the Pennsylvania mix to 8,360 psi (57.6 M Pa) for the Virginia mix with 50-60 pen. asphalt cement. The moduli of the Virginia mixes was indicative of the stiffness of the asphalt cement used in each mix. The coefficient of variation was 8%.

Table 14

FLEXURE TEST RESULTS

Mix	Failure Stress, psi		Failure ϵ , in.		Failure Modulus, psi	
	Avg.	C.V.*	Avg.	C.V.	Avg.	C.V.
California	335	12	0.146	7	5,000	15
Ohio	535	4	0.173	3	6,790	5
Utah	604	4	0.184	4	7,200	5
Pennsylvania	422	9	0.191	2	4,940	7
Virginia (AC-20)	637	12	0.187	5	7,600	12
Virginia (50-60 pen.)	722	6	0.193	3	8,360	6
Virginia (120-150 pen.)	444	10	0.147	6	6,560	8
Average		8		4		8

*Coefficient of variation - %.

Note: 1 in. = 25.4 mm; 1 psi = 6,890 Pa.

Resonant Frequency and Pulse Velocity Tests

Table 15 lists the average values of stiffness moduli obtained on the fatigue beams by the resonant frequency and pulse velocity test methods. The coefficient of variation was less than 10% for any of the mixtures; however, there was very little numerical difference between mixes.

The resonant frequency moduli appeared to follow the trend of the stiffness moduli from the other simple tests, with the California mix having the lowest and the Virginia (50-60 pen.) mix the highest moduli.

There is no apparent similar trend with the wave velocity moduli.

Table 15

RESONANT FREQUENCY AND WAVE VELOCITY TEST RESULTS

Mix	Resonant Frequency Moduli, psi x 10 ⁶	Wave Velocity Moduli, psi x 10 ⁶
California	0.92	4.40
Ohio	0.96	3.73
Utah	1.14	3.84
Pennsylvania	1.06	4.48
Virginia (AC-20)	1.14	3.60
Virginia (50-60 pen.)	1.24	3.67
Virginia (120-150 pen.)	1.06	3.68

Note: 1 psi = 6,890 Pa

Correlation of Simple Test and Fatigue Test Results

Constant Stress Fatigue Tests

Regression analyses were performed between fatigue properties and simple test values to determine the possibility of predicting fatigue behavior from a simple test.

The fatigue properties used for correlation were n_1 , n_2 , $\log K_1$, and $\log K_2$ from the fatigue equations $N_f = K_1(1/\sigma)^{n_1}$ and $N_f = K_2(1/\epsilon)^{n_2}$, where N_f is the number of cycles to failure, σ is the applied stress, ϵ is the initial strain, and K and n are constants. The stress at $N = 1$ cycles, $\sigma_N = 1$, from the fatigue curve was also used for correlation.

Simple test results of stiffness, strength, and vertical deformation were correlated with the fatigue properties. Asphalt cement properties were also correlated because examination of the data seemed to indicate a possible satisfactory correlation.

Correlation coefficients and standard error of estimates are listed in Table 16 for the 55 correlations. No accurate correlations were obtained that would allow the prediction of

Table 16

CORRELATION BETWEEN CONSTANT STRESS FATIGUE AND SIMPLE TESTS

Fatigue Characteristic	Stiffness				Strength			Vertical Deformation			
	Indirect Tensile	Punch	Flexure	Resilient Modulus	Transverse Frequency	Wave Velocity	Indirect Tensile	Punch	Flexure	Indirect Tensile	Punch
n_1^*	0.87 (0.67)	0.88 (0.64)	0.51 (1.15)	0.52 (1.15)	0.34 (1.26)	0.61 (1.07)	0.70 (0.96)	0.79 (0.82)	0.45 (1.20)	0.08 (1.34)	0.18 (1.32)
n_2^{**}	0.53 (0.79)	0.62 (0.73)	0.28 (0.90)	0.09 (0.93)	0.14 (0.92)	0.45 (0.84)	0.23 (0.91)	0.34 (0.88)	0.05 (0.93)	0.40 (0.86)	0.47 (0.82)
$\log k_1^*$	0.79 (1.74)	0.83 (1.60)	0.37 (2.66)	0.35 (2.68)	0.09 (2.85)	0.52 (2.44)	0.53 (2.43)	0.68 (2.10)	0.26 (2.76)	0.18 (2.81)	0.41 (2.61)
$\log k_2^{**}$	0.45 (2.49)	0.52 (2.38)	0.16 (2.76)	0.03 (2.79)	0.23 (2.71)	0.31 (2.65)	0.12 (2.77)	0.24 (2.71)	0.08 (2.78)	0.50 (2.42)	0.56 (2.32)
$\sigma_{n=1}^{***}$	0.91 (187)	0.81 (258)	0.72 (308)	0.76 (287)	0.77 (282)	0.55 (371)	0.93 (161)	0.81 (259)	0.71 (315)	0.39 (409)	0.10 (442)

$$*N = k_1 (1/\sigma)^{n_1}$$

$$**N = k_2 (1/\epsilon)^{n_2}$$

***Refer to definition on page 89.

Note: Correlation coefficient listed with standard error of estimate in parentheses.

the fatigue equation $N_f = K_2 (1/\epsilon)^{n_2}$. However, several correlations involving the fatigue curve $N_f = K_1 (1/\sigma)^{n_1}$ were discovered with reasonable correlation coefficients (greater than 0.89) and standard errors.

Reasonable correlations were obtained between the slope, n_1 , of the fatigue life-stress relationship and indirect tensile stiffness and punch stiffness. Also reasonable correlations were obtained between the stress calculated at $N = 1$ cycle, $\sigma_{N=1}$, from the fatigue curve and indirect tensile strength and indirect tensile stiffness.

The slope n_1 and $\sigma_{N=1}$ will define a fatigue life-stress relationship. The slope, n_1 , can be estimated from the indirect tensile stiffness or punch stiffness. A single point on the curve at $N = 1$ cycle can be estimated from the indirect tensile strength or stiffness. Therefore, there are several simple test values that can be used to predict the fatigue life of a bituminous mix. The selection of the simple test method or test methods will depend on simplicity, cost, and accuracy of prediction.

The indirect tensile test results can be used to predict a fatigue curve but the punch test will predict only the slope of the curve; therefore, the indirect tensile test is the logical choice. The correlation, $n_1 = 11.6 - 0.000396 E_{IT}$, can be used to predict the slope n_1 , of the constant stress fatigue curve from the indirect tensile stiffness. Also the stress at $N = 1$ cycle, $\sigma_{N=1}$, can be calculated from the correlation $\sigma_{N=1} = 12.6 \sigma_{IT} - 558$ where σ_{IT} is the indirect tensile strength; therefore, the fatigue curve can be defined.

The comparison between the experimental fatigue curves and predicted fatigue curves using the above procedure is illustrated in Figures 43-49. All of the predicted curves are within or very close to the 95% confidence limits of the experimental curves, with the exception of that for the Ohio mix. The predictive curve for the Ohio mix is positioned so that a higher fatigue life is predicted than obtained by the laboratory fatigue testing. The slopes of the predicted and experimental curves are comparable, except for the Virginia mix with 120-150 pen. asphalt cement.

Constant Strain Fatigue Tests

Regression analyses were performed on fatigue and simple test properties similar to the constant stress correlation. The property $\sigma_{N=1}$ was not used for correlation.

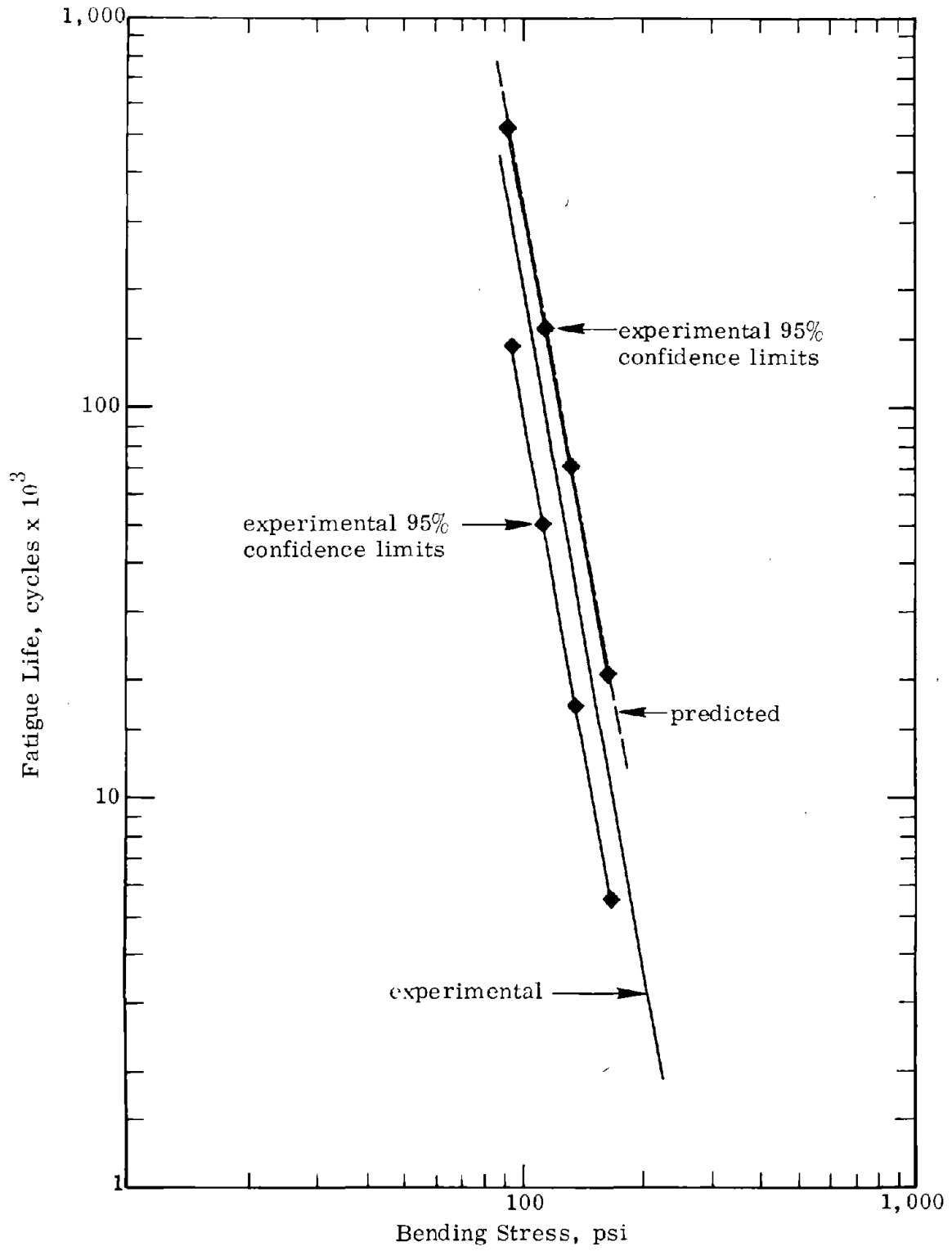


Figure 43. Constant stress fatigue curves (Virginia AC-20 mix).
1 psi = 6890 Pa

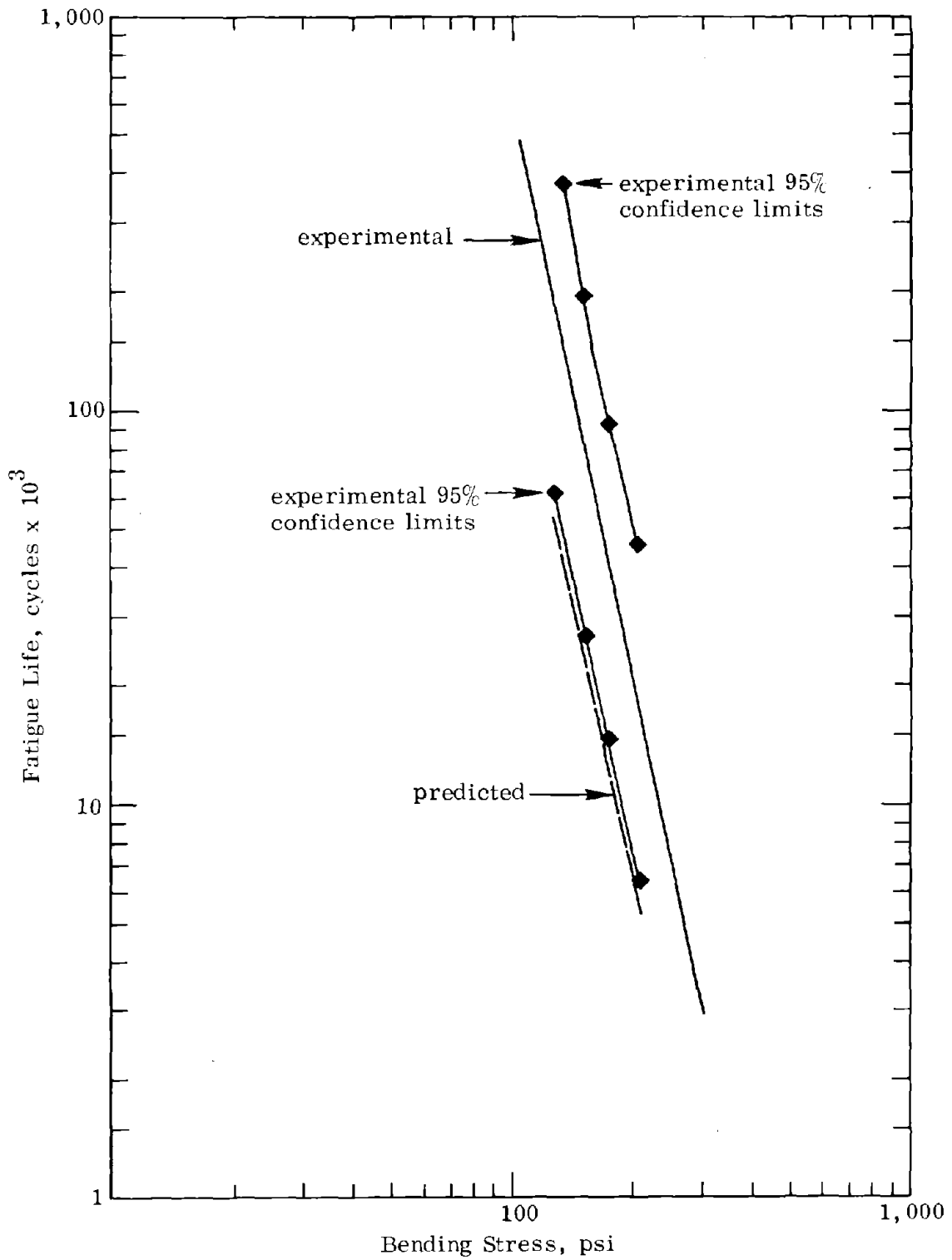


Figure 44. Constant stress fatigue curves (Virginia 50-60 pen. mix).
1 psi = 6890 Pa.

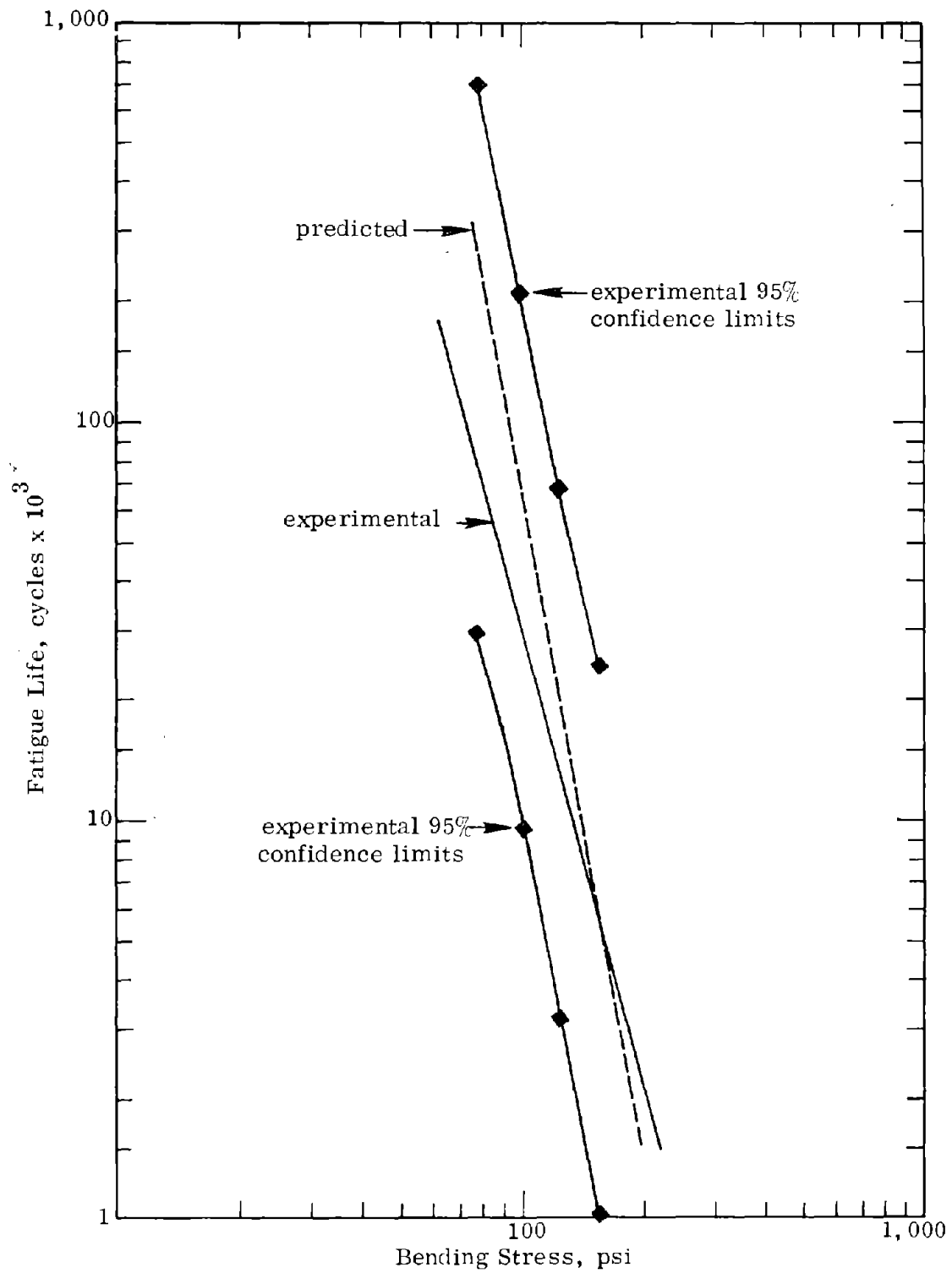


Figure 45. Constant stress fatigue curves (Virginia 120-150 pen. mix).
1 psi = 6890 Pa.

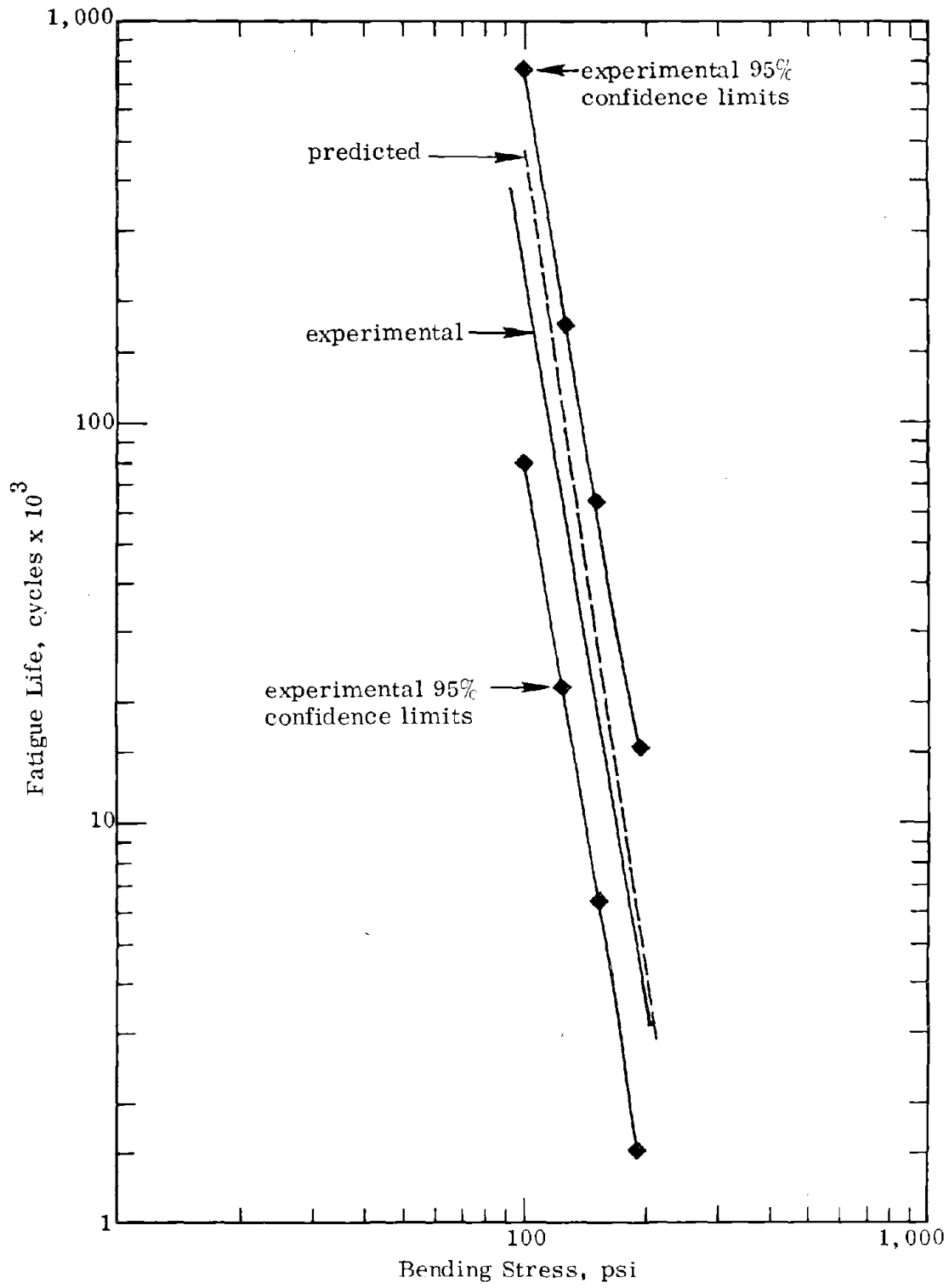


Figure 46. Constant stress fatigue curves (Pennsylvania mix).
1 psi = 6890 Pa.

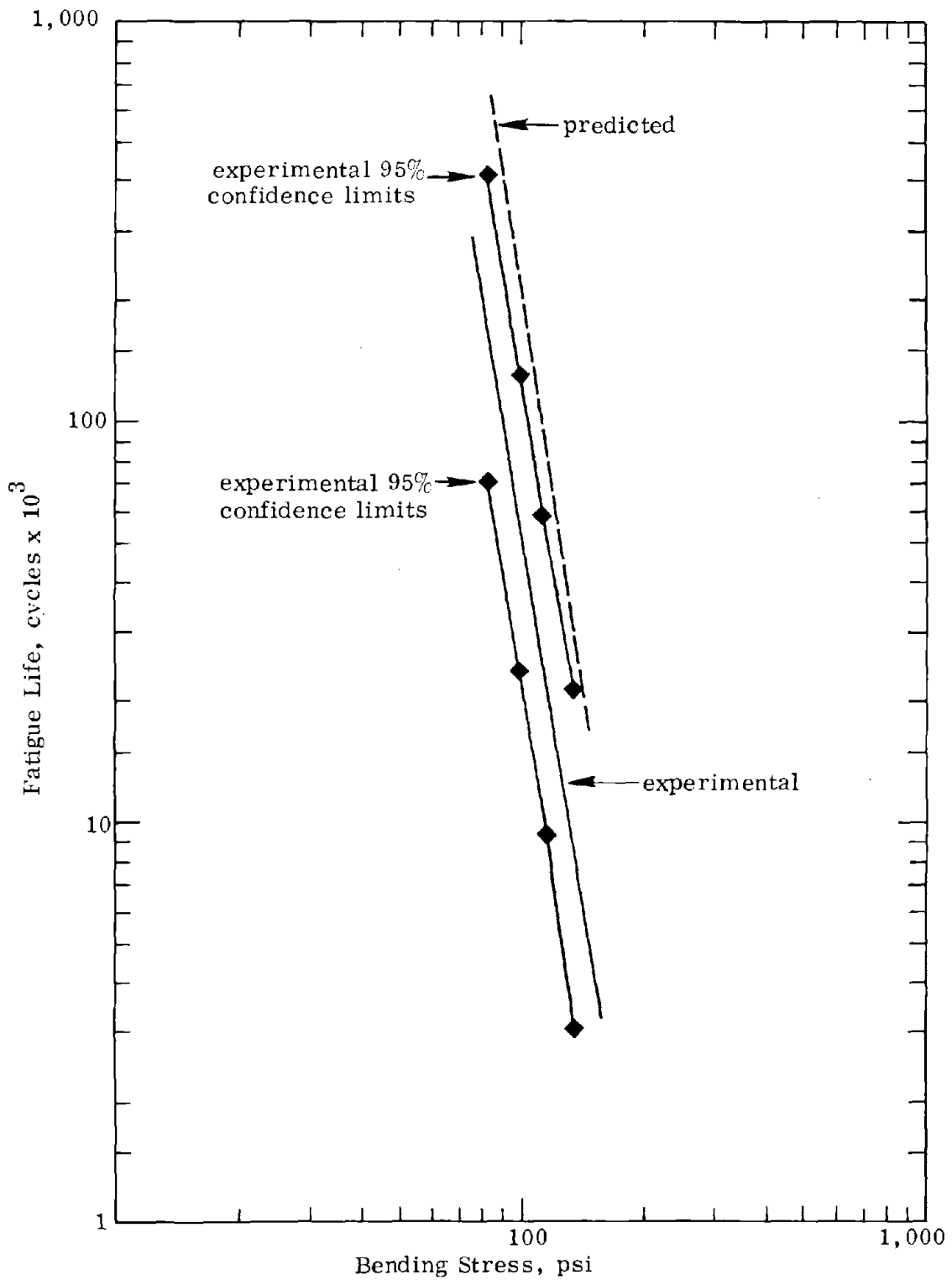


Figure 47. Constant stress fatigue curves (Ohio mix).
1 psi = 6890 Pa.

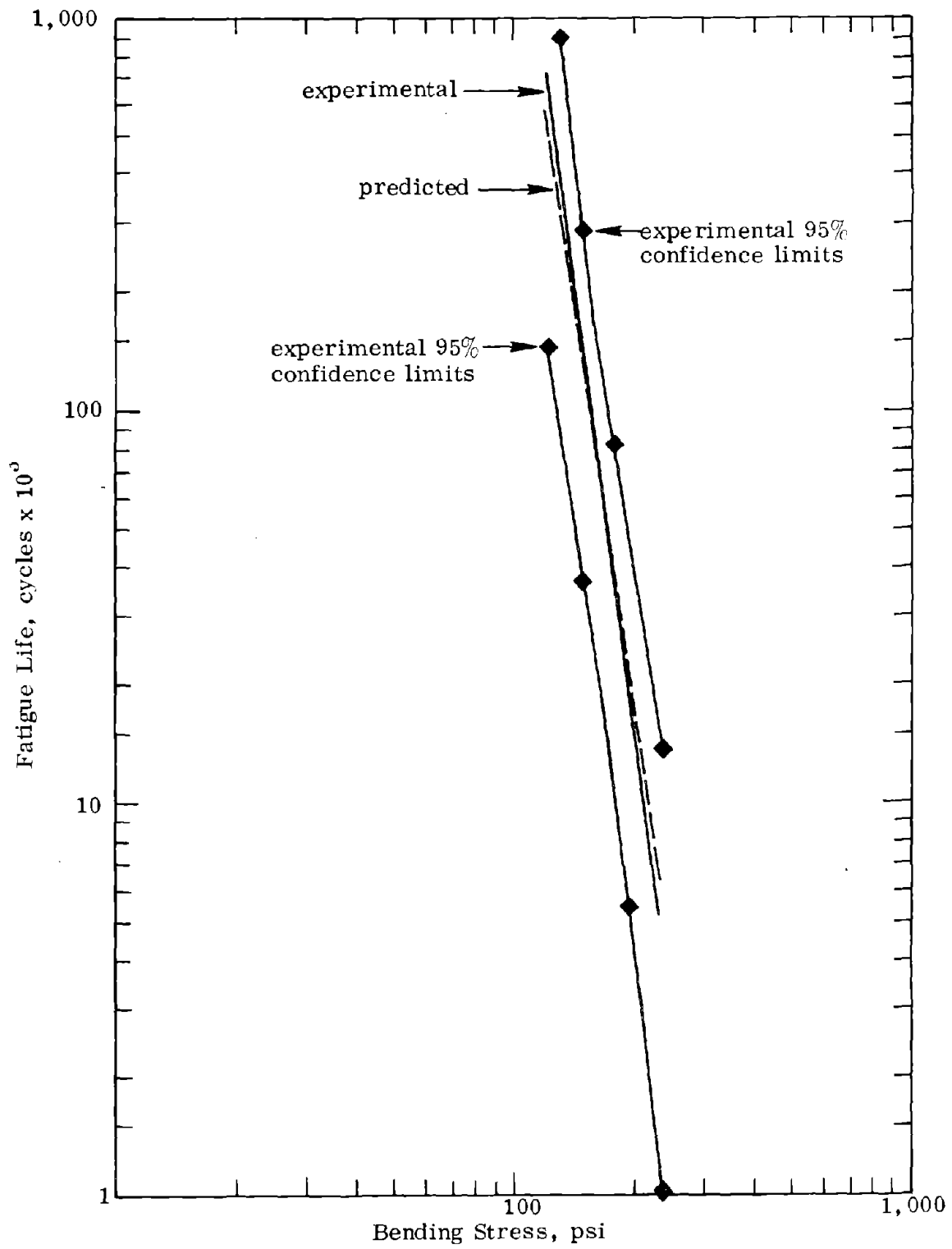


Figure 48. Constant stress fatigue curves (Utah mix).
1 psi = 6890 Pa.

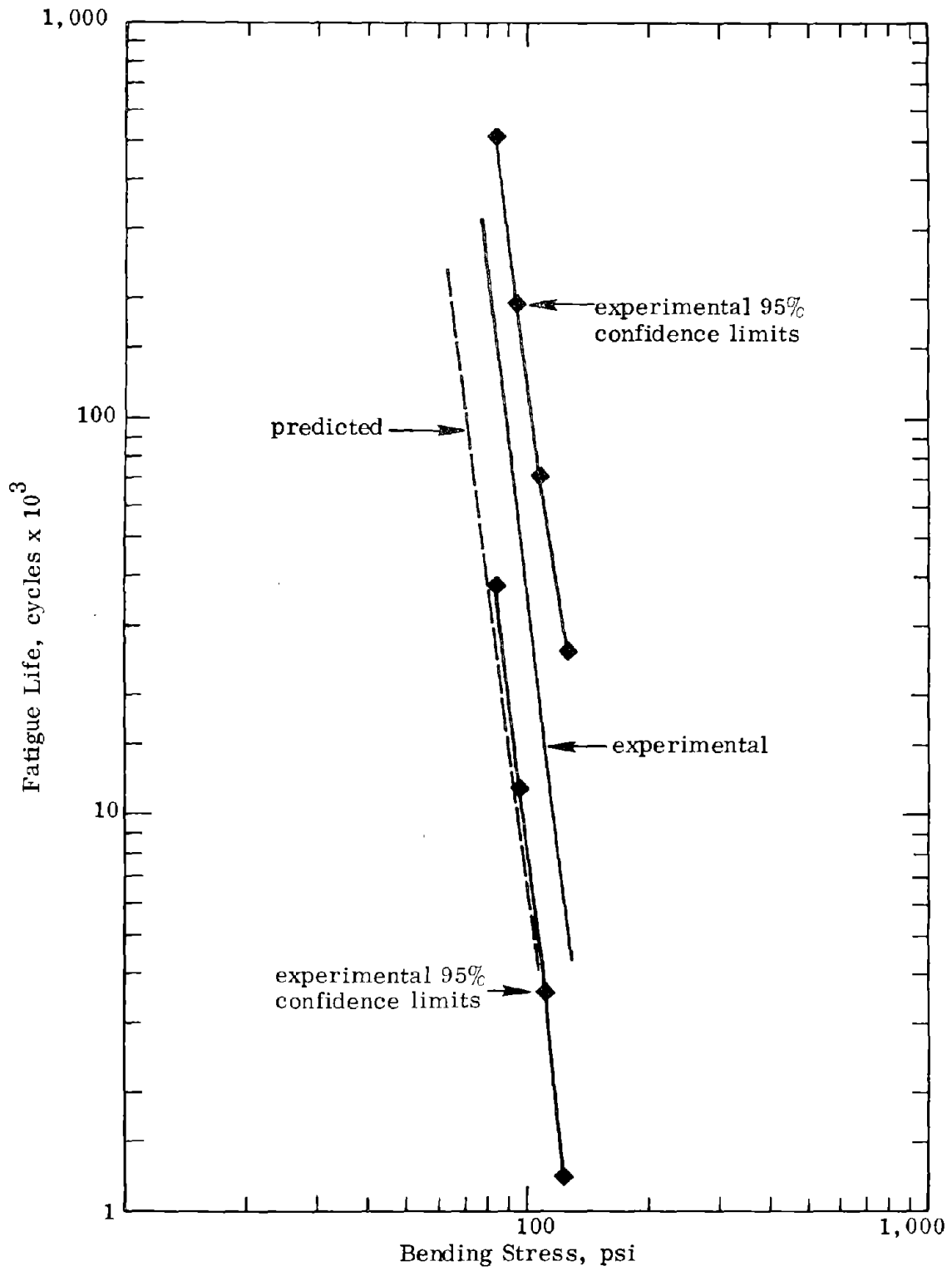


Figure 49. Constant stress fatigue curves (California mix).
1 psi = 6890 Pa.

Table 17 lists the correlation coefficients and standard error of estimates for the 44 correlations. No acceptable correlations were obtained that would allow the prediction of the constants K and n_1 for the stress fatigue curves. However, correlations were developed with acceptable error of estimates between the indirect tensile strength and the constants n_2 and K_2 for the strain fatigue curve.

The correlations $n_2 = 0.0374 \sigma_{IT} - 0.744$ and $\log K_2 = 7.92 - 0.122 \sigma_{IT}$ can be used to obtain the fatigue curve, $N = K_2 (1/\epsilon)^{n_2}$, for each mix.

The indirect tensile strength was used to predict the strain fatigue curves that are compared to the laboratory experimental fatigue curves in Figures 50-54. All of the predicted curves are within the 95% confidence band of the experimental fatigue curves.

CONCLUSIONS

1. Satisfactory correlations were developed between the stress-fatigue life curve properties obtained by constant stress fatigue testing and the indirect tensile test results.
2. Satisfactory correlations were developed between the strain-fatigue life curve properties obtained by constant strain fatigue testing and the indirect tensile test results.
3. The simple test properties that had the best correlations were the indirect tensile strength and the indirect tensile stiffness.
4. The indirect tensile strength and indirect tensile stiffness can be used to predict a constant stress fatigue curve (stress versus number of cycles). (Appendix C.)
5. The indirect tensile strength can be used to predict a constant strain fatigue curve (strain versus number of cycles). (Appendix C.)

RECOMMENDATIONS

It is recommended that the simple test procedure be used to design mixtures containing aggregate less than 1 in. (25.4 mm) for fatigue resistance.

It is also recommended that the simple test be used to obtain predicted fatigue curves for a variety of mixes in use by interested agencies in order to assess their individual needs concerning the fatigue design of bituminous concrete.

The simple test procedure should be used primarily to determine the relative fatigue properties of dense-graded bituminous concretes.

It is envisioned that the test method will be used to evaluate the relative fatigue properties of present mixes and also to design mixes with adequate fatigue properties in special situations. A special situation might be a case in which high deflections (strains) caused by unforeseen conditions will occur in the finished pavement. The bituminous concrete must be designed with better fatigue properties than the mix that is normally used if a reasonable service life is to be obtained.

Below, the general design procedure is illustrated for a location experiencing high deflections on which 6 in. (150 mm) of bituminous concrete is to be placed.

1. Decide whether the constant stress or constant strain failure mode will prevail in the pavement. It is generally conceded that thick bituminous concrete mats fail in the constant stress mode and that thin mats fail in the constant strain mode. Although there is not a well defined line between thick and thin mats, in this example it is assumed that thin mats are less than 3 in. (76 mm) and thick mats are greater than 3 in. (76 mm).

According to these assumptions, the asphaltic concrete in this example, being 6 in. (150 mm) thick, will fail in the constant stress mode and should be analyzed accordingly.

2. Obtain the indirect tensile strength and stiffness of a mix or mixes with a known fatigue performance. By using the equations in section 7.1 of Appendix C determine the fatigue equation and plot the relationship on log-log paper (Figure 55).

3. Obtain the indirect tensile strength and stiffness of the newly designed mix with unknown fatigue properties. Determine the fatigue equation as described above and plot the relationship on log-log paper.

Visual examination should reveal the fatigue behavior of the unknown mix as compared with that of a mix with known fatigue properties. A quantitative analysis is possible if material properties are known so that the anticipated stresses and/or strains can be calculated.

Table 17
CORRELATION BETWEEN CONSTANT STRAIN FATIGUE AND SIMPLE TESTS

Fatigue Characteristic	Stiffness						Strength		Vertical Deformation		
	Indirect Tensile	Punch	Flexure	Resilient Modulus	Transverse Frequency	Wave Velocity	Indirect Tensile	Punch	Flexure	Indirect Tensile	Punch
n_1^*	0.15 (1.22)	0.15 (1.22)	0.74 (.83)	0.44 (1.11)	0.62 (.97)	0.50 (1.07)	0.53 (1.05)	0.08 (1.23)	0.73 (.85)	0.64 (0.95)	0.68 (0.91)
n_2^{**}	0.79 (.63)	0.28 (.98)	0.46 (.90)	0.56 (.84)	0.84 (.56)	0.46 (.90)	0.81 (.59)	0.47 (.90)	0.59 (.83)	0.40 (0.94)	0.18 (1.00)
$\log k_1^*$	0.12 (3.29)	0.22 (3.24)	0.65 (2.51)	0.41 (3.03)	0.67 (2.48)	0.38 (3.07)	0.54 (2.79)	0.10 (3.30)	0.68 (2.45)	0.70 (2.36)	0.72 (2.29)
$\log k_2^{**}$	0.82 (1.82)	0.34 (3.00)	0.64 (2.46)	0.95 (2.69)	0.85 (1.67)	0.51 (2.75)	0.85 (1.69)	0.51 (2.74)	0.64 (2.46)	0.41 (2.91)	0.19 (3.14)

$$*N = k_1 (1/\sigma)^{n_1}$$

$$**N = k_2 (1/\epsilon)^{n_2}$$

Note: Correlation coefficient listed with standard error of estimate in parentheses.

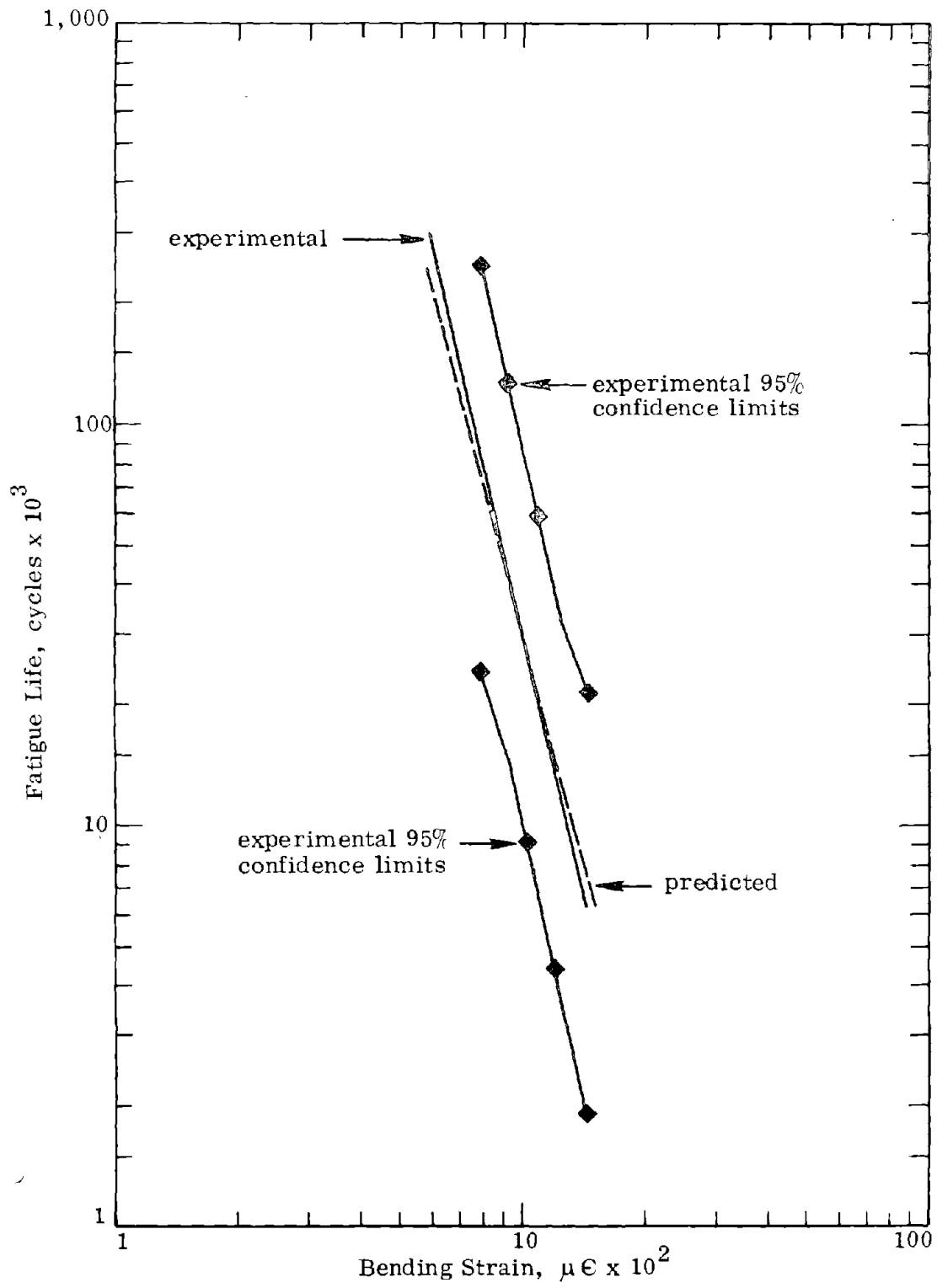


Figure 50. Constant strain fatigue curves (Virginia AC-20 mix).

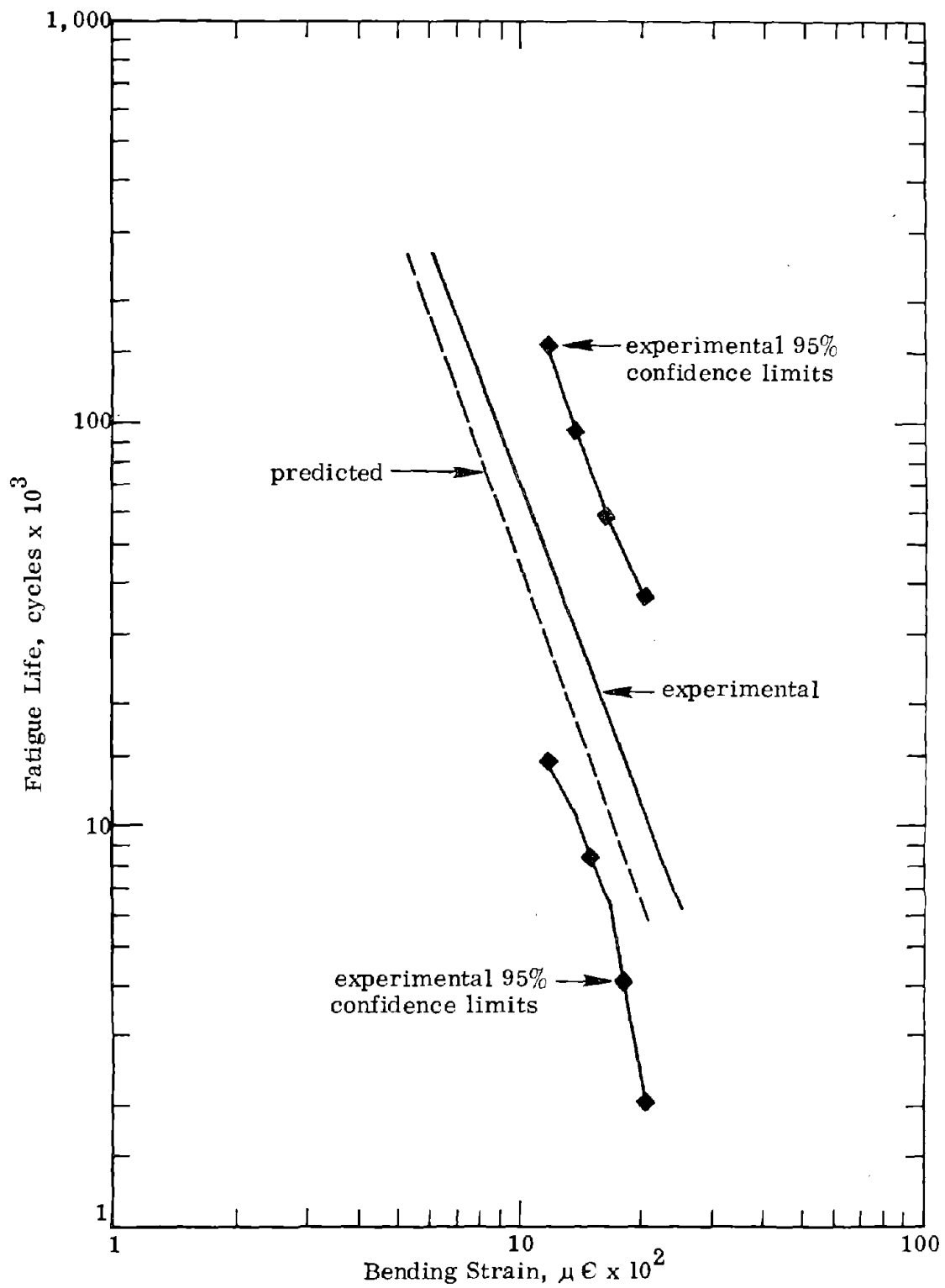


Figure 51. Constant strain fatigue curves (Pennsylvania mix).

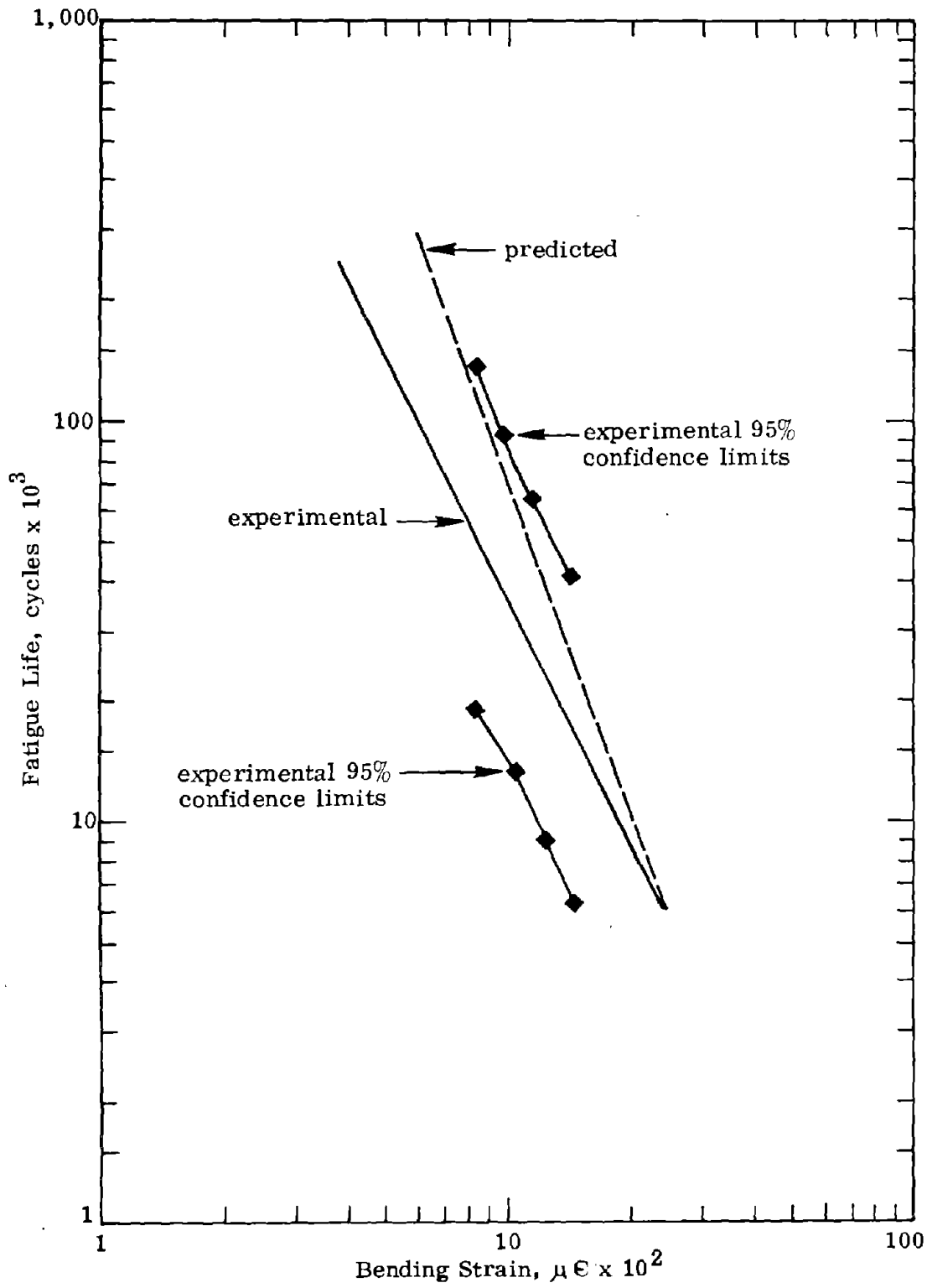


Figure 52. Constant strain fatigue curves (Ohio mix).

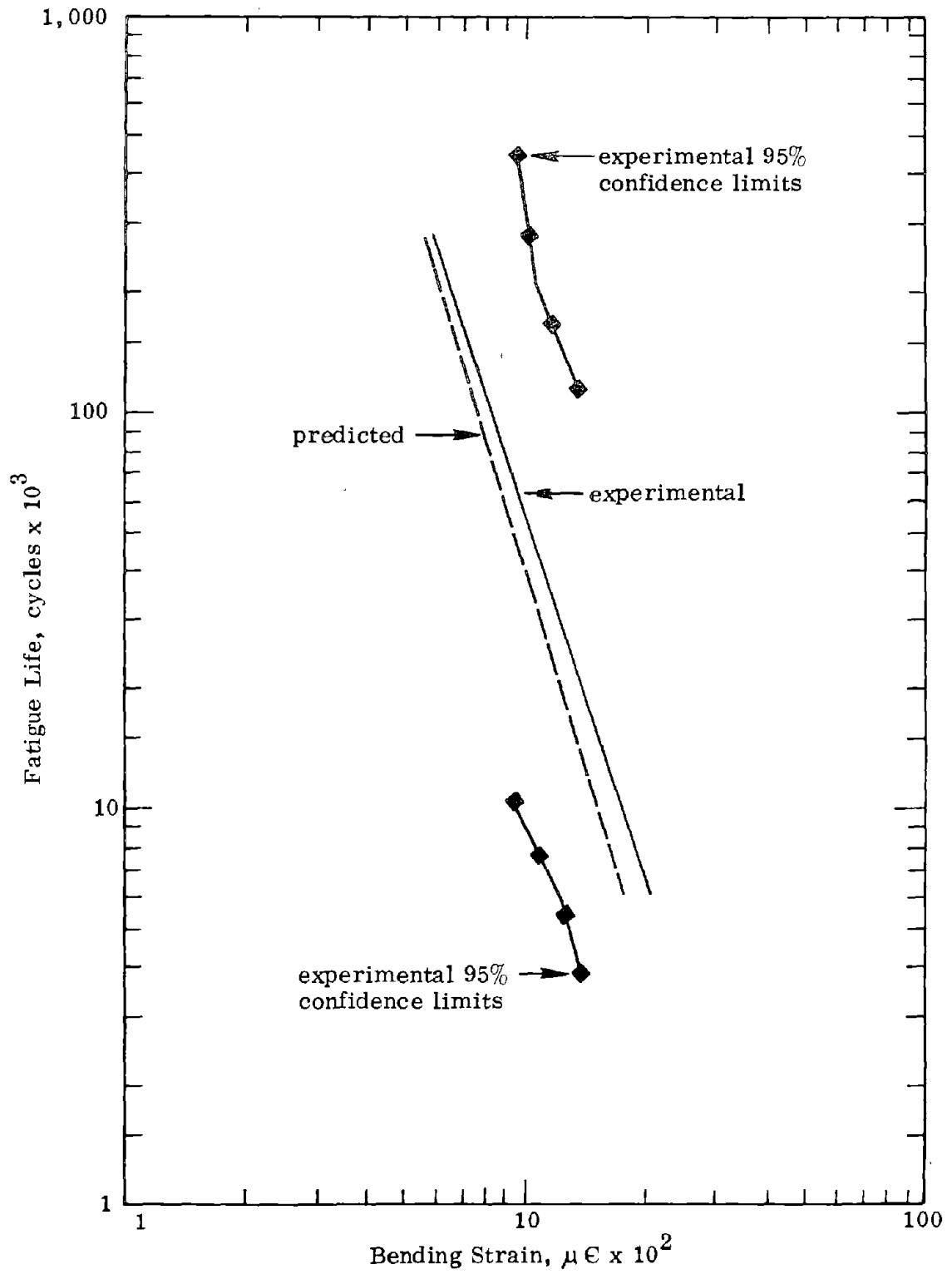


Figure 53. Constant strain fatigue curves (Utah mix).

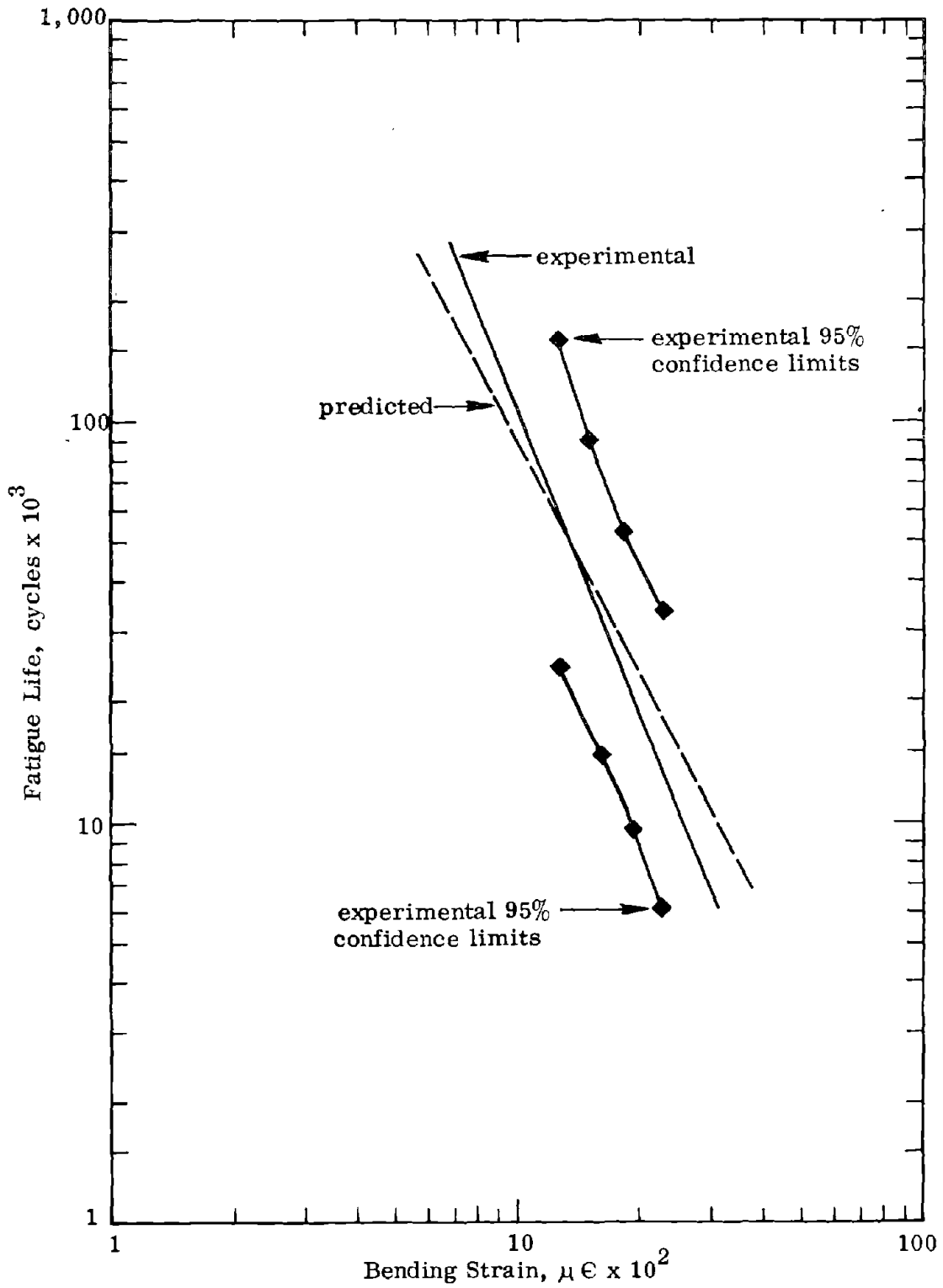


Figure 54. Constant strain fatigue curves (California mix).

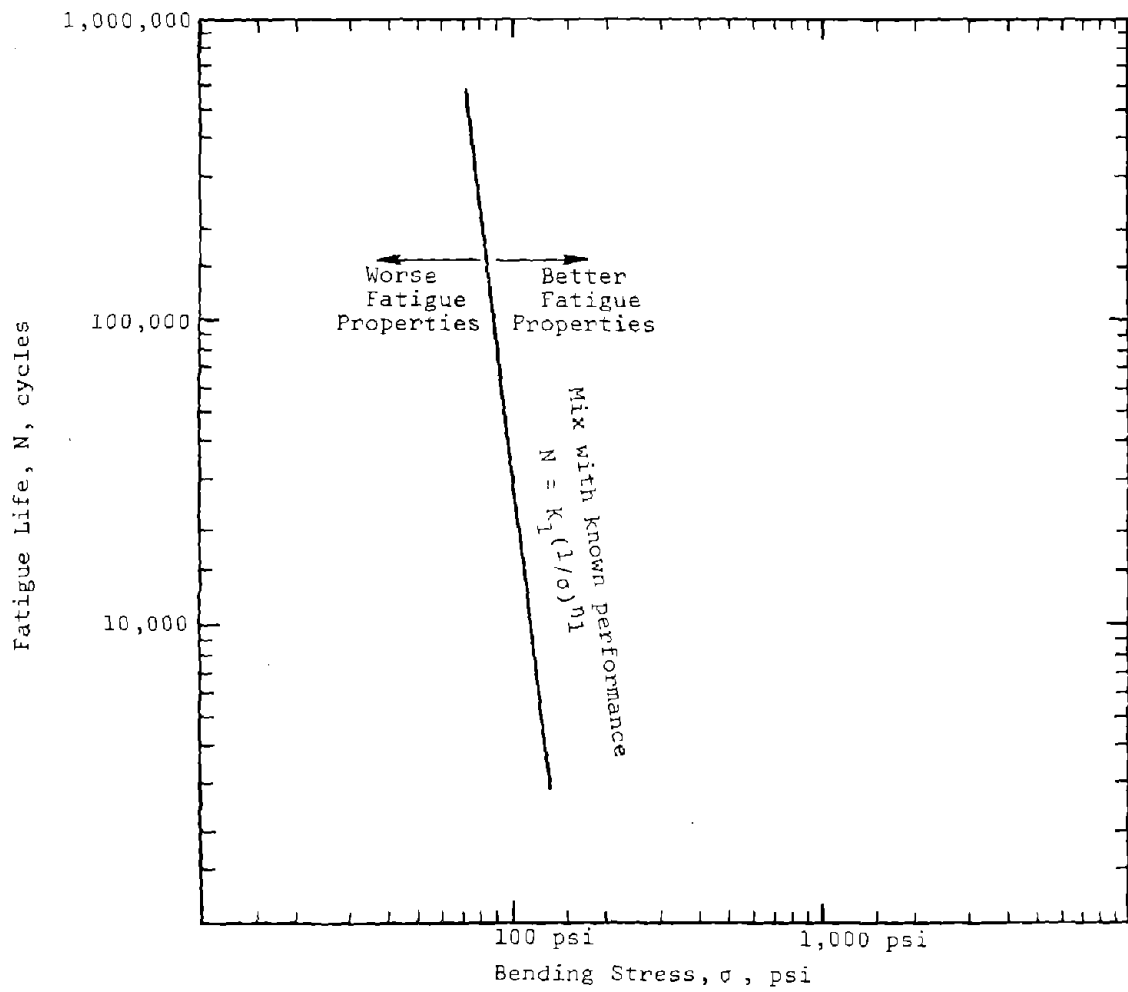


Figure 55. Fatigue design of bituminous concrete, constant stress failure mode.

REFERENCES

1. Grumm, Fred J., "Designing Foundation Courses for Highway Pavements and Surfaces," California Highways and Public Works, Vol. 20, No. 3, March 1942, pp. 6-9, 20.
2. Porter, O. J., "Foundations for Flexible Pavements." Proceedings, Highway Research Board, Vol. 22, 1942, pp. 100-143.
3. Hveem, F. N., "Pavement Deflections and Fatigue Failures," Bulletin, Highway Research Board, Washington, 1955, pp. 43-87.
4. Hennes, R. G., and H. H. Chen, "Dynamic Design of Bituminous Pavements," The Trend in Engineering, University of Washington, January 1959, pp. 22-25.
5. Nijboer, L. W., "Mechanical Properties of Asphalt Materials and Structural Design of Asphalt Roads," Proceedings, Highway Research Board, Vol. 33, 1954, pp. 185-198.
6. Van der Poel, C., "Road Asphalt," Building Materials, Their Elasticity and Inelasticity, edited by M. Rainer, New York, Interscience Publishers, 1954, pp. 361-413.
7. Monismith, C. L., "Flexibility Characteristics of Asphaltic Paving Mixtures," Proceedings, Association of Asphalt Paving Technologists, Vol. 27, February 1958, pp. 74-106.
8. Pell, P. S., "Fatigue Characteristics of Bitumen and Bituminous Mixes," Proceedings, International Conference on the Structural Design of Asphalt Pavement, Ann Arbor, Michigan, 1962, pp. 310-323.
9. Deacon, J. A., and C. L. Monismith, "Laboratory Flexural Fatigue Testing of Asphaltic Concrete with Emphasis on Compound Loading," Paper presented at the annual meeting of the Highway Research Board, Washington, D. C., January 1966.
10. Maupin, G. W., "Effects of Aggregate Shape on the Fatigue Behavior of an Asphaltic Surface Mixture," Virginia Highway & Transportation Research Council, Charlottesville, Virginia, June 1968.
11. Monismith, C. L., K. E. Secar, and E. W. Blackmer, "Asphalt Mixture Behavior in Repeated Flexure," Proceedings, Association of Asphalt Paving Technologists, Vol. 30, February 1961, pp. 188-222.

12. Kallas, B. F., and V. P. Puzinauskas, "Flexure Fatigue Tests on Asphaltic Paving Mixtures," Fatigue of Compacted Bituminous Aggregate Mixtures, ASTM STP 508, American Society for Testing and Materials, 1972, pp. 47-65.
13. Kirk, J. M., "Results of Fatigue Tests on Different Types of Bituminous Mixtures," Proceedings, Second International Conference on the Structural Design of Asphaltic Pavement, Ann Arbor, Michigan, 1967, pp. 571-575.
14. Jiminez, R. A., "Fatigue Testing of Asphaltic Concrete Slabs," Fatigue of Compacted Bituminous Aggregate Mixtures, ASTM STP 508, American Society for Testing and Materials, 1972, pp. 3-17.
15. Bazin, P., and J. B. Saunier, "Deformability, Fatigue and Healing Properties of Asphaltic Mixes," Proceedings, Second International Conference on the Structural Design of Asphalt Pavement, Ann Arbor, Michigan 1967, pp. 553-569.
16. Coffman, B. S., G. J. Ilves, and W. F. Edwards, "The Fatigue of Flexible Pavements," Report EES 296B-1, Transportation Research Center, Ohio State University, Columbus, Ohio, February 1971.
17. Majidzadeh, Karman, E. M. Kauffman, and C. L. Saraf, "Analysis of Fatigue of Paving Mixtures from the Fracture Mechanics Viewpoint," Fatigue of Compacted Bituminous Aggregate Mixtures, ASTM STP 508, American Society for Testing and Materials, 1972, pp. 67-83.
18. Epps, J. A., and C. L. Monismith, "Fatigue of Asphalt Concrete Mixtures - Summary of Existing Information," Fatigue of Compacted Bituminous Aggregate Mixtures, ASTM STP 508, American Society for Testing and Materials, 1972, pp. 19-45.
19. Taylor, I. F., "Asphaltic Road Materials in Fatigue," Thesis, University of Nottingham, October 1968.
20. Monismith, C. L., J. A. Epps, D. A. Kasianchuk, and D. B. McLean, "Asphalt Mixture Behavior in Repeated Flexure," Report No. TE 70-5, Office of Research Services, University of California, Berkeley, California, December 1970.
21. "An Introduction to MTS Closed-Loop Testing Systems," published by Materials Testing Systems Corporation.

22. Moore, Raymond K., and Thomas W. Kennedy, "Tensile Behavior of Subbase Materials under Repetitive Loading," Research Report 98-12, Center for Highway Research, University of Texas at Austin, October 1971.
23. Anagnos, James N., and Thomas W. Kennedy, "Practical Method of Conducting the Indirect Tensile Test," Center of Highway Research, University of Texas at Austin, August 1972.
24. Pell, P. S., "Fatigue of Asphalt Pavement Mixes," Proceedings, Second International Conference on the Structural Design of Asphalt Pavement, Ann Arbor, Michigan, 1967, pp. 577-593.
25. Hudson, W. Ronald, and Thomas W. Kennedy, "An Indirect Tensile Test for Stabilized Materials," Center for Highway Research, University of Texas at Austin, January 1968.
26. Timoshenko, S., and J. N. Goodier, "Stresses in a Circular Disk," Theory of Elasticity, Second Edition, McGraw-Hill, New York, N. Y., 1951, pp. 107-111.
27. Frocht, M. M., "Stresses in Circular Disks," Photoelasticity, Volume II, John Wiley and Sons, Inc., New York, N. Y., 1948, pp. 118-133.
28. Heukelem, W., and A. J. G. Klomp, "Road Design and Dynamic Loading," Proceedings, Association of Asphalt Paving Technologists, Vol. 33, February 1964, pp. 92-125.
29. Hadley, William O., W. Ronald Hudson, and Thomas W. Kennedy, "An Evaluation of Factors Affecting the Tensile Properties of Asphalt-Treated Materials," Center for Highway Research, University of Texas at Austin, March 1969.
30. Wright, P. J. F., "Comments on an Indirect Tensile Test on Concrete Cylinders," Magazine of Concrete Research, London, March 1956.
31. Hondros, G., "The Evaluation of Poisson's Ratio and Modulus of Materials of a Low Tensile Resistance by the Indirect Tensile Test," Australian Journal of Applied Science, Vol. 10, No. 3.
32. Hadley, William O., W. Ronald Hudson, and Thomas W. Kennedy, "Evaluation and Prediction of the Tensile Properties of Asphalt-Treated Materials," Center for Highway Research, University of Texas at Austin, May 1971.

33. Maupin, G. W. Jr., "Results of Indirect Tensile Tests Related to Asphalt Fatigue," Virginia Highway and Transportation Research Council, November 1971.
34. Marais, C. P., "Tentative Mix Design Criteria for Gap-Graded Bituminous Surfacing," National Institute for Road Research, Pretoria, South Africa, January 1974.
35. Schmidt, R. J., "A Practical Method for Measuring the Resilient Modulus of Asphalt-Treated Mixes," Highway Research Record 404, 1972, pp. 22-32.
36. Chen, W. F., "Double Punch Test for Tensile Strength of Concrete," American Concrete Institute, Vol. 67, December 1970, pp. 993-995.
37. Fang, H. Y., and W. F. Chen, "New Method for Determination of Tensile Strength of Soils," Highway Research Record 345, 1971, pp. 62-68.
38. Jimenez, R. A., "Testing for Debonding of Asphalt from Aggregates," Report to Arizona Highway Department, Research Project — Arizona HRP-1-10 (123), University of Arizona, April 1973.
39. Jimenez, R. A., "Evaluation of the Cohesimeter Test for Asphalt Concrete," Highway Research Record 51, 1964, pp. 44-56.
40. Mix Design Methods for Asphaltic Concrete, The Asphalt Institute, Third Edition, October 1969.
41. Hadley, William O., W. Ronald Hudson, and Thomas W. Kennedy, "Correlation of Tensile Properties and Cohesimeter Values of Asphalt Treated Materials," Center of Highway Research, University of Texas at Austin, June 1970.
42. Guericke, R., and F. Weinert, "The Behavior of Bituminous Mixtures in Laboratory Tests and under Road Conditions," The University of Michigan Third International Conference on the Structural Design of Asphalt Pavements, London, England, September 1972, pp. 233-240.
43. Epps, Jon A., and Carl L. Monismith, "Influence of Mixture Variables on the Direct Tensile Properties of Asphalt," Proceedings, Association of Asphalt Paving Technologists, Vol. 39, February 1970, pp. 207-241.
44. Mitchell, W. B., Jr., "The Indirect Tension Test for Concrete," Materials Research and Standards, American

Society for Testing Materials, Vol. 1, No. 10, October 1961, pp. 780-787.

45. Busby, Edward O., and Lloyd F. Rader, "Flexural Properties of Asphalt Concrete at Low Temperatures," Proceedings, Association of Asphalt Paving Technologists, Vol. 41, February 1972, pp. 163-187.
46. Freeme, Charles R., and Claude P. Marais, "Thin Bituminous Surfaces: Their Fatigue Behavior and Prediction," Special Report 140, Highway Research Board, 1973.
47. Leslie, J. R., and W. J. Cheesman, "An Ultrasonic Method of Studying Deterioration and Cracking in Concrete Structures," American Concrete Institute Journal, Vol. 46, September 1949.
48. Correspondence with R. A. Jimenez.

APPENDIX A

FINGERPRINTING DATA ON ORIGINAL ASPHALT CEMENTS

Card No.	N#20	N#21	N#22	N#23	N#24
Sample Identification	Virginia	Pennsyl- vania	Ohio	Utah	California
Composition of asphalt, %	AC-10				
Fraction A (asphaltenes)	19.5	25.8	23.1	20.6	24.1
Fraction N (nitrogen bases)	21.2	24.9	16.9	21.1	24.5
Fraction A1 (first acidaffins)	19.0	22.5	18.3	18.0	21.4
Fraction A2 (second acidaffins)	27.8	19.4	28.6	23.0	20.9
Fraction P (paraffins)	12.5	7.4	13.1	17.3	9.1
(N-A1) / (F+A2)	1.00	1.77	0.84	0.97	1.53
N/P	1.70	3.36	1.29	1.22	2.69
Max, %	3.65	1.12	2.87	4.39	1.61
Refractive index of Fraction P (N _D ²⁵)	1.4821	1.4774	1.4810	1.4809	1.4753
Asphalt viscosity at 60°C (140°F), P	2341	2743	3325	1187	1117
Penetration at 25°C (77°F), 100g, 5 sec.	69	94	78	83	191
Maltenes viscosity at 25°C (77°F), P	15081	3508	5541	14429	1256
at 60°C (140°F), P	105.3	31.75	39.94	36.92	20.05
at 135°C (275°F), cS	91.53	74.60	61.82	55.89	27.78
Molecular weight of Fraction A	5540	5850	6560	4995	6660
Weight change in Thin Film Oven Test, %	-0.01	-1.22	-0.14	-0.61	-1.72
Pellet abrasion loss at 25°C (77°F), mg/rev.					
Unaged	0.07	0.07	0.03	0.14	0.00
Aged 7 days at 60°C (140°F)	0.31	1.76	0.21	0.17	0.36
Average of unaged and aged 7 days	0.19	0.91	0.12	0.16	0.18
Pellet abrasion loss at 25°C (77°F), %					
Unaged	1.6	1.7	0.7	3.6	0.1
Aged 7 days at 60°C (140°F)	7.7	44.4	5.2	4.2	9.0
Average of unaged and aged 7 days	4.7	23.0	3.0	3.9	4.5

APPENDIX B

ASPHALT CEMENT SLIDING PLATE VISCOSITIES

72° F (22°C) at .05 sec⁻¹, poises

Mix Identification	Pennsylvania	Ohio	Utah	California	Virginia AC-20	Virginia 50-60 pen.	Virginia 120-150 pen.
Original Asphalt Cement	2.10 x 10 ⁶	2.85 x 10 ⁶	3.27 x 10 ⁶	5.46 x 10 ⁵	4.00 x 10 ⁶	5.70 x 10 ⁶	1.58 x 10 ⁶
Asphalt Cement Recovered from Beams	4.90 x 10 ⁶	4.42 x 10 ⁶	3.80 x 10 ⁶	7.43 x 10 ⁵	7.20 x 10 ⁶	1.15 x 10 ⁷	2.65 x 10 ⁶

APPENDIX C

PREDICTION OF FATIGUE LIFE RELATIONS BY INDIRECT TENSILE TEST

1. Scope

- 1.1 This method covers procedures for testing asphalt concrete mixtures to predict constant stress and constant strain fatigue relations.
- 1.2 The method is applicable to mixtures containing aggregate particles less than 1 inch (25.4 mm) in size.

2. Applicable Documents

- 2.1 ASTM Standards
 - D 1559 Resistance to Plastic Flow of Bituminous Mixtures Using Marshall Apparatus
 - D 1561 Preparation of Test Specimens of Bituminous Mixtures by Means of the California Kneading Compactor

3. Apparatus

- 3.1 Testing Machine — A testing machine capable of applying a maximum load of 5,000 lb. (22 kN) at a constant rate of 2 inches/min. (51 mm/min.)
- 3.2 Measurement System — The measurement system consists of a two-channel recorder, load and displacement measuring devices, suitable signal amplification and excitation equipment. The system should be capable of measuring loads to 5,000 lb. (22 kN) with a minimum sensitivity of 20 lb. (89 N) per mm of chart paper. The system should be capable of measuring horizontal deformation to a sensitivity of 0.0004 inch (10 μ m) per mm of chart paper.
 - 3.2.1 Horizontal Deformation Measurement — Horizontal deformation can be measured by two LVDT's mounted as shown in Figure 1A. Other transducer devices are satisfactory provided the sensitivity required in Section 3.2 is provided.

- 3.2.2 Load Measurements — Loads are measured by an electronic load cell or other acceptable electronic means.

4. Specimens

- 4.1 Laboratory Molded Specimens — Specimens (2.5 in. x 4 in. diam.) (63.5 mm x 102 mm diam.) can be prepared by ASTM Methods D 1559 or D 1561. Eight specimens should be tested for each condition and the results averaged.
- 4.2 Pavement Cores — Pavement cores (2.5 in. x 4 in. diam.) (63.5 mm x 102 mm diam.) may be tested. The core mixture should conform to Section 1.2.

5. Procedure

- 5.1 Measure and record diameter and thickness of specimen to 0.05 in. (1 mm).
- 5.2 Bring specimen to test temperature $72^{\circ}\text{F} \pm 1^{\circ}\text{F}$ ($22^{\circ}\text{C} \pm 0.5^{\circ}\text{C}$).
- 5.3 The specimen is placed in a loading apparatus similar to that shown in Figure 31. The steel loading strips are 0.5 inch (13 mm) wide and have a 2-inch (51 mm) contact radius.
- 5.4 The specimen is loaded at a vertical deformation rate of 2 inches (51 mm) per minute until the maximum load is attained. Load and horizontal deformation are recorded simultaneously.
- 5.5 If the specimen temperature and testing temperature are not coincident, then testing should be completed within 3 minutes.

6. Calculations

- 6.1 Compute the indirect tensile strength, σ_{IT} , and indirect tensile stiffness, E_{IT} , by the following equations:

$$\sigma_{IT} = \frac{2P}{\pi h d}$$
$$v = \frac{0.0673 \text{ DR} - 0.8954}{-0.2494 \text{ DR} - 0.0156}$$

$$E_{IT} = \frac{P}{X_T h} (0.9976 \nu + 0.2692)$$

where

- P = ultimate load, lbs. (N)
- h = specimen thickness, in. (m)
- d = specimen diameter, in. (m)
- X_T = horizontal deformation, in. (m)
- Y_T = vertical deformation, in. (m)
- DR = deformation ratio, $\frac{Y_T}{X_T}$
- ν = Poisson's ratio
- σ_{IT} = indirect tensile strength, psi (Pa)
- E_{IT} = indirect tensile stiffness, psi (Pa)

7. Fatigue Curve Prediction

- 7.1 Constant Stress Fatigue Curve — The fatigue relation $N_f = K_1 (1/\sigma)^{n_1}$, can be calculated from the following equations:

$$n_1 = 11.6 - 0.000396 E_{IT}$$

$$K_1 = e^{n_1 \ln (12.6 \sigma_{IT} - 558)}$$

where

$$N_f = \text{cycles to failure (collapse)}$$

$$\sigma = \text{maximum bending stress}$$

- 7.2 Constant Strain Fatigue Curve — The fatigue relation $N_f = K_2 (1/\epsilon)^{n_2}$ can be calculated from the following equations:

$$n_2 = 0.0374 \sigma_{IT} - 0.744$$

$$\log K_2 = 7.92 - 0.122 \sigma_{IT}$$

where N_f = cycles to failure (a 1/3 reduction in initial stiffness calculated at approximately 200 cycles).
 ϵ = initial bending strain (based on center point deflection of specimen at approximately 200 cycles).

Note: After the constants n_1 , n_2 , K_1 , and K_2 , are calculated, values for N_f are determined by substituting representative values of σ (stress level) or ϵ (strain level) in the respective equations. These will normally be in the range of 70 psi to 300 psi for stress, and 300 $\mu\epsilon$ to 2000 $\mu\epsilon$ for strain. The chosen values of σ or ϵ and corresponding values of calculated N_f values are then plotted on log - log paper.

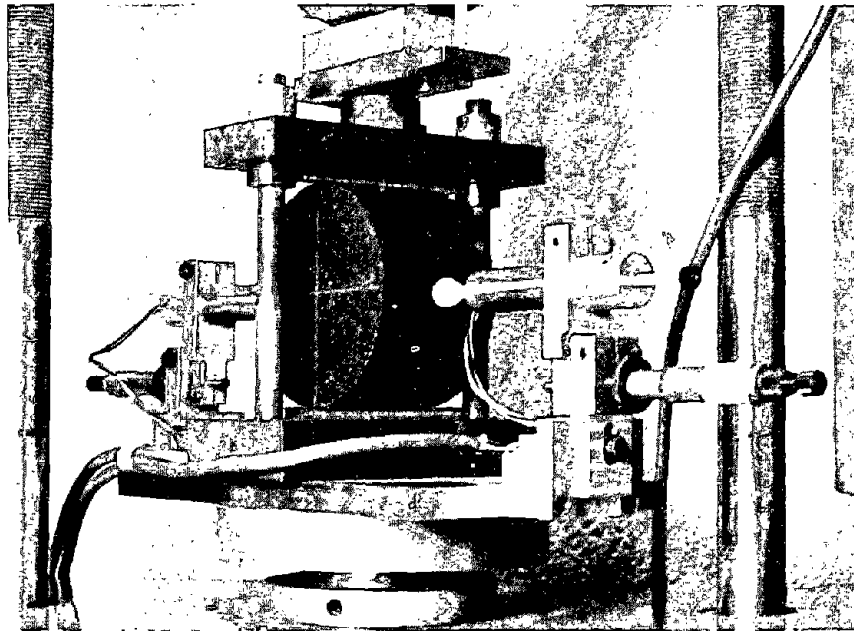


Figure 1-A. Indirect tensile test.

